

G78299

INVESTIGATIONS ON SOME TITANIA SUPPORTED CATALYSTS



**THESIS SUBMITTED
TO
COCHIN UNIVERSITY OF SCIENCE AND TECHNOLOGY
IN PARTIAL FULFILMENT OF THE REQUIREMENTS
FOR THE DEGREE OF**

DOCTOR OF PHILOSOPHY

**IN
CHEMISTRY
UNDER
THE FACULTY OF SCIENCE
BY**

AHMED YASIR. VAKAYIL

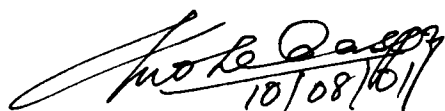
**DEPARTMENT OF APPLIED CHEMISTRY
COCHIN UNIVERSITY OF SCIENCE AND TECHNOLOGY
KOCHI – 682 022, KERALA, INDIA**

AUGUST 2001

10th August 2001

CERTIFICATE

This is to certify that the work embodied in the thesis entitled "*INVESTIGATIONS ON SOME TITANIA SUPPORTED CATALYSTS*" is an authentic record of the research work carried out by **Mr. Ahmed Yasir. Vakayil** under our supervision in the partial fulfillment of the requirements for the degree of **Doctor of Philosophy** in Chemistry of Cochin University of Science and Technology, Kochi and further that no part thereof has been presented before for any other degree.



10/08/01

Dr. P.N. Mohan Das
Dy. Director
Head, BSMR Division
Regional Research Laboratory
(CSIR)
Thiruvananthapuram- 695 019



Dr. K.K. Mohammed Yusuff
Professor
Dept. of Applied Chemistry
Cochin University of Science
and Technology
Kochi- 682 022

CONTENTS

Declaration

Certificate

Acknowledgements

Preface

Chapter 1 INTRODUCTION

1.1	General introduction	1
1.2	Industrial applications of titania	2
1.3	Titania as a catalyst or support	6
1.4	Metal -support -interactions in titania supported catalysts	11
1.5	Anatase to rutile transformation	14
1.6	Literature survey	20
1.6.1	Reactions carried out over titania supported catalysts	20
1.6.1.1	Hydrodesulfurization (HDS)	20
1.6.1.2	Partial oxidation	21
1.6.1.3	Carbon monoxide hydrogenation	23
1.6.1.4	Selective catalytic reduction (SCR)	24
1.6.1.5	Coal liquefaction	26
1.6.1.6	Ammonia synthesis	27
1.6.1.7	Isomerization	28
1.6.1.8	Carbon monoxide oxidation	28

1.6.1.9	Miscellaneous	30
1.6.1.10	Photo catalysis	31
1.6.2.	Preparation method	33
1.6.2.1	Sol - gel method	33
1.6.2.2	Ion-exchange method	35
1.6.2.3	Wet-impregnation method	36
1.6.2.4	Co-precipitation	38
1.6.2.5	Thermal hydrolysis	38
1.6.2.6	Miscellaneous	40
1.7	Scope and objective of the present investigation	41
Chapter 2	MATERIALS AND EXPERIMENTAL METHODS	43
2.1	Materials used	43
2.2	Experimental procedure	44
2.2.1	Preparation of TiO ₂ (anatase) by thermal hydrolysis	44
2.2.2	Preparation of NiO/TiO ₂ catalysts	46
2.2.2.1	Co-precipitation method	46
2.2.2.2	Ion-exchange method	47
2.2.2.3	Wet-impregnation method	47
2.2.3	Preparation of Fe ₂ O ₃ /TiO ₂	47
2.2.3.1	Co-precipitation method	48
2.2.3.2	Ion-exchange method	48
2.2.3.3	Wet-impregnation method	48
2.2.4	Preparation of CeO ₂ /TiO ₂ catalysts	48
2.2.4.1	Co-precipitation method	48
2.2.4.2	Ion-exchange method	49
2.2.4.3	Wet-impregnation method	49

2.2.5	Preparation of V ₂ O ₅ /TiO ₂ catalysts	49
2.2.5.1	Co-precipitation method	49
2.2.5.2	Ion-exchange method	50
2.2.5.3	Wet-impregnation method	50
2.3.	Pelletization	50
2.4	Dispersion studies	50
2.4.1	Oxygen chemisorption method	51
2.4.2	Carbon monoxide chemisorption method	53
2.5	Catalytic activity studies	53
2.5.1	Carbon monoxide methanation activity studies	54
2.5.2	Toluene oxidation activity studies	55
2.6	Crystallite size calculation	56
2.7	Rutile percentage calculation	56
2.8	Chemical analysis	57
2.8.1	Estimation of TiO ₂	57
2.8.2	Estimation of NiO	58
2.8.3	Estimation of CeO ₂	58
2.8.4	Estimation of V ₂ O ₅	59
2.8.5	Estimation of Fe ₂ O ₃	59
2.9	Instrumental methods employed	60
2.9.1	Surface area analyzer	60
2.9.2	Gas chromatograph	60
2.9.3	Catalytic reactor	60
2.9.4	Furnace and temperature programmer	60
2.9.5	X- ray diffractometer	61
2.9.6	Scanning electron microscope	61

2.9.7	UV- Visible spectro photometer	61
2.9.8	TGA and DTA	61
RESULTS AND DISCUSSION		
Chapter 3	STUDIES ON TiO₂ PREPARED BY THERMAL HYDROLYSIS	62
3.1	Chemical analysis	63
3.2	Surface area studies	64
3.2.1	Concentration of titanyl sulfate solution	64
3.2.2	Temperature of hydrolysis	65
3.2.3	Duration of hydrolysis	66
3.2.4	Calcination temperature	66
3.3	XRD studies	68
3.4	TGA and DTA studies	72
3.5	Conclusions	74
Chapter 4	STUDIES ON NiO/TiO₂ CATALYSTS	77
4.1	XRD studies	78
4.2	Surface area studies	86
4.3	Dispersion studies	90
4.4	SEM studies	91
4.5	Methanation activity studies	94
4.6	Conclusions	101
Chapter 5	Fe₂O₃/TiO₂ CATALYSTS	103
5.1	XRD studies	104
5.2	Surface area studies	112
5.3	Dispersion studies	115
5.4	Studies on toluene oxidation activity	117
5.5	Conclusions	122

Chapter 6	CeO₂/TiO₂ CATALYSTS	124
6.1	XRD studies	124
6.2	Surface area studies	132
6.3	Dispersion studies	136
6.4	Toluene oxidation studies	136
6.5	Conclusions	139
Chapter 7	V₂O₅/TiO₂ CATALYSTS	141
7.1	XRD studies	141
7.2	Surface area studies	150
7.3	SEM studies	153
7.4	Dispersion studies	156
7.5	Toluene oxidation studies	157
7.6	Conclusions	161
Chapter 8	SUMMARY AND CONCLUSIONS	163
	REFERENCES	167

PREFACE

Titania is a versatile metal oxide with multiple applications. It has gained much attention in catalyst industry due to its application as a catalyst by itself and as a support for metal or metal oxide catalysts. Titania supported catalysts are reported to be much more active compared to conventional silica or alumina supported ones in some reactions. It is noteworthy and interesting that many Indian industries are now trying titania based catalysts as a substitute for their existing alumina or silica or zeolite based ones, but many are in a state of infancy in terms of implementation, presumably due to the non-availability of catalytic grade TiO_2 or manufacturing technologies in India and also due to the lack of systematic data dealing with anatase to rutile transformation, which may occur during the metal oxide loading. Most of the TiO_2 manufacturing companies are aiming only on the pigmentary properties. Also, most of the investigations found in literature were carried out on a commercially available imported TiO_2 , called Degussa p-25, which is a mixture of anatase and rutile. At this juncture, it thought worthwhile, to carry out investigation on some titania supported catalysts. For this purpose, high surface area TiO_2 (anatase) was prepared through controlled thermal hydrolysis of titanyl sulfate solution and some metal oxides were loaded on this TiO_2 in the amorphous state by ion exchange and wet-impregnation methods. Another method, called co-precipitation using hydrazine hydrate was also adopted to prepare the same catalysts to compare the properties. The details of the present investigation are presented in this thesis.

This thesis consists of 8 Chapters. The Chapter 1 deals with a detailed discussion about the importance of titania as a catalyst or support, preparation methods available, anatase to rutile transformation and metal – support – interactions in titania supported catalysts. The detailed experimental procedure adopted for the preparation of some titania supported catalysts and the various analytical and physical techniques employed are included in Chapter 2. The Chapters 3 to 7 deals with the results and discussion of titania prepared through thermal hydrolysis, NiO/TiO₂, Fe₂O₃/TiO₂, CeO₂/TiO₂ and V₂O₅/TiO₂ catalysts prepared through all the three methods described above and their catalytic activity studies respectively. Chapter 8 deals with the summary and conclusion. The references to the literature are given at the end of this thesis.

INTRODUCTION

Chapter 1

INTRODUCTION

1.1 General introduction

Titanium is the 9th most abundant element in the earth's crust and is the 4th most abundant structural element¹. Being highly reactive, it is never found in the metallic form in nature. It is always found combined with oxygen and other metal oxides. Since it falls in group IVB of the periodic table, it shows the characteristic valency of 4, but, in addition to this, di, tri and penta valent states are also reported in some compounds. Titanium forms oxides with all of the above-mentioned valencies, or to say more specifically, seven phases of its oxide exist with the general formula TiO_{2n-1} . As the value of 'n' increases from 4 to 10, the structure approaches more and more closely to that of rutile TiO_2 . Thus wide range of possible compounds and structures exist in the TiO system,² however, the dioxide is the most stable under ordinary conditions. Titanium minerals occurring in nature are ilmenite ($FeTiO_3$), rutile, anatase, brookite, perovskite ($CaTiO_3$), sphene ($CaTiSiO_5$) and geikielite ($MgTiO_3$).² Ilmenite is by far the most common and its reserves are wide spread through out the world including India. Indian ilmenite deposits are reported to be rich in TiO_2 content.¹

As the stable dioxide, TiO_2 exists in 3 polymorphs, corresponding to the naturally occurring mineral anatase, rutile and brookite respectively². Out of these, rutile is the thermodynamically most

stable form. Anatase and brookite are meta stable, which readily get converted to rutile on calcination at higher temperature.²

1.2 Industrial applications of TiO₂

Titania is one of the top 20 inorganic chemicals of industrial importance. Although it is used in some non-pigmentary applications, the chemical and industrial interests on TiO₂ are almost solely derived from its pigmentary properties. It has been used as a pigment from the very beginning of 20th century.³

The important properties of a pigment are i) opacity - the ability to opacify the medium to which it is applied or the surface on which it is dispersed, ii) hiding power - the power to obscure a background of contrasting colours either by absorption or by scattering, iii) tinting strength – the ability to lighten a colourant, iv) gloss - surface finish, v) chalking resistance - the resistance to the disintegration of organic binders, which results in the formation of powdery chalk or free pigment particles on the surface, etc. Most of the above mentioned properties are in some way or other, related to refractive index, particle size, surface area, etc. Better pigmentary properties are observed in the oxides having higher refractive index and surface area. Since anatase is highly photoactive compared to rutile, the disintegration of organic binder occurs in anatase based pigments in presence of u.v radiations or radiations having wavelength less than 400 nm. The coated surface becomes powdery and moves away by wind or rain there by exposing the underlying section for further attack, which leads to the fading of colour. For the same reason, anatase is reported to be ‘poor’ in some of the

pigmentary properties.³ Hence, anatase is usually preferred in interior paints, while rutile is preferred in exterior ones including enamels and emulsions. Since, both anatase and rutile have different physical properties, they cannot be substituted by each other, but in some applications both can be used.

In the manufacture of quality papers, anatase is preferentially used as a filler - to fill the crevices between the paper fiber and as opacifier and brightner, to improve smoothness and printability. Since it is a wide band gap semiconductor, it can absorb u.v light and emit radiations of higher wavelength, which is the main requirement for optical brightners.³ Its lower density compared to that of rutile reduces the problems in handling of the paper at wet stage. It is less abrasive due to its lower hardness (compared to rutile), which results in lower consumption of cutting blades used in paper industry.³

The high refractive index and chemical inertness make TiO_2 an ideal pigment for plastics. Even though some plastics are used in their natural colours, most of them are blended with pigment to obtain attractive colours, as well to opacify them. Addition of rutile confers resistance to u.v degradation. Anatase grade is used in textile industry for de-lustering of synthetic fibres.³ Addition of TiO_2 into ceramic materials improves their acid resistance and lowers the sintering temperature.⁴ It also finds application in rubber, cosmetics, soap, pharmaceuticals, printing ink, roofing granules, floor coverings,^{2&3} etc.

TiO_2 has found versatile applications in low as well as high temperature fields. Mesoporous TiO_2 electrodes are used in photovoltaic

applications.⁵ The microstructure of TiO_2 influences the photovoltaic response of the solar cell and thereby increases the overall efficiency of the system.⁵ It is hence regarded as an important electrode material for extensive applications in low cost solar cells⁶⁻⁸ and in electrochromics.⁹ In recent years, much effort has been focused towards the development of renewable energy conversion and storage devices. For economically and environmentally viable devices, the right choice of material is of crucial importance. An important material in this respect is TiO_2 , whose combination of semi conducting as well as chemical stability makes it a suitable candidate for use in rechargeable lithium batteries.¹⁰⁻¹⁴ Titania crystal lattice has the ability to accommodate charge in the form of small foreign ions, such as H^+ and Li^+ .¹⁵ These ions can be inserted and extracted from TiO_2 electrodes using an electric field as driving force through a process referred to as intercalation. The insertion of positively charged ions has to be balanced with an uptake of electrons to preserve overall charge neutrality.¹⁵ For practical devices, the extent, reversibility and speed of intercalation are of prime importance. A common way to meet these demands is by using nano-structured electrodes. The large effective surface area provides a concomitant large number of adsorption sites for the intercalating ions.¹⁵

Titania coatings have been studied for a wide variety of uses, such as antifouling, antibacterial, de-odourising agent and in wet type solar cells.⁶ Because of high refractive index, dielectric constant, good oil absorption ability, tinting strength and chemical stability, even under strongly acidic or basic conditions, TiO_2 is used in optical coatings, beam

splitters and in antireflection coatings.¹⁶⁻¹⁹ The fabrication and characterization of titania thin films have attracted the attention of many researchers.^{20&21}

In view of its chemical stability, high refractive index and high dielectric constant, it has also got applications in opto-electronic devices,²² optical wave-guides,²³ filters²³ and NO₂ gas sensors.²⁴ Because of its wide chemical stability and non-stoichiometric phase region, it shows different electrical characteristics with oxygen partial pressure, which makes it suitable for use in high temperature oxygen and humidity sensors in pure form or mixed with other metal oxides,²⁵⁻²⁷ with enhanced mechanical properties.²⁸ Titania based oxygen sensors can be used to monitor automobile engine performance and the feed back from the detector can control the air fuel ratio to give optimum low pollution performance.²

Titania nano particles are widely used for the preparation of micro porous membranes,²⁹ which are used for the separation, with or without chemical reaction.^{30&31} Layered hydrated titania (H₂Ti₄O₉.nH₂O) and some titanates can readily inter change with some alkali or alkaline earth metals,³²⁻³⁴ because of which they find application in ion-exchange materials. The possibility of using hydrated titania as an ion-exchange agent for treatment of liquid radioactive wastes from nuclear reactor installations and for the separations of uranium from seawater has also been reported.^{35&36}

Synthetic gems have been produced from rutile, since its refractive index is significantly higher than that of diamond, which makes

it a very spectacular gem.³⁷ Strontium titanate gems under various trade names, viz. Fabulite and Wellington, are available in the world market.² Gemstone grade SrTiO_3 was first developed at the National Lead Company in mid 1950s.³⁸

Titanates, like barium titanate, lead titanate, lead zirconate titanate (PZT), lead lanthanum zirconate titanate (PLZT), barium strontium titanate (BST), strontium bismuth titanate (SBT), etc have found applications in ultrasonic transducers, radio and communication filters, medical diagnostic transducers, stereo tweeters, buzzers, gas igniters, positive temperature coefficient sensors, ultra sonic motors, electro-optic light valves, thin film capacitors and ferroelectric thin film memories.³⁹ The wide applications of BaTiO_3 include multi player capacitor, thermistor, piezo electric actuator, non-linear resistor, thermal switch, passive memory storage device,⁴⁰ chemical sensor (due to its surface sensitivity to gas adsorption),⁴¹ etc.

Titania has gained much attention in catalyst industry due to its applications as a catalyst or catalyst support for metal or metal oxide catalysts used in heterogeneous catalysis including photo catalysis of industrially and environmentally important reactions. A brief outline is given in the succeeding section.

1.3 TiO_2 as a catalyst or support

Catalysts are those materials, which can accelerate or facilitate a particular chemical reaction, without undergoing any change or without being consumed in the process and hence it can be regenerated in its original form, but some times in a lower or higher oxidation state.

Photo catalysts can increase the rate of chemical reactions in presence of light, i.e. photochemical reactions. The major functions of a support are to provide higher surface area, better dispersion of active component over it, give thermal and mechanical stability, reduce the quantity of required active component for a particular reaction and there by to increase the overall efficiency of the catalyst, etc. Historically, a large number of processes have been based on heterogeneous catalytic systems. The ease of product isolation is the most attractive feature of heterogeneous catalysis.

Even before Berzelius coined the term 'catalysis' in 1836, human beings have used catalysts in the fermentation of drinks (wine) and preparation of food materials like cheese. All biological processes, in living beings, function through enzymatic (catalytic) processes. It is likely that even the very first organic molecules that formed on earth were produced by catalysis. During the last two centuries, the phenomenon of catalysis was slowly understood and exploited by mankind in many ways. The application of catalysis has improved the well being of human race and their quality of life. Today, catalysis plays a vital role or occupies the center stage in almost 95 % of all the processes in the chemical manufacturing, petroleum and other petrochemical industries.

Titania impregnated with metals like Pt, Rh, Ru or Ni was used in Fischer-Tropsch synthesis of hydrocarbon from CO and H₂.^{42&43} Titania impregnated with Pt was also reported for photo catalytic splitting of water to give hydrogen.⁴⁴⁻⁴⁶ The introduction of titania based catalysts

in commercial air pollution control equipment in Japan in 1970s⁴⁷ and the titania based single crystal electrode for solar energy conversions, which is considered by researchers working in the area of energy conversions as a promising method for harnessing sunlight into storable chemical energy,⁴⁸ were the major breakthroughs and landmarks in the field of titania based catalysis. Since then, it became most popular, economical, harmless catalyst of choice and subject of many scientific studies, which is mirrored in the multitude of literature and patents available in this area.

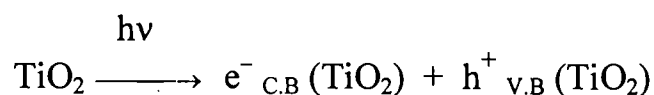
Pure TiO₂ is used as a catalyst in amination of methanol, isomerisation of 1-butene and β-pinene,⁴⁹ photo degradation of chlorinated hydrocarbons,⁵⁰⁻⁵² photolysis of water⁵³ and in degradation of organic pollutants.^{54&55}

Metals or metal oxides supported on TiO₂ are used as a catalyst in photo degradation of chloro fluoro carbons,⁵⁶ dichloro acetic acid,⁵⁷ partial oxidation of methane to synthesis gas,⁵⁸ ammonia synthesis,⁵⁹ methanation using CO,⁶⁰ hydro desulfurisation,⁶¹ reduction of NO_x,⁶² selective oxidation of o-xylene,⁵⁹ etc. Titania supported catalysts are reported to be highly active compared to conventional SiO₂ or Al₂O₃ supported ones.⁶³⁻⁶⁵ Titanium based Ziegler-Natta catalyst is extensively used in industry for the production of polyethylene and polypropylene with high degree of stereo regularity.⁶⁶⁻⁷¹ Titanium-β, a large pore Ti metal doped zeolite has shown to be an active catalyst for oxidation of branched and cyclic alkenes and alkanes using H₂O₂ or tert.butyl hydro peroxide, as the oxidant, with high selectivity. The activity is ascribed to the presence of titanium in the zeolite framework.⁷²⁻⁷⁴ In 1983, Enichem,

Italy, opened up an active research in the area of titano silicates⁷⁵ and is regarded as another milestone in heterogeneous catalysis including photo catalysis. The need for catalysts with large pore size and different coordination environment of the catalytically active titanium centers, recently led to the discovery of ETS-10 and ETS-4.^{76&77}

Heterogeneous semiconductor photo catalysis represents an emerging area of environmental catalysis,⁷⁸⁻⁸² with significant potential to detoxify noxious organic pollutants and reduction of heavy metal ions in industrial wastes,⁸³⁻⁸⁷ in an effective manner. A variety of semiconductor materials have been investigated due to the growing interest in the development of inexpensive and efficient methodologies to reduce environmental problems. Among the semiconductors, TiO₂ is the most frequently investigated one, due to its ability to degrade a variety of harmful organic pollutants including halogenated and non-halogenated ones, adaptability to work in a specially designed reactor system,⁸⁸ even in presence of solar u.v light⁸⁹ and due to its efficiency in the mineralisation of aquatic pollutants in a short time.⁸⁸

Photo irradiation of TiO₂ with photon energy greater than the band gap energy creates electrons and holes.^{90&91}



Consequently following the irradiation, the TiO₂ acts as either electron or hole donor to reduce or oxidize the materials present in the surrounding

media. These electrons and holes are responsible for the photochemical reactions taking place on the surface of TiO_2 . However, the photo induced charge separation in pure TiO_2 has a very short lifetime, because of the charge recombination (this would adversely affect the efficiency of the catalyst). Therefore a great deal of concerted effort has been focused to prevent charge recombination before a designated reaction occurs. One way to accomplish this is to scavenge photo generated electrons or holes with some other molecules, which are strongly adsorbed to TiO_2 surface.^{92&93} Extensive research is being carried out on utilization of solar energy much effectively for photoreactions by a technique called photosensitization, in which coloured metal oxides or dyes were doped or adsorbed on TiO_2 surface.⁹⁴⁻⁹⁶ However, the separation of TiO_2 following the photo catalytic process, is done by charge neutralization, coagulation and flocculation, which include an additional cost for chemicals and the requirement for crucial process control. These problems are minimized by immobilizing TiO_2 on to various substrates, such as glass beads, sand, silica gel, quartz, optical fiber and glass fiber in the form of mesh or on a glass reactor wall.⁹⁷ Titania coated magnetite is also reported with enhanced settling properties by applying a magnetic force, without the need for further down stream processes and there by reuse of photo catalyst is made easier.⁹⁸

Pollution prevention, rather than remediation, has the long-term value for improving the environment. The sustainable approach currently available is the development of new technologies for controlling the emissions of gaseous pollutants in to the atmosphere and the

discharge of effluent to the surrounding water body. For these purposes, catalysis and catalytic technology, especially titania based ones, hold the key to a range of less polluting processes and technologies, which can control both air and water pollution.

Although much has been learnt about catalysis during the past few decades, the level of understanding has not progressed to the point, where predictions based on first principles can be made. In particular, there is no real fundamental understanding of why a given substance is or not a good catalyst for a given reaction. Despite these limitations, major advances in catalytic technology are continuously emerging, as evidenced by many impressive applications of catalysis in industry.⁹⁹

1.4 Metal - support interactions in TiO₂ supported catalysts

Transition metal oxides offer an additional dimension for chemisorption compared to non-transition metal oxides in that, the number of electrons on the metal cations can be changed relatively easily. Also, it is often possible to reduce the surface of transition metal oxides to a lower oxide upon chemisorption, some thing that is generally impossible for non-transition metal oxides.¹⁰⁰ One of the most important driving forces for the study of metal - metal oxide surface interactions over the last few decades, or so, is due to their application in catalysis.

Much of the interest in metal on metal oxides stems from the observation that strong interaction may exist between small metal particles and their supports, when they are supported on reducible transition metal oxides in catalysts.

Since TiO_2 is a reducible catalyst support and its electronic structure is simpler than those of most of the other transition metal oxides, the majority of metal - support interaction studies were performed on TiO_2 .¹⁰⁰

There exists an extensive literature devoted to understanding the origin and nature of metal - support interactions and hence it would be very appropriate to briefly summarize these aspects in TiO_2 supported catalysts.

The original and perhaps the most striking observation of the metal - support interaction was the report that when Pt, Rh, Ru, Pd, Ir, Os, etc were supported on TiO_2 powders and when the catalyst was reduced at high temperature in hydrogen, the chemisorption behaviour of the metals changed drastically compared to that for the same catalyst not reduced at high temperature,¹⁰² where as these metals normally chemisorbed both hydrogen and CO at room temperature. Catalysts that had been reduced at high temperature would no longer adsorb either hydrogen or CO, although the original amounts of metals were still present on the catalyst support. This is due to the metal - support interactions. Tauster *et al*² called it as strong - metal - support interaction (SMSI). Subsequent heating of the catalyst in oxygen, at least, partially restored the normal chemisorption behaviour. A number of other dramatic changes in catalytic behavior would also be accompanied with the existence of SMSI state, but the hydrogen and CO chemisorption properties are the key ones and they are the ones that have been used by the majority of researchers to investigate SMSI.¹⁰⁰

One of the first speculations to the origin of SMSI was that the charge state of the catalyst metal was changed by the interaction with the electrons on the transition metal ions in the support; this different charge state then altered the chemisorption and catalytic properties of the supported metal.¹⁰⁰ For example, the studies on Na deposited on TiO₂ indicated that, Na adsorbed on TiO₂ ionically, donating its 3s electrons to the Ti⁴⁺ ions in TiO₂ and creating surface Ti³⁺ ions; hence, the Na - TiO₂ interaction is strong.³ Similarly, Ti deposited TiO₂ also showed electron transfer from Ti to empty 3d orbitals of Ti⁴⁺ ions of TiO₂, resulting in the creation of reduced Ti³⁺ species.¹⁰³ Like wise, in the case of Fe/TiO₂,¹⁰⁴ Ni/TiO₂¹⁰⁵ and Cu/TiO₂,¹⁰⁶ formation of Ti³⁺ species on the surface are also reported. In the case of Pt/TiO₂ and Rh/TiO₂, they are reported to be accepting electrons from Ti³⁺ ions at high temperature reduced state.^{107&108}

However, charge transfer from metal to support is insufficient to explain the phenomena and one of the other reason was the physical blocking of many of the catalytically active sites on the metal particles by lower oxides of the support, that had migrated on to the surface of the metal particles. This process is referred to as encapsulation or decoration. It ultimately proved to be the primary cause of SMSI, although there are still some unanswered questions about this effect.¹⁰⁰ Although encapsulation is the accepted explanation for most of the SMSI phenomena, it must necessarily be accompanied by electronic and bonding effects, which presumably constitute the driving force for the migration of lower oxides onto the metal particles.¹⁰⁰

It is evident from literature that, the chemical and physical interactions between metal particles and the support bring about changes in the morphology of the supported metal particles. It would affect their chemisorption behaviour and consequently the selectivity and activity of the supported catalyst. This type of interaction is reported to occur only in catalysts, especially TiO₂ supported group VIII metals reduced at high temperature (ca. > 500⁰C).¹⁰⁰ The literature also reveals that the high temperature reduction effect was different from metal to metal. It may be attributed to the characteristic properties of each metal, such as work function, Fermi level, electronic configuration,¹⁰⁰ etc.

1.5 Anatase to rutile transformation

A variety of solids exhibit transformation from one crystal structure to another as the temperature or pressure is varied. This phenomenon is known as polymorphism. As mentioned earlier, titania also exhibits polymorphism, i.e. it exists in three crystal modifications, viz. anatase, brookite and rutile.¹⁰⁹

Brookite is orthorhombic, while anatase and rutile are octahedrally coordinated tetragonal in structure. Brookite phase is very rarely formed under normal conditions, hence, most of the investigations reported in literature are focused on anatase and rutile, which have got different physical properties as illustrated in Table 1.1

The crystal structure of anatase and rutile are shown in Fig1.1A and 1.1B. In both structures, each Ti atom is surrounded by six oxygen atoms and each oxygen atom is surrounded by three Ti atoms and hence the formula TiO₂.³ It is apparent from Figs1.1A and 1.1B that,

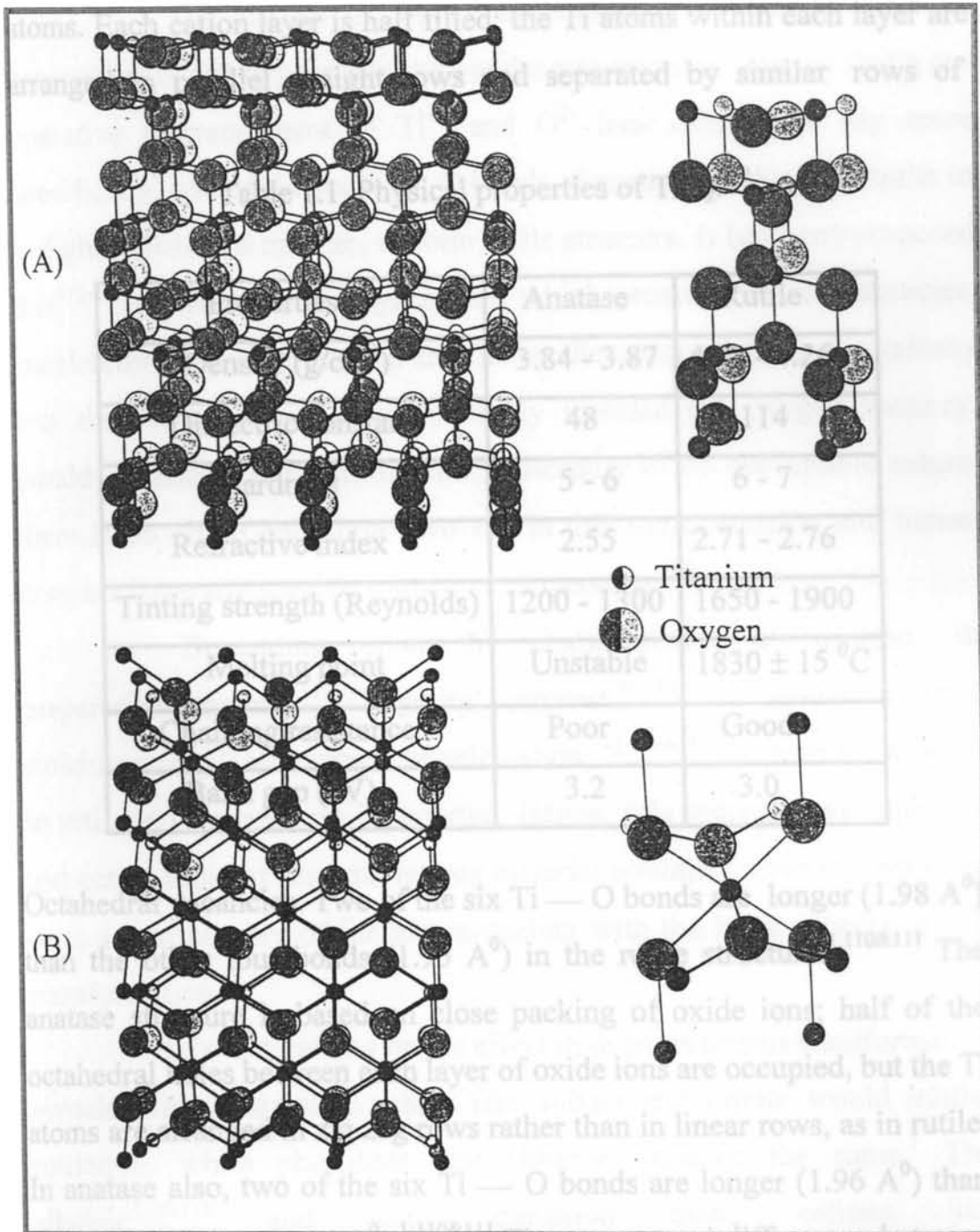


Fig. 1.1 Crystal structure of A) anatase and B) rutile

rutile structure consists of distorted hexagonal close packing of oxygen atoms. Each cation layer is half filled; the Ti atoms within each layer are arranged in parallel straight rows and separated by similar rows of

Table 1.1 Physical properties of TiO_2 .¹⁻³

Properties	Anatase	Rutile
Density (g/cm^3)	3.84 - 3.87	4.24 - 4.26
Dielectric constant	48	114
Hardness	5 - 6	6 - 7
Refractive index	2.55	2.71 - 2.76
Tinting strength (Reynolds)	1200 - 1300	1650 - 1900
Melting point	Unstable	1830 ± 15 °C
Chalking resistance	Poor	Good
Band gap (eV)	3.2	3.0

Octahedral vacancies. Two of the six Ti — O bonds are longer (1.98 \AA^0) than the other four bonds (1.95 \AA^0) in the rutile structure.^{1,110&111} The anatase structure is based on close packing of oxide ions; half of the octahedral holes between each layer of oxide ions are occupied, but the Ti atoms are arranged in zig zag rows rather than in linear rows, as in rutile. In anatase also, two of the six Ti — O bonds are longer (1.96 \AA^0) than that of the other 4 (1.94 \AA^0).^{1-110&111} These structural differences between anatase and rutile, make the transformation irreversible.

The anatase to rutile transformation involves an over all contraction of the oxygen structure and a movement of ions, so that a co-operative rearrangement of Ti^{4+} and O^{2-} ions occurs. To say more specifically, two of the six Ti — O bonds of anatase break and re-unite in a slightly distorted manner, to form rutile structure. It has been proposed that¹¹²⁻¹¹⁴ the removal of oxygen ions, which generates lattice vacancies, accelerates the transformation and hence, the cations, having the valency less than four, which correspondingly increase the oxygen vacancy, would enhance the transformation.¹¹² Because of its irreversible nature, there is no phase equilibria involved in this transformation and hence, does not have any specific transition temperature.¹⁰⁹

Depending upon the characteristics of anatase, its preparation method,¹¹⁵ impurity contents,^{110&115-120} deviation from stoichiometry,¹¹⁶ atmosphere of calcination,^{112-114&119} etc, a wide variation in rutilation temperature is reported. Hence, it is currently an important and active topic of research among material scientists, even though there exist a vast number of literatures dealing with the basic aspects of this transformation.

Investigations on the effect of dopants on this transformation revealed that, normally, anions like sulfate and nitrate would inhibit rutilation, while phosphate and chloride enhance the same.¹ The alkaline^{112&115} and some transition metal cations like Fe^{3+} ^{109,115,118,119,121&122} Cu^{2+} ^{112,115&123} Mn^{4+} ^{115,121&123} Co^{2+} ¹²¹ Ni^{2+} ¹²¹ Zn^{2+} ¹²⁴ etc are reportedly enhancing the transformation. Addition of

AlCl_3 enhanced rutilation by increasing the primary particle size and rate of sintering.¹²⁰ Dopants like SnCl_4 enhanced rutilation, since both tin and titanium are in octahedral coordination with oxygen and also due to the formation of SnO_2 with rutile structure during calcination, which in turn acts as rutile nuclei.¹²⁰ According to Diing *et al*,¹²² SnO_2 enhances rutilation by reducing either the onset temperature or the transformation temperature range. Most of the authors unanimously agreed^{112,114,115,118&119} that the enhancement or inhibiting effect of additives is dependent on their ability to enter TiO_2 lattice, there by creating oxygen vacancies or interstitial Ti^{3+} ions respectively. The colour change observed in pure anatase during rutilation is an indication of oxygen loss to form lattice defects.¹ These lattice defects act as colour centers.¹¹⁴

Studies on the effect of various atmospheres have shown that in vacuum conditions, the transformation was inhibited due to the presence of interstitial Ti^{3+} ions.^{112&114} Lida *et al*¹²¹ have reported that the transformation rate was increased in hydrogen atmosphere due to the formation of oxygen vacancies. Similar observations were put forward by many authors.^{112,113&114} Gennari *et al*^{118&119} claimed an enhanced rutilation in presence of Fe_2O_3 in air, and chloride atmospheres. In general chemically reducing atmosphere enhances the transition by formation of oxygen vacancies in the anatase lattice, which in turn favours the rupture of $\text{Ti} - \text{O}$ bonds necessary for crystallographic rearrangement.^{112,114&123}

Significant grain growth has been reported in TiO_2 during this transformation by different authors.^{114-118&121-126} Mackenzie *et al*¹²⁶ have shown that those reaction atmospheres, which favour the formation of rutile also favour the particle growth. Yoganarasimhan and Rao¹¹⁶ claimed a marked increase in crystallite size and particle size in the region of transformation due to the expansion of unit cell of anatase prior to the transformation. According to them smaller particle size and larger surface area would favour the transformation. Rao¹²⁷ classified this transformation under nucleation and growth mechanism. Gamboa *et al*¹¹⁴ also agreed with this mechanism. Reddy *et al*¹²⁸ demonstrated that the formation of gaseous TiCl_4 is responsible for TiO_2 grain growth occurring at a faster rate in chloride atmosphere than in air. Nobile jr¹²⁵ concluded by his studies on iron doped TiO_2 that the TiO_2 grain growth and rutilation are simultaneous processes and are inter-related. He argued with the support of a mechanism that, the Ti^{3+} ions formed on the surface of TiO_2 were responsible for enhancement of rutilation. Many authors.^{112,116,118&123} also investigated the kinetics of anatase to rutile transformation.

In spite of large number of literature available on this transformation, there is no systematic data available dealing with anatase to rutile transformation in presence of different percentages of dopants prepared under different methods. Also most of the studies were carried out by impregnating the metal ions on to crystalline TiO_2 and in some cases,^{109,118,119&125} a smaller percentage of rutile was already present in

TiO₂ even before loading metal oxides. All these would undoubtedly affect the investigation.

1.6 Literature survey

A thorough survey of the literature shows that titania supported catalysis is an emerging field with multiple applications, which is reflected in the availability multitude of patented and other literature. A great deal of concerted effort has been directed towards synthesizing TiO₂ with better properties, which make it suitable to use as catalyst by itself and as a support for various other metal and metal oxide catalysts.

A number of studies have been carried out using TiO₂ based catalysts, out of which some of the important typical applications are only given in the succeeding sections.

1.6.1 Reactions carried out over titania supported catalysts

1.6.1.1 Hydro de-sulfurisation (HDS)

The removal of sulfur from sulfur containing feedstock, as H₂S is known as hydro de-sulfurisation, which is an important process used in petroleum industry and is one of the most widely studied branches of catalysis. The most common catalysts employed are molybdena-alumina catalyst.¹²⁹ Molybdena supported on TiO₂ is reported by a few researchers¹³⁰⁻¹³² for this reaction. It has been shown that at low molybdena loading, titania supported catalysts are more active than alumina supported ones. Takeuchi *et al*^{133&134} reported HDS of thiophene in naphtha on Ni-Mo-TiO₂ catalyst and is reported to be more active than alumina supported ones. Matsuda *et al*¹³⁵ used MoO₃/TiO₂ catalyst for H₂S adsorption and removal from waste gas streams or from natural gas.

The important advantage, they claimed was that, the adsorbent can be regenerated easily by passing oxygen through the adsorbent bed. One of the important advantages of TiO₂ based catalyst in commercial HDS processes is that, usually, a commercial HDS catalyst is sulfided prior to use, but TiO₂ based catalyst showed a high activity without pre-sulfidation.

1.6.1.2 Partial oxidation (Selective oxidation)

Partial oxidation is an interesting and promising approach for producing synthesis gas from methane and oxygen or air to give hydrogen and CO with a ratio suitable for Fischer-Tropsch synthesis and methanol synthesis. Ir/TiO₂ is reported to be a better catalyst for this reaction.¹³⁶

The effect of TiO₂ supported catalysts in selective catalytic oxidation of hydrocarbons is currently a topic of investigation. There have been numerous investigations on V₂O₅/TiO₂ catalysts. This catalyst was reported for selective oxidation of furan to maleic acid.¹³⁷ The selectivity was determined by the number of V₂O₅ layers on the support. A high selectivity was reported with five layers of V₂O₅ over TiO₂.¹³⁷ V₂O₅/TiO₂ possess high activity and selectivity in processes of industrial importance, such as, oxidation of o-xylene¹³⁸⁻¹⁴² and naphthalen¹⁴³ to phthalic anhydride. Buta diene¹³⁸ and benzene^{144&145} to maleic anhydride, oxidative ammonolysis of various hydrocarbons¹⁴⁶⁻¹⁴⁸ are also reported over this catalyst. Reddy *et al*¹⁴⁹ reported that, this catalyst is quite superior to other alternatives due to their high activity and resistance to SO₂ poisoning. It is generally accepted that the active phase is the

vanadia part of the catalyst and the most appropriate support is anatase.¹³⁹⁻¹⁴² Many scientists, to explain the unique activity of this catalyst, put several hypotheses forward. Thus, Vejux and courtine¹⁵⁰ have noted that the crystallographic fitting between the (010) face of V_2O_5 and the prevailing anatase planes (001), (100) and (010). Thus there is a possibility of epitaxial growth of V_2O_5 during its deposition with predominant exposure of the (010) vanadia face, characterized by the presence of $V = O$ groups¹⁵¹ and these groups are responsible for the enhancement of selective oxidation.¹⁵¹ Bond *et al*¹⁵² supposed that at low vanadia content, isolated tetrahedral hydroxo vanadyl groups are formed. The peculiar catalytic properties of this catalysts are due to the joint effect of an easily reducible $V = O$ bond and an acid hydroxyl group from the same active centers.¹⁴¹ Spectroscopic studies of sub monolayer coverages of vanadia on titania have shown that the dispersed vanadia is present as a combination of monomeric vanadyl and polymeric vanadate species,¹⁵³⁻¹⁵⁷ with distribution of both these structures varying with vanadia loading¹⁵⁷ and when the vanadia loading was raised above the dispersive capacity of the titania support, crystallites of V_2O_5 were formed.^{154-156&158}

V_2O_5 supported on TiO_2-ZrO_2 ¹⁵⁹ or TiO_2-SiO_2 ¹⁴⁹ mixed oxides was also proposed for the improved selective catalytic oxidation reactions. Murakami *et al*¹⁴⁴ and Inomata *et al*¹⁴⁵ reported the benzene oxidation over titania and alumina supported ones with the following order $V_2O_5/TiO_2 > V_2O_5 > V_2O_5/Al_2O_3$ and the activation energy for this reaction on V_2O_5/TiO_2 was reported to be much smaller (ca. 80 KJ/mol)

than that on unsupported V_2O_5 (ca. 92 KJ/mol) or on V_2O_5/Al_2O_3 (ca.120 KJ/ mol). These data indicate the promoting effect of TiO_2 support. In spite of the catalyst containing V_2O_5 on titania has been the subject of considerable interest due to its successful application in selective catalytic oxidation reactions; the nature of active species taking part in the reaction is still controversial.

1.6.1.3 Carbon monoxide hydrogenation

Catalytic hydrogenation of CO is a profoundly important reaction widely exploited by many chemical industries for the production of gasoline, alcohol, methane and other higher hydrocarbons. This reaction for the synthesis of long chain hydrocarbon is referred to as Fischer-Tropsch synthesis. Group VIII metals supported on silica, alumina or titania are generally used.¹⁶⁰ But depending on the metal used, the product would be different. The selectivity of this reaction varied with support material.¹⁶¹

Carbon monoxide hydrogenation using Fe/TiO_2 catalyst led to the formation of methane.¹⁶²⁻¹⁶⁴ While Rh/TiO_2 gave methanol and other hydrocarbons.⁶⁰ Methane was reported to be formed over Ni catalyst.¹⁶⁰ Sebatier won Nobel prize in 1912 for the successful production of methane over unsupported Ni catalyst.¹⁶⁰ Sen *et al*¹⁶⁵ and Vannice *et al*^{43&166} reported Ni/TiO_2 catalyst with better activity for methanation than unsupported one and Ni/SiO_2 . Smith *et al*¹⁶⁷ also strongly supported the above observation.

The CO and hydrogen chemisorption behaviour of Ni/TiO_2 was investigated by many researchers.¹⁶⁸⁻¹⁷⁰ The chemisorption was

reported to be decreasing in the catalyst reduced at high temperature (ca. > 500°C). The peculiar behaviour of this catalyst was due to SMSI as discussed earlier, which was induced during high temperature reduction.¹⁶⁸ The titania moieties migrated to the Ni surface during reduction would reduce the sticking coefficient of CO adsorption.^{168 & 170} So, it is very clear that the rate of CO adsorption is strongly dependent on the support material^{43&167} and change of support would change the rate of CO hydrogenation.^{43&167} Rabo *et al*¹⁷¹ investigated the methanation using Ni over a range of supports and made a conclusion that the specific activity for hydrogenation would be in the order Ni/TiO₂ > Ni/Al₂O₃ > Ni/SiO₂-Al₂O₃ > Ni/SiO₂.

Many researchers have reported, high activity in CO hydrogenation to synthesize gasoline, over alloy catalysts, like 42Ni29Fe29Co and 50Co50Ni supported on TiO₂.¹⁷²⁻¹⁷⁵

1.6.1.4 Selective catalytic reduction of NO_x (SCR)

The emission of NO_x from power plants, nitric acid plant and from other industries caused serious environmental problem. So, the removal of NO_x is particularly important from a standpoint of pollution control.

Selective catalytic reduction using NH₃ is the most commonly used method to abate NO_x emission and was commercialized in recent years.⁴⁷ By the end of 1982, about hundred plants have been constructed and are operating in Japan.⁴⁷ In early stages of development of the NO_x reduction process, several base metal oxide catalysts, such as

Fe, Fe-Cr and Fe/Al₂O₃, were reported⁴⁷ with high activity. These catalysts, however, lost their activity in a few hundred hours, due to SO_x poisoning, which was present along with NO_x. Hence, the commercialization of SCR of NO_x was not realized until the advent of TiO₂ based catalysts, which are resistant to sulfur poisoning and were reported to be maintaining their activity for more than five years.⁴⁷ So, now, TiO₂ has become a catalyst support of choice for this reaction. A number of Japanese^{176&177} and US¹⁷⁸ patents available on TiO₂ based NO_x reduction catalyst disclose this fact more clearly.

The SCR catalysts are mainly composed of TiO₂ and the second component selected from V₂O₅, MoO₃, Fe₂O₃, CoO, NiO, MnO₂, Cr₂O₃, CuO, etc. On the whole, a catalyst composed of TiO₂ and one of the n-type semiconductor (V₂O₅, MoO₃, Fe₂O₃, etc) showed high activity for NO - NH₃ reaction, while a catalyst composed of TiO₂ and one of the p-type semiconductor (CoO, NiO, etc) showed high activity for NO₂ - NH₃ reaction.⁴⁷ But, NO₂ - NH₃ reaction was also reported on V₂O₅/TiO₂ catalyst.¹⁷⁹ A large number of literatures are available on the investigation of the surface structure of V₂O₅/TiO₂ catalyst and its NO_x reduction capacity.¹⁸⁰⁻¹⁹⁴ The high activity of this catalyst is attributed to the nature of the adsorption sites on the catalyst surface.

Inomata and co-workers¹⁸⁰⁻¹⁸³ found that the sites responsible for the catalytic activity of bulk as well as supported vanadia towards the NO - NH₃ reaction in presence of oxygen are the V⁵⁺=O groups, whose concentration is directly related with activity. On the basis of isotopic transient studies Janssen *et al*^{184&185} proposed dual site

mechanism for this reaction with the participation of two neighbouring $V^{5+}=O$ species as active sites. On the other hand, Gasier *et al*¹⁸⁶ concluded that not the $V=O$ species, but the acid hydroxyl group, i.e. $V-OH$ group, present on vanadia surface could be the active site. But, Topsoe *et al*¹⁸⁷ noted that the $V=O$ species are also involved in this reaction along with $V-OH$ group. Some others believe, on the contrary, that an amorphous disordered multiple layers of V_2O_5 are present on the whole surface.^{183,188&189} Isolated monovanadate structures have been detected at low vanadia coverage on SiO_2 , Al_2O_3 , TiO_2 , ZrO_2 and HfO_2 supported vanadia catalysts by some authors.^{154,190&191} According to them, VO_x species condense into chain or 2D domains and ultimately into bulk V_2O_5 crystallites as VO_x loading was increased. Eckert *et al*¹⁵⁵ and Coustemer *et al*,¹⁹² by spectroscopic studies revealed that V^{5+} centers evolve from tetrahedral coordination at low coverage to octahedral coordination at higher coverage on TiO_2 and Al_2O_3 . In spite of these investigations on this catalyst, there is still no agreement on the nature of the active sites and the mechanism of the NO_x reduction process,¹⁹³ but, it is generally accepted that the vanadia part of the catalyst is essential for this reaction.

1.6.1.5 Coal liquefaction

Concern about the supply of clean burning fuels has stimulated interest in coal liquefaction process. The conversion of coal to liquid fuel involves increasing the hydrogen content of the material. In the liquefaction process it is not sufficient to break down the coal

structure into the basic condensed ring units, but it must be broken to yield a product that is liquid at room temperature.⁹⁹

Tanabe *et al*¹⁹⁵ reported direct hydrogenation of coal using various metal oxides catalysts, including TiO₂ based ones, such as, MoO₃/TiO₂ and Fe₂O₃/TiO₂. Hydrogenation of coal was carried out under a pressure of 100 Kg/cm³ and a temperature of 400⁰C. The ratio of benzene soluble fraction from hydrogenated coal reached 68% for MoO₃/TiO₂ compared to 51% for MoO₃/SiO₂. These results suggest that TiO₂ is not only acting as a support, but also promoting the hydro cracking activity.

1.6.1.6 Ammonia synthesis

The gas phase equilibrium reaction between hydrogen and nitrogen to form NH₃ is well known to chemists as the basis of the famous Haber - Bosch process, which represents the typical example for a heterogeneously catalyzed reaction. Practical catalysts are multifunctional catalysts, which consist mainly of the reduced form of Fe₃O₄ doped with small percentage of Al₂O₃, K₂O, CaO, SiO₂ and MgO.¹⁶⁰

Aika *et al*,¹⁹⁶ who studied the ammonia synthesis over Ru supported on several supports, found the activity to depend strongly on the type of support used. These authors attributed this to variations in the electronic interaction of the metal with the support. Sueiras *et al*¹⁹⁷ also support this conclusion.

Santos *et al*,^{65&198} who studied ammonia synthesis over Fe/TiO₂ catalyst found that a small degree of surface poisoning by titania

caused a drastic decrease of activity. Nobile jr⁵⁹ investigated the kinetics of NH₃ synthesis over Fe/TiO₂, hydrazine pre treated Fe/TiO₂, K or Cs promoted Fe/TiO₂. The pre-treatment of Fe/TiO₂ catalyst with hydrazine increased the ammonia synthesis turn over frequency by more than an order of magnitude than untreated one, because of inhibition of onset of Fe - TiO₂ interaction by hydrazine. Alkali promotion also increased the activity.

1.6.1.7 Isomerization

Hattori *et al*^{199&200} and Itoh *et al*²⁰¹ reported the isomerization of butene over TiO₂ and TiO₂/SiO₂ catalyst. Maximum activity was obtained for a catalyst with 9:1 TiO₂: SiO₂ composition. The acidic properties are reported to be responsible for the activity.¹⁹⁹⁻²⁰⁵ Some authors²⁰¹⁻²⁰³ also reported the isomerization of 1-butene and β-pinene over pure TiO₂.

Sohn *et al*²⁰⁴ investigated the isomerization of 1-butene to cis and trans 2-butene over NiO/TiO₂ catalysts modified by anions like SO₄²⁻, PO₄³⁻, SeO₄²⁻ and BO₃³⁻ and showed the order of activity NiO-TiO₂/SO₄²⁻ >> NiO-TiO₂/PO₄³⁻ > NiO-TiO₂/BO₃³⁻ > NiO-TiO₂/SeO₄²⁻ > NiO-TiO₂. According to them the higher activity of SO₄²⁻ modified one is due to the improved acidic properties of this catalyst. Similar was the order of activity for ethylene dimerization carried out using these catalysts.^{204&205}

1.6.1.8 Carbon monoxide oxidation

Carbon monoxide oxidation to CO₂ is an extremely important reaction from environmental point of view, since this reaction is applicable in automotive exhaust decontamination. This reaction is

readily catalyzed by transition metals, particularly Pt group metals. The CO oxidation can be performed on Pt catalyst supported on either Al_2O_3 or TiO_2 .⁴⁷ If the reaction gas contains even trace amount of SO_x , Pt/ Al_2O_3 catalyst is deactivated in short time. A drastic decrease in specific surface area and pore volume takes place, resulting from the formation of aluminium sulfate.⁴⁷ An advantage of using TiO_2 based catalyst, is that it is resistant to SO_x poisoning. Matsuda *et al*⁴⁷ made this conclusion by investigating CO oxidation in presence and absence of SO_2 over Pt/ TiO_2 , Pd/ TiO_2 and Ru/ TiO_2 . An inhibition of the reaction due to the presence of SO_2 was observed with all the catalysts. The effect, however, was smallest in the case of Pt/ TiO_2 , which had maintained its initial activity even in presence of 500 ppm SO_2 for a longer period.

Tanaka and White²⁰⁶⁻²⁰⁸ studied, in detail, the CO adsorption and CO_2 dissociation on Pt/ TiO_2 catalyst. Akubuiro *et al*²⁰⁹ carried out the kinetic study of this reaction over Pt/ TiO_2 . Lane and Wolf²¹⁰ investigated the effect of TiO_2 crystal phases on this reaction over Pt/ TiO_2 catalyst. They convincingly argued that, the crystalline form of support plays dominant role in determining the activity, where as the reduction temperature plays only a minor role. After low (200°C) or high (500°C) temperature reduction, the rutile supported Pt exhibited greater activity than SiO_2 or anatase supported ones. Though the reason for this better activity of rutile supported one was not clear, a speculative oxygen transfer mechanism from the support is presented (here the rutile support acts as an oxygen source and provides a means for oxygen transfer to the adsorbed CO). These authors argued that the rutile support tends to give

up its oxygen, more freely, since it has 19 Kcal/mole lower energy for oxygen desorption compared to anatase.²¹⁰

1.6.1.9 Miscellaneous

Metals or metal oxides supported on TiO₂ are reported⁵⁶ to be used in catalytic conversion of chloro fluoro carbon (CFC). By considering the hazardous nature of CFC, this reaction is of vital importance. Pd/TiO₂, CeO₂/TiO₂, La₂O₃/TiO₂, Pt/TiO₂, NiO/TiO₂ and CoO/TiO₂ were the catalysts used.⁵⁶

Enantio selective hydrogenation of prochiral C = C bonds using heterogeneous chiral catalyst is a challenging subject in organic synthesis. (E)- α -phenyl cinnamic acid was hydrogenated to yield (S)-(+)-2,3-diphenyl propionic acid on cinchonidine modified Pt/TiO₂ catalyst, with much higher optical yield than palladium supported on activated carbon.²¹¹⁻²¹⁴

Ir/TiO₂ is reported for hydrogenation of n-butane and 2,2, dimethyl propane.²¹⁵ The same catalyst was reported for partial oxidation of CH₄ to synthesis gas (CO and H₂).¹³⁶

Catalytic oxidation process plays an important role in the industrial production of fine chemicals and several other commodities. Propylene oxidation to acrolein is reported²²⁰ over Fe-Sb-Ti mixed oxide catalyst with higher activity. Liquid phase epoxidation of olefins is known to proceed in the presence of hydro peroxides as oxidant over catalytic system that contain titanium.²¹⁷

Micro porous crystalline titanate silicates are another class of titanium containing catalysts, which are reported to be catalyzing the

oxidation of unsaturated hydrocarbons with aqueous H_2O_2 , oxidation of alcohols to ketone, hydroxylation of aromatic hydrocarbon and amines to oxime.²¹⁷ Another titano silicate,⁷⁴ called titanium- β , is a suitable catalyst for oxidation of branched and cyclic alkenes in presence of organic hydroperoxides with high selectivity. The development of titano silicalites,²¹⁷ which are ZSM type molecular sieves, are interesting due to their hydrophobic nature, which favours the diffusion of non-polar substrates to the active sites. The hydrophobic micro pores of this catalyst are assumed to exclude water from its voids and thus protect the catalyst from deactivation.

1.6.1.10 Photo catalysis

It has been recognized that TiO_2 is the most efficient photo catalyst for many industrially and environmentally important reactions.⁸¹ Photooxidation of salicylic acid is reported by Dagan *et al*⁵⁵ on pure TiO_2 . Photo decomposition of tri chloro acetic acid and CHCl_3 over TiO_2 were reported by Wang *et al*.²¹⁹ Reductive dehalogenation of 1,1,2- tri chloro fluoro ethane (CFC113) took place upon illumination of air free suspension of TiO_2 containing formate ions.⁵² Photo reduction of CCl_4 and CHBr_3 occurred in suspensions of TiO_2 .^{220&221} Kutty *et al*⁵⁴ studied the photo degradation of phenol over nano sized TiO_2 (anatase) powder.

Kominami *et al*^{222&223} put forward a couple of conditions to obtain better photo activity, viz. titania should necessarily possess large surface area to adsorb substrates and high crystallinity to diminish electron - hole recombination. They investigated the photo mineralization of acetic acid in presence of air. They claimed better activity for their

catalysts prepared by hydrothermal crystallization in presence of organic solvents, compared to commercially available Degussa p-25 and Ishihara ST-01.

The photo degradation of metal - EDTA complexes, especially that of Cu, Fe and Zn over TiO_2 were studied by Kagaya *et al.*,²²⁴ with complete removal of metal ions. This reaction is profound in the treatment of industrial effluent containing metal ions. Photo oxidation of mono chloro acetic acid and pyridine in presence of oxygen and ozone over TiO_2 were reported with activity and much lower specific energy consumption in presence of ozone.²²⁵

Lee *et al.*⁵¹ carried out the photo degradation of 1,4 - dichloro benzene. Rutile was reported by Sopyan *et al.*²²⁶ for the photo oxidative decomposition of gaseous acetaldehyde. Muneer *et al.*²²⁷ studied the photo degradation of acid blue 40, a textile dye, in aqueous suspension of TiO_2 . Addition of some anions, like SO_4^{2-} and PO_4^{3-} enhanced the photo degradation of paraquant, a very toxic herbicide.^{228&229}

Iron doped TiO_2 is reported for photo reduction of molecular N_2 , which has ecological significance and is a part of natural N_2 -cycle.²³⁰ $\text{Fe}_2\text{O}_3/\text{TiO}_2$ mixed oxide catalyst was found to be used in photo detoxification of water containing dichloro acetic acid.⁵⁷ Titania supported on SiO_2 or Al_2O_3 is reported for photo decomposition of salicylic acid and phenol²³¹ with improved activity than pure TiO_2 . Titania species anchored within the micro pores of Y-zeolite and meso porous zeolites exhibited a high and unique photo activity for the reduction of CO_2 with water at 55°C ,^{232&233} which is known as reductive

fixation of CO₂. The titano silicalite is used for the photo decomposition of NO into N₂, O₂ and N₂O at 22⁰C.²³⁴ Photo degradation of acetophenone in aqueous medium is reported by Xu *et al*²³⁵ on TiO₂ supported on micro porous zeolite X and Y and on meso porous molecular sieves. Titanium exchanged clays are reported for photo degradation of dichloro methane with improved activity than pure titania.²³⁶

1.6.2 Preparation methods

Some of the important methods adopted to prepare TiO₂ based catalysts are presented below.

1.6.2.1 Sol - gel method

The sol - gel method has emerged an important means of preparing inorganic metal oxides in recent years. It is a wet chemical method and a multi step process involving both chemical and physical processes such as hydrolysis, polymerization, drying and densification. The name sol - gel is given to this process because of the distinctive increase in viscosity, which occurs at a particular point in the sequence of steps. A sudden increase in viscosity is a common feature in sol - gel processing indicating the onset of gel formation. Usually, metal alkoxides are used as precursors.²³⁷

Vorkapic *et al*²³⁸ prepared titania nano particles by this method. To prepare titania sol, a specific amount of HNO₃ was mixed with pure distilled water/alcohol mixture in a glass bottle and placed in a temperature-controlled bath. Temperature was raised gradually with stirring and titanium tetra alkoxide (ethoxide, propoxide or butoxide) of desired quantity was added drop wise. The hydrolysis and condensation

reactions were started immediately upon mixing. The samples obtained were calcined at desired temperatures. They also reported that the particle size of titania was decreased with increasing the length of alkoxy group.

Pure titania films were prepared by mixing titanium tetra isopropoxide, which was dissolved in ethanol with acidified water at room temperature.²³⁹ Similarly, titanium tetra ethoxide was also used as precursor by Yanagisawa *et al.*²⁴⁰ Inoue *et al.*²⁴¹ synthesized amorphous titania gel by slowly adding methanol containing TiCl_4 solution to a mixed solution of NH_4OH , methanol and water at room temperature. The surface area obtained was ranging between $62.3 \text{ m}^2/\text{g}$ to $76.9 \text{ m}^2/\text{g}$.

Wang *et al.*²¹⁹ described a modified type of sol - gel hydrolysis precipitation of titanium tetra isopropoxide, followed by hydrothermal treatment. The as prepared gel was amorphous. In hydrothermal treatment, the gel was directly subjected to crystallization at $80^\circ\text{C}/24\text{hrs}$ or $180^\circ\text{C}/96\text{hrs}$. Dagon *et al.*⁵⁵ described acid catalyzed sol - gel method. The sol was prepared by mixing titanium tetra isopropoxide with anhydrous ethanol, water and HNO_3 at room temperature with stirring. A series of gels with a constant molar ratio of 1: 0.08 between titanium tetra isopropoxide and acid with different alcohol and water contents were prepared. The surface area of annealed sample was between $65 \text{ m}^2/\text{g}$ and $188 \text{ m}^2/\text{g}$.

Masson *et al.*²⁴² prepared titania aero gel by supercritical evacuation of solvent from gels prepared through hydrochloric acid controlled hydrolysis - condensation reactions of titanium tetra isopropoxide in isopropanol. The aero gel formed was anatase with

prismatic shape. Kundu and others¹⁶³ investigated preparation of Fe₂O₃/TiO₂ mixed oxide through sol - gel method. A sol of titania was prepared by hydrolysis of titanium tetra isopropoxide in acetic acid and ethanol, stirred for 1hr. Another solution of FeCl₃.6H₂O in water was added to the above mixture. The solution was stirred and kept at room temperature for gelation. It was finally calcined at different temperatures.

Beydoun *et al*⁹⁸ used this method for preparing titania coated magnetite photo catalyst with improved separation properties. This method involved the hydrolysis of titanium tetra iso butoxide in presence of magnetite particles, resulting in the deposition of titania layer on to the surface of the magnetite particles. Anderson *et al*²³¹ prepared TiO₂/Al₂O₃ photo catalyst by sol - gel method, using titanium tetra isopropoxide and aluminium tri isopropoxide. Similarly, TiO₂/SiO₂ was prepared by Kim *et al*²⁴³ using tetra ethyl orthosilicate instead of aluminium tri isopropoxide.

1.6.2.2 Ion-exchange method

Only a very few literature is available on this method for preparing TiO₂ supported catalysts. Arunarkavally *et al*²⁴⁴ used this method for the preparation of Ni/TiO₂ catalyst. Titania (Degussa p-25) was refluxed at 100⁰C for 20hrs in an ammoniacal solution of nickel nitrate at pH 11. After the blue solution turned clear, the mixture was filtered hot and dried at 100⁰C. Similarly Espinos *et al*²⁴⁵ prepared the same catalyst by using TiO₂ (Aerosil p-25) and nickel nitrate at pH 11.5. Here the ion-exchange was carried out at 25⁰C for 120hrs.

1.6.2.3 Wet-impregnation method

This is the most common method found in literature for preparing TiO₂ supported catalysts. Nagakawa *et al*¹³⁶ prepared Ir/TiO₂ by this method using an aqueous solution of iridium tetra chloride and titania. Rh/TiO₂⁶⁰ was prepared by adding TiO₂ (Degussa p-25) in to an aqueous solution of RhCl₃.3H₂O. The slurry was dried over night at 40⁰C.

Ng and Gulari⁶¹ impregnated molybdena on TiO₂ (Degussa p-25) from an aqueous solution of ammonium hepta molybdate. Surface area ranging between 37 m²/g and 45.3 m²/g was obtained. Takita *et al*⁵⁶ reported a series of TiO₂ supported metal catalysts for catalytic conversion of CFC. The metals were impregnated to hydrous titania from an aqueous solution of respective metal nitrate, the water was evaporated to dryness and then calcined at 500⁰C for 5hrs. But they have not made any detailed investigations on the phase changes of titania and there is no mention about the surface area. Instead, they concentrated only on the activity and product selectivity.

Vanadia supported on titania catalyst was prepared by Satsuma *et al*.²⁴⁶ by impregnating V₂O₅ from a solution of ammonium meta vanadate in nitric acid or oxalic acid solution on TiO₂. Two types of TiO₂ were used as support, viz. JRC TIO-3 (rutile with surface area 49.5 m²/g) and JRC TIO-4 (> 60 % anatase with surface area 50.1 m²/g). Surface area after loading V₂O₅ was ranging between 36 m²/g and 45 m²/g. The samples prepared from an oxalic acid solution of ammonium meta vanadate showed much higher activity in selective oxidation of benzene to maleic anhydride. Kancheve *et al*¹⁷⁹ prepared the same

catalyst by adsorption of VO^{2+} ions from a solution of ammonium meta vanadate in nitric acid at pH 0.5 on TiO_2 (Degussa p-25). Went *et al*²⁴⁷ described an impregnation method in which they have prepared TiO_2 by hydrolysis of titanium tetra isopropoxide in water. The TiO_2 formed was 95% anatase and 5% brookite. V_2O_5 was impregnated using vanadium oxalate solution. Surface area obtained was $28 \text{ m}^2/\text{g}$ to $79 \text{ m}^2/\text{g}$.

In a series of cases $\text{V}_2\text{O}_5/\text{TiO}_2$ was prepared by impregnation of VOCl_3 ,^{152&248-250} $\text{VO}(\text{OiBu})_3$ ^{152&248-251} and $\text{VO}(\text{acac})_2$ ^{152,252&253} on titania. But these methods need completely non-aqueous media, hence are much complicated.

Georgiadou *et al*²⁵⁴ described a modified type of impregnation and they called it as equilibrium deposition filtration method (EDF). Here the anatase powder was added to ammonium meta vanadate solution, the pH of the suspension was regulated using nitric acid or ammonium hydroxide and then stirred the suspension for 20 hrs at 25°C . It was then filtered and calcined at different temperatures. The samples were prepared at different pH, viz. 4.5, 6 and 8. The decrease in pH caused an increase in the amount of vanadia deposited on TiO_2 surface. Similar method was found to be used by Kim *et al*²⁵⁵ for preparing $\text{MoO}_3/\text{TiO}_2$. Molybdena was adsorbed on TiO_2 (Degussa p-25) from a solution of ammonium hepta molybdate under different pH conditions. At 3.98 pH, monolayer coverage of MoO_3 was obtained and at more acidic pH, crystalline MoO_3 was formed over monolayer.

Lane and Wolf²¹⁰ impregnated Pt on TiO_2 (Degussa p-25) by using chloro platinic acid. Courbon *et al*²⁵⁶ prepared Pt/TiO_2 and

Ni/TiO₂ by adding desired quantities of hexachloro platinum acid and nickel hexamine nitrate respectively to a stirred suspension of TiO₂ (Degussa p-25), which was subsequently evacuated at 80⁰C. Arunarkavally *et al*²⁴⁴ reported Ni/TiO₂ (Degussa p-25). Sen and Falconer¹⁶⁵ also prepared Ni/TiO₂ catalyst by this method. Ishihara *et al*¹⁶² reported 50Co50Ni/ TiO₂ alloy catalyst by this method.

Foger and Jaeger²¹⁵ synthesized Ir/TiO₂ catalyst using chloro irridic acid and TiO₂. Three types of TiO₂ were used, viz. Degussa p-25, Tioxide and Rutile (Tioxide). Tau and Bennett¹⁶² prepared Fe/TiO₂ catalyst by using ferric nitrate and TiO₂ (Degussa p-25). Nobile jr and Davis jr^{125&59} used ferric nitrate dissolved in nitric acid for the preparation of this catalyst. They used dimethyl formamide as the solvent in some samples.

1.6.2.4 Co-precipitation

In the usual procedure, solution of metal salts and the support are contacted with aqueous alkali or ammonium hydroxide or ammonium carbonate to cause the precipitation. The precipitate can be readily converted to respective oxides by calcination. But in the case of TiO₂ supported catalysts, the co-precipitation was not yet reported.

1.6.2.5 Thermal hydrolysis

Pure TiO₂ used in catalysis was prepared by hydrolysis or thermal hydrolysis of titanium tetra alkoxide, oxy chloride or sulfate.

Cortesi *et al*²⁵⁸ developed and patented a process and apparatus for preparing spherical sub micron particles of TiO₂ by reacting steam with gaseous stream containing aero sol of titanium tetra

isopropoxide. Tanaka *et al*¹³⁵ prepared TiO₂ by hydrolysis of commercially available Ti(SO₄)₂ at 90⁰C. Yanagisawa *et al*²⁴⁰ prepared TiO₂ by hydrolysis of TiCl₄ at different pH and by the hydrolysis of titanium tetra ethoxide. According to their studies acidic conditions resulted in the formation of all the three phases of TiO₂, where as basic conditions accelerated the formation of anatase. Kim *et al*²⁵⁹ used TiCl₄ as the starting material to synthesize TiO₂ by controlled thermal hydrolysis. Kondo *et al*^{260&261} reported sub micron sized TiO₂ anatase prepared by hydrothermal processes using titanium tetra ethoxide. Iwasaki and others²⁶² synthesized nano crystalline (2.2 nm to 15 nm) TiO₂ anatase particles from an alcohol - water solution of titanyl sulfate by thermal hydrolysis. Yokota and Naka²⁶³ prepared amorphous titania having 50 micron diameter by urea hydrolysis of titanyl sulfate.

Rubio *et al*²⁶⁴ prepared spherical fine titania powder with a surface area of 80 m²/g by vapour phase hydrolysis of titanium tetra butoxide - butanol mixture. Gablenz and others²⁶⁵ prepared fine TiO₂ powder by spray hydrolysis of titanium tetra isopropoxide in a modified mini spray drier. The calcined sample has the surface area of 113.3 m²/g. But the process is very complicated and hence the reproducibility of the results is doubtful. Serpone *et al*²⁶⁶ and Kormann *et al*²⁶⁷ synthesized nano sized anatase (ca. 2 nm) by hydrolysis of TiCl₄ below 0⁰C. But, according to them, the reproducibility is very poor.

Kominami *et al*²²² synthesized TiO₂ (anatase) photo catalyst of surface area ranging between 12 m²/g and 111 m²/g by high temperature (300⁰C) hydrolysis of titanium tetra butoxide in organic

media in an autoclave in presence of water (15ml). The organic solvents used were toluene and hexanol. Toluene gave better surface area.

Kutty and Ahuja⁵⁴ prepared nano sized TiO₂ anatase and rutile powder from TiOCl₄ solution by hydrothermal method at 180⁰C. According to them depending on the anion concentration in the aqueous medium, either anatase or rutile could be obtained (i.e. 100 % anatase could be obtained if the ratio between the concentrations of SO₄²⁻ to Cl⁻ ions is > 0.3). The surface area obtained by this method was 26 m²/g to 85 m²/g.

1.6.2.6 Miscellaneous

Ferroni *et al*²⁴ prepared TiO₂ thin film on silicon substrate by R.F magnetron sputtering of Ti_{0.1}W_{0.9} target, followed by annealing in air at 800⁰C for 12 hrs. Lee *et al*²²⁶ used two new techniques for preparing titania, viz. i) ultra sonic nebulization and flame hydrolysis and ii) ultra sonic nebulization and furnace pyrolysis. Titanium tetra chloride and di isopropoxy titanium bis acetylacetonate respectively were used.

There are two distinct technologies, which are widely used for manufacturing pigment grade TiO₂.³ One is the sulfate process and the other is chloride process. The sulfate process is the classical one, which has been in use for many years. It involves the precipitation of hydrated titania by controlled thermal hydrolysis of titanyl sulfate solution (which is obtained by digesting ilmenite with sulfuric acid). Finally, the precipitate is calcined at >1000⁰C. Although this process is more suited for anatase grade TiO₂, rutile can also be manufactured by adding rutile nuclei (seeding agents) at the time of precipitation. The chloride process

involves chlorination of ilmenite or synthetic rutile or natural rutile or titania slag to form titanium tetra chloride. The TiCl_4 obtained is purified and then subjected to vapour phase oxidation to obtain rutile titania.

Even though an incredibly vast number of literature devoted to catalysis exist, important ones, relevant to the subject of present investigation, has only been referred here.

1.7 Scope and objective of the present investigation

It is evident from the literature that the preparation of fine metal oxides, especially TiO_2 , has been the subject of many scientific studies during the last two decades, considering their particular demand for use in catalysis. Hence, now, the preparation of fine TiO_2 powder is a subject of profound importance, in basic as well as applied research. As we know, the catalytic activity of a material is highly dependent on the physical properties, its preparation is of fundamental importance to obtain desired properties, necessarily required to catalyze a particular reaction. But, only limited methods are available in literature for the preparation of TiO_2 supported catalysts. The methods utilizing titanium tetra alkoxides or tetra chlorides were described in literature. But, it is very difficult to handle these compounds of titanium, as they vigorously hydrolyze even in presence of atmospheric moisture and phase pure TiO_2 anatase cannot be prepared in presence of chloride ions. Commercial non-availability of catalytic grade titania is the major concern of many of the catalyst industries, as the TiO_2 manufacturers are aiming only at the pigmentary properties rather than any other physical properties. The present investigation is there fore carried out with the following objectives.

- To prepare and characterize high surface area titania through thermal hydrolysis of titanyl sulfate solution and to study the possibility of ion-exchange and wet-impregnation on this titania in the amorphous state.
- To synthesize and characterize phase pure titania (anatase) supported catalysts by co-precipitation using hydrazine hydrate and compare the properties with their counter parts prepared through the other two methods.
- To carryout detailed investigation on the catalytic activity of all these samples.
- To examine thoroughly the onset and completion temperatures of anatase to rutile phase transformation in presence of different percentages of NiO, Fe₂O₃, V₂O₅ and CeO₂ and the after effects, of rutilation, if any, on physical properties and catalytic activities.

With these objectives, NiO/TiO₂, Fe₂O₃/TiO₂, CeO₂/TiO₂ and V₂O₅/TiO₂ catalysts with different percentages were prepared through three different methods and characterized. Methanation activity of NiO/TiO₂ samples and toluene oxidation activity of Fe₂O₃/TiO₂, CeO₂/TiO₂ and V₂O₅/TiO₂ samples were also carried out.

Chapter 2

MATERIALS AND EXPERIMENTAL METHODS

In this chapter, a brief description of the reagents used and the procedural details of the preparation of TiO_2 through thermal hydrolysis of titanyl sulfate solution and the preparation of NiO/TiO_2 , $\text{Fe}_2\text{O}_3/\text{TiO}_2$, $\text{CeO}_2/\text{TiO}_2$ and $\text{V}_2\text{O}_5/\text{TiO}_2$ catalysts. The experimental details regarding the catalytic activity studies and the details of instruments used and the analytical methods adopted for the physico-chemical characterization of the above samples are also outlined.

2.1 Materials used

Chemicals used

All the chemicals used were of analytical grade. The following chemicals were used:

Aluminium foil (s.d. fine - chem Ltd), Ammonia (s.d. fine - chem Ltd), Ammonium meta vanadate (s.d. fine - chem Ltd), Ammonium Sulfate (s.d. fine - chem Ltd), Ammonium thiocyanate (s.d. fine - chem Ltd), Barium chloride (RANBAXY), Cerium nitrate (MERCK), Dimethyl glyoxime (MERCK), Diphenyl amine sulfonate (s.d. fine - chem Ltd), Ferric nitrate (s.d. fine - chem Ltd), Hydrazine hydrate (99%, s.d. fine - chem Ltd), Hydrochloric acid (s.d. fine - chem Ltd), Hydrofluoric acid (RANBAXY), Hydrogen peroxide (30%, s.d. fine - chem Ltd), Manganous sulfate (s.d. fine - chem Ltd), Mercuric chloride (s.d. fine - chem Ltd), Nickel nitrate (MERCK), Oxalic acid (s.d. fine - chem Ltd), Phosphoric acid (s.d. fine - chem Ltd), Poly vinyl alcohol

(s.d. fine - chem Ltd), Potassium bisulfate (s.d. fine - chem Ltd), Potassium dichromate (s.d. fine - chem Ltd), Sodium bicarbonate(s.d. fine - chem Ltd), Stannous chloride (s.d. fine - chem Ltd), Sulfuric acid (s.d. fine - chem Ltd) and Toluene (99%, RANBAXY).

Gases used

Air (Sterling Gases, Kochi).

Carbon monoxide (Air Products, UK)

Hydrogen (Sterling Gases, Kochi)

Helium (IOL, Mumbai)

Nitrogen (West Cost Industries Gases, Kochi)

Oxygen (Manorama Oxygen Ltd, Kochi)

2.2 Experimental procedure

2.2.1 Preparation of TiO₂ (anatase) through thermal hydrolysis

Titanyl sulfate solution having specific gravity 1.523 at 40⁰C is an intermediate product in the commercial manufacture of TiO₂ by sulfate route, which is obtained by acidulating ilmenite with sulfuric acid to solubilize titanium as its sulfate. This solution was supplied by Travancore Titanium Products Ltd., Thiruvananthapuram. The composition of the titanyl sulfate solution is given in Table 2.1

Titanyl sulfate solution (containing 70 gpl TiO₂) was taken in a round bottom flask fitted with water condenser. The solution was then refluxed at 100⁰C for 5hrs. The precipitated hydrated TiO₂ was transformed to a 1000 ml beaker, washed six times by decantation after adding large quantities of distilled water each time. Finally it was washed with 25 % ammonia solution to remove any adsorbed sulfate ions present.

The whole precipitate was transferred into a large silica crucible and dried in air oven at 110⁰C for 3 hrs. Another sample of titania was prepared by refluxing for 7 hrs using the same quantity of titanyl sulfate solution. Two more samples of titania were also prepared by refluxing at 200⁰C using the same quantity of titanyl sulfate solution for 5 hrs and 7hrs. All these experiments were repeated with different concentrations of titanyl sulfate solution (containing 35 gpl, 23.33 gpl or 17.5 gpl TiO₂) to get 12 additional samples of titania.

Table 2.1 Composition of titanyl sulfate solution.

Constituents in grams per litre (gpl)	
Total TiO ₂	140
Reduced TiO ₂	2.3
Total acid	266
Reduced iron	101

The hydrated titania obtained was calcined at different temperatures, viz. 350⁰C, 450⁰C, 550⁰C, 600⁰C, 700⁰C, 800⁰C and 1000⁰C. The one having highest surface area (prepared by refluxing the titanyl sulfate solution - containing 35 gpl TiO₂ - at 100⁰C for 5hrs) was used for the preparation of the titania supported catalysts by co-precipitation, ion-exchange and wet-impregnation method.

2.2.2 Preparation of NiO/TiO₂

Catalysts with three different composition of NiO were prepared through three different methods.

2.2.2.1 Co-precipitation

Pure hydrated titania containing 82 % TiO₂ (1.22g) was dissolved in conc. H₂SO₄ (25ml) and (NH₄)₂SO₄ (20g) by boiling. Boiling was continued till a clear solution was obtained. It was then cooled, diluted four times with distilled water and kept in an ice bath. Ni(NO₃)₂.6H₂O (0.209g) dissolved in distilled water (20ml) was added to the above titanium sulfate solution and mixed well. Hydrazine hydrate (99%) was added drop by drop to this solution with continuous stirring till the precipitation was complete (pH became 9 at this stage). It was then kept aside for 3 hrs to settle down the precipitate and the supernatant liquid was decanted. Distilled water (approx. 500 ml) was added to the precipitate, stirred well and decanted after settling. This was repeated till the washings were free from sulfate ions (tested using 2 % barium chloride solution). The precipitate was filtered using Whatman No: 42 filter paper and oven dried at 110⁰C for 8 hrs. This oven dried sample was made into different portions and calcined at different temperatures, viz. 350⁰C, 450⁰C, 600⁰C, 800⁰C and 900⁰C for 6 hrs each in order to investigate the changes in physical properties with calcination. The sample was labeled as CN1. Samples CN2 and CN3 were also prepared similarly by taking 0.441g or 0.700g of nickel nitrate respectively.

2.2.2.2 Ion-exchange on pure hydrous titania

Hydrated titania (1.22g) was taken in a 250 ml round bottom flask and was made into slurry by adding distilled water (25ml). The pH of the slurry was adjusted to 11 by adding ammonia solution (30%). Nickel nitrate (0.209g) dissolved in distilled water (20ml) was added to this slurry. The whole slurry was then refluxed for 15 hrs at 105⁰C. The pH was maintained at 11 by adding ammonia solution occasionally. The residue was then filtered and dried in an air oven at 110⁰C for 8 hrs. It was then made into different portions and these samples were calcined at 350⁰C, 600⁰C, 700⁰C, 800⁰C and 1000⁰C or 6 hrs each. This sample was labeled as IN1. By the same procedure, the samples IN2 and IN3 were also prepared using the same quantity of nickel nitrate as in CN2 and CN3 respectively.

2.2.2.3 Wet-impregnation

Hydrated titania (1.22g) was taken in a 250ml beaker. Nickel nitrate (0.209g) dissolved in distilled water (20ml) was added to the hydrated titania, stirred well and evaporated to dryness on a hotplate with intermittent stirring. The residue was then oven dried at 110⁰C for 8 hrs and calcined at different temperatures, viz. 350⁰C, 600⁰C, 700⁰C, 800⁰C and 1000⁰C for 6 hrs each. This sample was labeled as WN1. By adopting the same procedure, the samples WN2 and WN3 were also prepared using the same quantity of nickel nitrate as in CN2 and CN3 respectively.

2.2.3 Preparation of Fe₂O₃/TiO₂

Three different samples of Fe₂O₃ loaded titania were prepared by the following methods.

2.2.3.1 Co-precipitation

The samples of $\text{Fe}_2\text{O}_3/\text{TiO}_2$, CF1, CF2 and CF3 were prepared by adopting the procedure described in section 2.2.2.1, using 0.2715g, 0.5732g or 0.9104g of ferric nitrate (dissolved in 20ml distilled water) respectively. The samples were oven dried at 110°C for 8 hrs and finally calcined at 450°C , 550°C , 650°C , 700°C and 800°C for 6 hrs each.

2.2.3.2 Ion-exchange

By following the same procedure described in section 2.2.2.2, the samples IF1, IF2 and IF3 were prepared by using 0.2715g, 0.5732g or 0.9104g of ferric nitrate (dissolved in 20ml distilled water) respectively. The oven dried samples were calcined at various temperatures, viz. 350°C , 800°C , 900°C and 1000°C for 6 hrs each.

2.2.3.3 Wet-impregnation

The wet-impregnation was carried out by the same procedure given in section 2.2.2.3. The samples prepared by using 0.2715g, 0.5732g or 0.9104g of ferric nitrate (dissolved in 20ml distilled water) were labeled as WF1, WF2 and WF3 respectively. These samples were calcined at 350°C , 550°C , 700°C , 800°C and 900°C for 6 hrs each.

2.2.4 Preparation of $\text{CeO}_2/\text{TiO}_2$

Three different samples of CeO_2 loaded TiO_2 were prepared using the following procedure.

2.2.4.1 Co-precipitation

The co-precipitation was carried out as described in section 2.2.2.1. Here the samples (CC1, CC2 and CC3) were prepared by using 0.1354g, 0.2858g or 0.454g of cerium nitrate solution (dissolved in 20ml

distilled water) respectively. The calcination was done at 350⁰C, 450⁰C, 800⁰C, 900⁰C and 1000⁰C for 6 hrs.

2.2.4.2 Ion-exchange

The samples, IC1, IC2 and IC3 were prepared by taking the same quantity of cerium nitrate used for CC1 (0.1354g), CC2 (0.2858g) and CC3 (0.454g) respectively. The procedure explained in section 2.2.2.2, was used for the preparation. Calcination was done at 350⁰C, 900⁰C, 1000⁰C and 1100⁰C for 6 hrs.

2.2.4.3 Wet-impregnation

The procedure adopted was similar to that described in the section 2.2.2.3. The samples prepared by using 0.1354g, 0.2858g or 0.454g of cerium nitrate (dissolved in 20ml distilled water) were labeled as WC1, WC2 and WC3 corresponding to CC1, CC2 and CC3 respectively. These samples were calcined at 350⁰C, 900⁰C, 1000⁰C and 1100⁰C for 6 hrs.

2.2.5 Preparation of V₂O₅/TiO₂

The samples of V₂O₅ loaded titania were prepared as follows:

2.2.5.1 Co-precipitation

Co-precipitation was carried out as explained in section 2.2.2.1, using 0.0690g, 0.1458g or 0.2315g of ammonium meta vanadate (dissolved in 10ml of 2% oxalic acid solution). The samples were marked as CV1, CV2 and CV3 respectively. They were calcined at 350⁰C, 450⁰C, 600⁰C and 650⁰C for 6 hrs.

2.2.5.2 Ion-exchange

By taking the same quantities of ammonium meta vanadate, samples, IV1 (0.0690g), IV2 (0.1458g) and IV3 (0.2315g) were prepared. The procedure adopted was same as described in section 2.2.2.2. Calcination was done at 350⁰C, 450⁰C, 600⁰C and 800⁰C for 6 hrs.

2.2.5.3 Wet-impregnation

Samples, WV1, WV2 and WV3 were prepared under this method as described earlier using the same quantities of ammonium meta vanadate as in CV1 (0.0690g), CV2 (0.1458g) and CV3 (0.2315g) respectively. These samples were calcined at 350⁰C, 450⁰C, 600⁰C and 700⁰C for 6 hrs.

2.3 Pelletization

All the samples were made into pellets before carrying out the chemisorption studies and catalytic activity studies. For this, the samples were made into a paste using 2% aqueous solution of polyvinyl alcohol (which acts as a binder) and were palletized by a hand press. The pellets were calcined at 250⁰C for 2 hrs and finally sieved through the sieves ASTM No: 9 and ASTM No: 12. The pellets retained on ASTM No: 12 sieve were only used for chemisorption and activity studies. All the pellets were nearly 0.2mm in thickness.

2.4 Dispersion studies

The percentages of NiO and V₂O₅ present on the surface of TiO₂ were estimated by oxygen chemisorption method and the percentage of Fe₂O₃ on TiO₂ was estimated by CO chemisorption method. The

experimental set up used for both methods were same and is shown in Fig. 2.1.

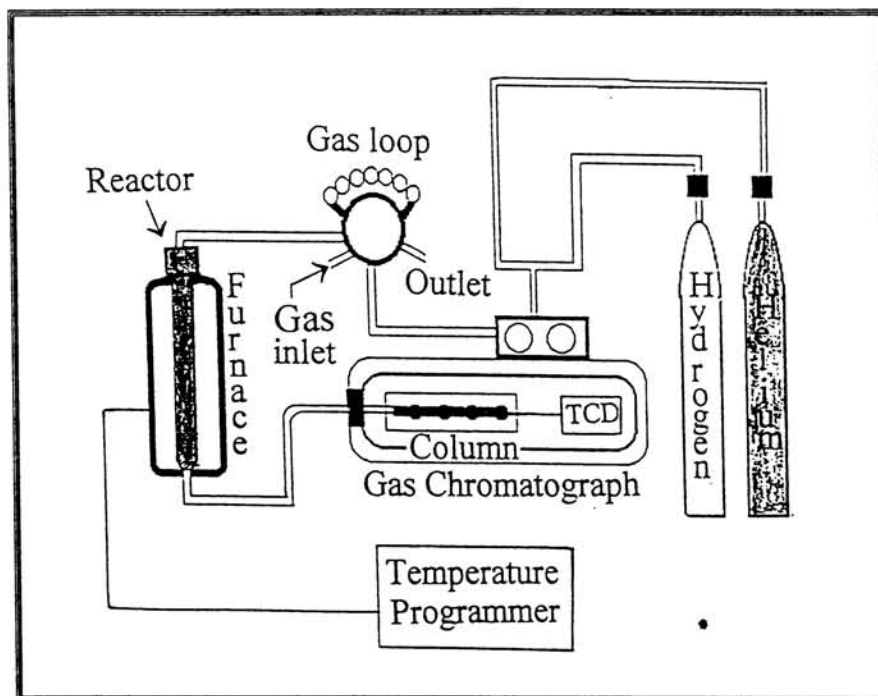


Fig. 2.1 Experimental setup for dispersion study.

2.4.1 Oxygen chemisorption method

Dispersion of NiO on NiO/TiO₂

Pelletized and sieved sample (0.5g) was loaded in a micro catalytic reactor (ID = 6mm and OD = 10mm). The NiO present on the surface of the pellet was reduced to Ni by heating at 390°C for 1 hr in hydrogen flow at a rate of 30ml per minute. Helium gas was purged through the catalyst bed for 0.5 hr at the same temperature in order to

remove residual hydrogen, if present on the catalyst. The reactor was then cooled to room temperature (27⁰C). Pure oxygen gas (0.24ml) was then injected through the manual gas-sampling valve connected to the reactor through a 0.24ml loop. This pulse of oxygen was carried by helium gas stream through the catalyst bed and was chemisorbed on the catalyst depending on the Ni content on the surface. The oxygen that was not chemisorbed on the catalyst was carried by the helium gas to the Thermal Conductivity Detector (TCD) of a Gas Chromatograph connected to the outlet of the reactor. Porapak-Q column was used for this experiment. Several injections of oxygen (0.24ml each) were given till a 100 % oxygen slip occurred. The 100 % oxygen slip was confirmed from the integrated data of 0.24ml oxygen, which was directly injected into the Gas Chromatograph. From the integrated data of the curves corresponding to un-chemisorbed oxygen, the number of oxygen atoms chemisorbed was calculated. The number of Ni atoms present on the catalyst surface was calculated from the number of oxygen atoms chemisorbed by taking the stoichiometry 1:1 for Ni and oxygen.

Dispersion of vanadia on V₂O₅/TiO₂

Here the catalyst sample (0.5g) was reduced at 370⁰C for 2hrs by a steady stream of hydrogen (30ml/minute) as above and the chemisorption was carried out at the reduction temperature i.e. at 370⁰C. All the remaining steps were similar to that described above. The number of vanadium atoms present on the surface of the catalyst pellet was

calculated from the number of oxygen atoms chemisorbed by taking the stoichiometry 1:1 for vanadium and oxygen.^{49,149&268}

2.4.2 Carbon monoxide chemisorption

Dispersion of Fe₂O₃ on Fe₂O₃/TiO₂

Pelletized sample (0.5g) was loaded in the micro catalytic reactor. The experimental set up is same as given in Fig. 2.1. The sample was reduced at 400⁰C for 2 hrs in hydrogen stream (at a rate of 30ml per minute). The reactor was then cooled to room temperature (27⁰C) and kept in a freezing mixture to keep the temperature below 0⁰C. Carbon monoxide (0.24ml) was injected through the manual gas-sampling valve connected to the Gas Chromatograph. All the remaining procedure is as described earlier. The number of iron atoms present on the surface was calculated using the stoichiometry of 2:1 for iron and carbon monoxide.^{59,125&162}

From the dispersion data, the crystallite size of the respective metal particles present on the surface was calculated^{269&162} using an approximate relation $d = 80/D$, where, d = surface average crystallite size, D = percentage dispersion.

2.5 Catalytic activity studies

Carbon monoxide methanation activity studies were carried out using NiO/TiO₂ samples and toluene oxidation activity was done using the CeO₂/TiO₂, Fe₂O₃/TiO₂ and V₂O₅/TiO₂ samples.

2.5.1 Carbon monoxide methanation by pulse method

The CO methanation activity studies of CN1, CN2, CN3, IN1, IN2, IN3, WN1, WN2 and WN3 samples calcined at different temperatures were carried out by the following procedure. The experimental set up is similar to that of dispersion studies shown in Fig.2.1.

The pelletized sample (0.5g) was loaded in the micro catalytic reactor (ID = 6mm and OD = 10mm) used in dispersion studies. The sample was then reduced for 1hr in hydrogen stream at a rate of 30ml per minute at 390⁰C. Helium gas was then purged through the catalyst bed for 10 minutes to remove residual hydrogen. The reactor was then cooled to 275⁰C and hydrogen gas was again passed through the catalyst bed at the same rate. A pulse of pure CO (0.24ml) was injected through the manual gas-sampling valve of the Gas Chromatograph, which can pass through the catalyst bed. The output gases, un-reacted CO and CH₄ were quantitatively analyzed by the on-line Gas Chromatograph connected to the outlet of the reactor. The column used was spherocarb and the detector was TCD. The output signals were evaluated and the percentage conversion of CO to CH₄ was determined by peak area of the signals with reference to calibration area of known volume of corresponding gases. The experiments were repeated by injecting CO (0.24ml each) at different temperatures, viz. 300⁰C, 325⁰C, 350⁰C and 375⁰C to find out the temperature for maximum conversion. The suitable optimum temperature for maximum conversion was found to be 350⁰C. Hence the activity studies of all the other samples were done at 350⁰C.

2.5.2 Toluene oxidation activity studies (gas phase)

The toluene oxidation activity studies were carried out on $\text{CeO}_2/\text{TiO}_2$, $\text{Fe}_2\text{O}_3/\text{TiO}_2$ and $\text{V}_2\text{O}_5/\text{TiO}_2$ samples calcined at different temperatures as per the procedure described below. The complete experimental setup is as shown in Fig. 2.2.

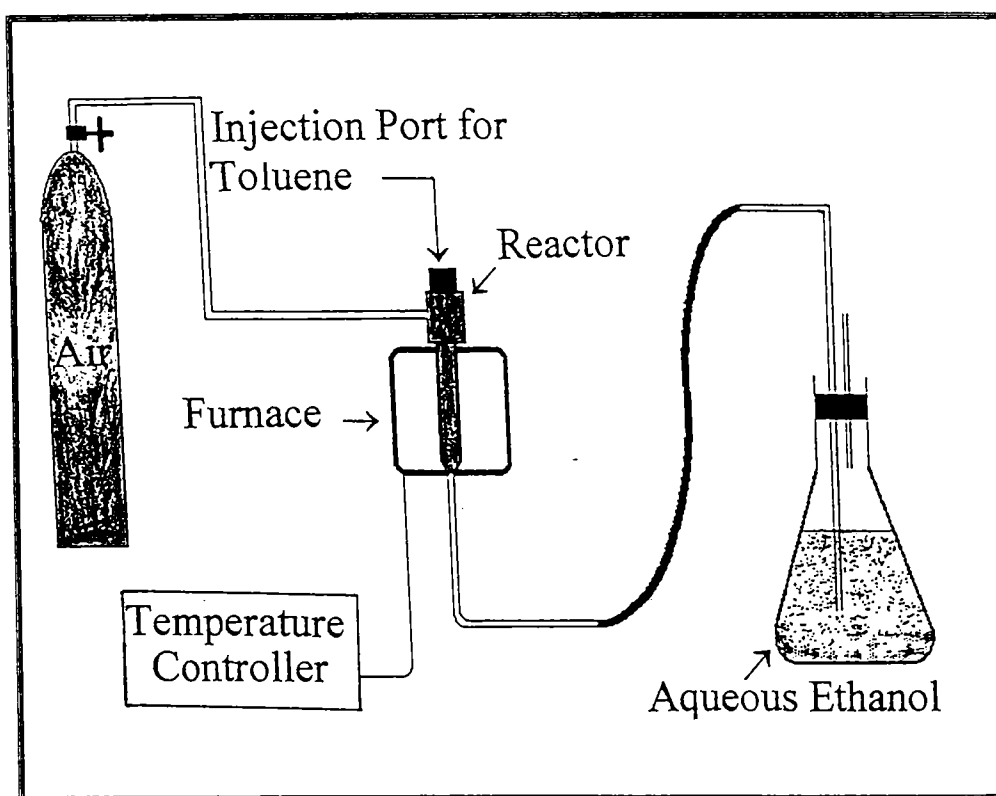
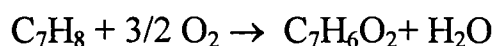


Fig. 2.2 Experimental setup for toluene oxidation study.

The pelletized catalyst sample having nearly the same dimension (0.5g) was loaded in the micro catalytic reactor and was diluted with porcelain beads. It was then heated at 400°C for 1 hr in air at

a flow rate of 30ml per minute and 0.2ml of toluene was injected through the top of the reactor by keeping it at the same temperature. The outlet gas was scrubbed into a 50ml of 25% aqueous ethanolic solution previously neutralized with NaOH, taken in well-stoppered conical flask with a small outlet. After scrubbing for 15 minutes, the conical flask was disconnected from the unit and the benzoic acid formed was estimated by titrating against standard 0.1N NaOH solution using phenolphthalein as indicator as per the procedure cited in reference.²⁷⁰ The proposed reaction is:



2.6 Crystallite size calculation

The crystallite size (not the particle size) of anatase was calculated using a computer program based on Scherrer relation. For this purpose, the width at half height of the peak corresponding to [101] plane of anatase was measured. The Scherrer relation states that the XRD peak broadening is inversely proportional to crystallite size²⁷¹ and the crystallite size can be calculated from the equation $D = 0.9\lambda / \beta \cos \theta$. Where, D = crystallite size, λ = wavelength used, β = corrected half width of the peak and θ = angle of diffraction.

2.7 Rutile percentage calculation

The rutile percentage in each sample was calculated using the equation²⁷² $(1 + 0.794 I_A/I_R)^{-1}$ multiplied by 100. Where, I_A and I_R are

the peak intensities of [101] and [110] planes of anatase and rutile respectively.

2.8 Chemical analysis

A brief description of chemical analysis methods adopted for the estimation of TiO_2 ,²⁷³ NiO ,²⁷⁴ CeO_2 ,²⁷⁵ V_2O_5 ,²⁷⁶ and Fe_2O_3 ²⁷⁷ is given below.

2.8.1 Estimation of TiO_2

Aluminium reduction method

The estimation was carried out using the procedure described in literature.²⁷³ The sample (0.2g) was fused with excess amount of potassium bisulfate (15g). The mass was cooled and dissolved in 20% H_2SO_4 (150ml) and the solution was made up to 250ml in a standard flask. A known volume of the made up solution was pipetted into a 500ml Erlenmeyer flask and conc. HCl (30ml) was added to it. The solution was boiled well and removed from the heating mantle. Highly pure aluminium foil (2g) was attached to the glass rod of the reaction setup. The rubber stopper carrying the glass rod with aluminium foil and the delivery tube was immediately inserted into the Erlenmeyer flask. The other end of the delivery tube was placed below the level of saturated sodium bicarbonate solution taken in a beaker, to prevent the re-oxidation. The flask was heated again. Towards the end of the reaction, the flask was swirled to ensure complete mixing and reduction. When the aluminium foil was dissolved, the solution was gently boiled for 3 - 5 minutes keeping the delivery tube immersed in the sodium bicarbonate solution. The solution was cooled to a temperature less than 60°C . As the

solution was cooled, the sodium bicarbonate solution was drawn inside the flask and the CO_2 evolved would give the necessary protective atmosphere. The solution was cooled and titrated against standard N/16 ferric alum solution using ammonium thiocyanate solution as indicator.

2.8.2 Estimation of NiO

Nickel estimation was done as per the standard procedure.²⁷⁴ The sample (0.5g) was fused with potassium bisulfate (38g). The mass was cooled and dissolved in 20% H_2SO_4 (300ml). Titania was precipitated out by adding ammonia. The filtrate was collected and was made acidic by adding conc. hydrochloric acid (10ml). The solution was then heated to 70 - 80°C and 1% ethanolic solution of dimethyl glyoxime (25ml) was added. Dilute ammonia solution was added drop wise with constant stirring until the precipitation began and then in slight excess. The precipitate was filtered through a sintered glass crucible and washed with cold water until free from chloride and sulfate. Completion of precipitation was tested by adding dimethyl glyoxime to the filtrate. The residue was dried at 110°C for 1 hr and weighed.

2.8.3 Estimation of CeO_2

Ceria was estimated as per the procedure.²⁷⁵ The sample (0.5g) was fused with potassium bisulfate, dissolved in dilute H_2SO_4 and made up to 250ml, as described in TiO_2 estimation. A known volume of the made up solution was pipetted out into a 250ml beaker and the pH of the solution was adjusted to 1. The solution was heated to boiling and hot saturated solution of oxalic acid (15ml) was added slowly with stirring. The whole solution was boiled for a few minutes and allowed to

cool to room temperature. The solution was then set aside for overnight for completing the precipitation. The precipitate was washed initially with saturated oxalic acid solution and then with water and was filtered through Whatman No: 42 filter paper. The residue was ignited at 500⁰C for 0.5 hr. Re-dissolved in hydrochloric acid and was precipitated again. The precipitate was finally ignited at 900⁰C for 2 hrs and weighed as CeO₂.

2.8.4 Estimation of V₂O₅

Vanadia was estimated spectrophotometrically²⁷⁶ using u.v-visible spectrophotometer. The sample (0.5g) was fused with potassium bisulfate. Then it was dissolved in dilute H₂SO₄ and made up to 250ml, as described in the case of TiO₂ estimation. A known volume of the made up solution was pipetted and diluted to 80ml. Hydrofluoric acid (48%, 2ml) was added to prevent colour interference by titanium. Then H₂O₂ (3%, 3ml) was added and diluted to 100ml. The absorbance was noted at 450 nm against a similarly prepared standard.

2.8.5 Estimation of Fe₂O₃

Ferric oxide was estimated as per the standard procedure.²⁷⁷ The sample (0.2g) was fused with potassium bisulfate, dissolved in dilute H₂SO₄ and made up to 250ml, as described in section 2.8.1. A known volume of the made up solution was pipetted out into a 250ml Erlenmeyer flask, conc. hydrochloric acid (5ml) was added and heated for 5 minutes. Stannous chloride (6%, 2 - 3 drops) was added till the yellow colour disappeared and then one drop in excess was added. The excess SnCl₂ was removed by adding saturated HgCl₂ solution (15ml).

Then 10ml of acid mixture (1:1 H_2SO_4 and H_3PO_4) and 10ml of Zimmermann solution (this solution was prepared by adding a cooled mixture of 100ml conc. H_2SO_4 and 300ml water to a solution of 50g of $\text{MnSO}_4 \cdot 4\text{H}_2\text{O}$ in 250ml water. 100ml of syrupy phosphoric acid was also added) were added. It was then titrated against standard 0.1N potassium dichromate solution after adding three drops of diphenyl amine sulfonate indicator to a violet end point.

2.9 Instrumental methods employed

2.9.1 Surface area analyzer

Surface area measurements were done by BET method of nitrogen adsorption at liquid nitrogen temperature using Gemini 2360 V4.01 instrument by taking accurately 0.5g of the sample.

2.9.2 Gas Chromatograph

The Gas Chromatograph used was Chemito 8510 series, with a manual gas-sampling valve and 0.24 ml loop connected to it. The columns used were porapak-Q and spherocarb and the thermal conductivity detector (TCD) was used to detect the out let gases.

2.9.3 Micro catalytic reactor

The catalytic reactor was made out of stainless steel. It has 15cm height and 10mm and 6mm outer and inner diameters respectively.

2.9.4 Furnace and temperature programmer

A vertical tube furnace with a local made temperature programmer (Century Systems CS 7533) was used in these studies. Ordinary muffle furnace was used for calcination purpose.

2.9.5 X - Ray Diffractometer

Philips automatic powder diffractometer, PW 1710 with $\text{CuK}\alpha$ wavelength was used for XRD studies.

2.9.6 Scanning Electron Microscope

JSM-5600 instrument was used for SEM analysis. The sample was prepared as follows: 0.1g of the sample was dispersed in acetone by sonication and one drop was placed on a copper stud, dried and gold sputtered. Then the SEM analysis was performed.

2.9.7 UV-Visible spectrophotometer

The estimation of V_2O_5 was done using UV-Visible spectrophotometer, Shimadzu 1601.

2.9.8 TGA and DTA

The thermo gravimetric analysis and differential thermal analysis were done using Shimadzu TGA-50H and Shimadzu DTA-50 in the atmosphere of air.

Chapter 3

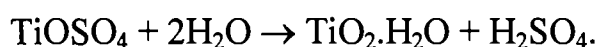
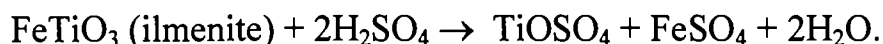
STUDIES ON TITANIA PREPARED THROUGH THERMAL HYDROLYSIS

Tiitania acts as catalyst or as support in various reactions. Its catalytic activity, to a great extent, is determined by physical properties such as surface area, crystallinity, etc. and these properties mainly depend on the preparative conditions. Most of the reactions reported in literature were carried out on the commercially available imported TiO_2 , called Degussa p-25, which is a mixture of 70 % anatase and 30 % rutile and has surface area of $50 \text{ m}^2/\text{g}$.²⁷⁸ Several methods are available for the preparation of TiO_2 , which are described in detail in Chapter 1. It is very difficult to handle TiCl_4 or alkoxides and strict control of reaction conditions are required, as they vigorously hydrolyse in presence of atmospheric moisture.²⁵⁹ The high price of alkoxides limits the commercialization of titania manufacture using the hydrolysis of alkoxides. Furthermore, phase pure TiO_2 anatase cannot be prepared by hydrothermal crystallization in presence of chloride ions, which would lead to the formation of rutile phase rather than anatase.^{1&118}

Hence extensive work has been going on for preparing highly pure anatase having high surface area. Thermal hydrolysis of titanyl sulfate solution, which can give highly pure anatase with good crystallinity, is a widely used commercial process for the production of pigment grade TiO_2 . The commercial plants add nuclei (seeding agents)

to hasten the hydrolysis, which would lead to the precipitation of a mixture of ortho and meta titanic acids. This precipitate is normally calcined at ca. $>1000^{\circ}\text{C}$, to achieve desired pigmentary properties. Commercial plants would also add anti rutilating agents like ammonium dihydrogen phosphate. Hence some adsorbed sulfate and phosphate ions would be present as impurity with commercial TiO_2 . All these would adversely affect the physical properties and hence the catalytic activity.

Hence a detailed investigation for the preparation of TiO_2 through thermal hydrolysis of titanyl sulfate solution under different conditions to obtain better properties in terms of surface area and crystallinity was undertaken and the results are reported here. The proposed reaction, taking place during thermal hydrolysis is:



3.1 Chemical analysis

Chemical analysis was done as per the standard procedure discussed in Chapter 2 and the results are given in Table 3.1

Table 3.1. Chemical analysis data for titania samples.

Calcination temperature ($^{\circ}\text{C}$)	TiO_2 (%)
Oven dried (110)	82.00
270 /4hrs	86.73
350 /4hrs	92.83
350 /6hrs	99.34

The oven dried sample contained 82 % TiO_2 , which showed that the precipitate formed was meta titanic acid ($\text{TiO}_2 \cdot \text{H}_2\text{O}$). On increasing the calcination temperature and duration, the percentage of TiO_2 was found to increase. It is clear from Table 3.1 that, the calcination at 350°C for 6 hrs is necessary to remove the water molecules completely. So, all further studies were carried out with the samples calcined at 350°C for 6 hrs.

3.2 Surface area studies

All the titania samples, prepared by thermal hydrolysis under different conditions, were calcined at 350°C for 6 hrs and the surface area of these samples were measured. The results of surface area studies are shown in Fig. 3.1. The surface area was found to be highly dependent on the conditions of thermal hydrolysis like, concentration of titanyl sulfate solution, temperature and duration of thermal hydrolysis, etc. The calcination temperature has also got marked effect on the surface area of TiO_2 .

3.2.1 Concentration of titanyl sulfate solution

As the concentration of titanyl sulfate solution was decreased, the surface area of TiO_2 formed by thermal hydrolysis was found to increase initially and then decrease markedly under all conditions. The samples prepared from titanyl sulfate solution containing 35gpl TiO_2 have got much higher surface area. As the concentration of titanyl sulfate solution was decreased further to 23.33gpl and 17.5gpl TiO_2 , the surface area of TiO_2 also decreased, which could be due to the

increased possibility of the growth of hydrated titania particles on boiling the very dilute titanyl sulfate solution.

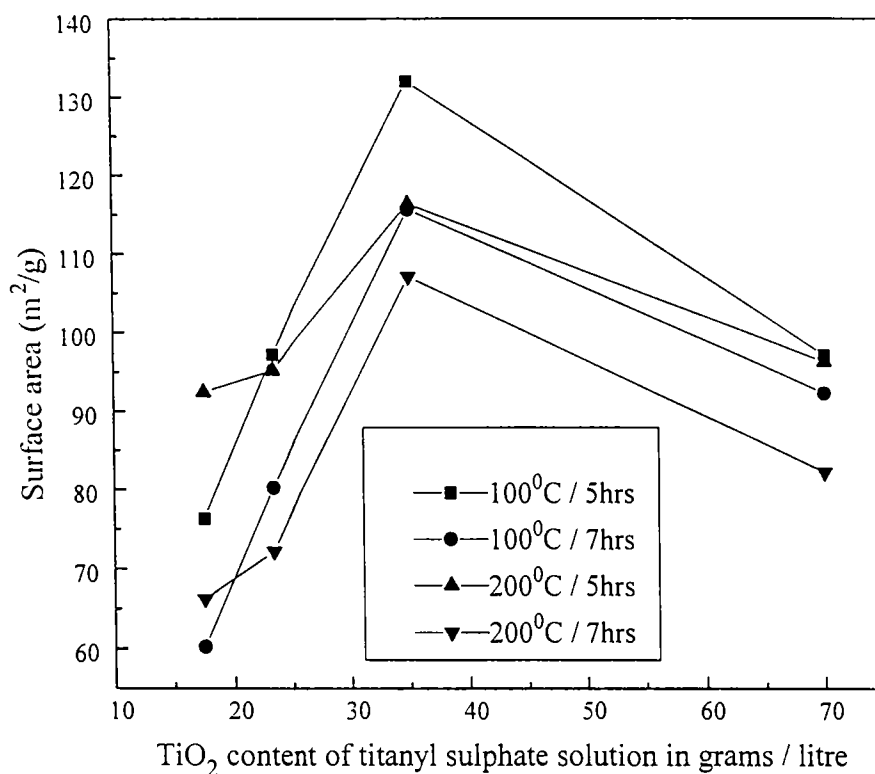


Fig. 3.1. Variation in surface area of TiO₂ prepared by thermal hydrolysis under different conditions

3.2.2 Temperature of hydrolysis

Usually, in commercial plants, the thermal hydrolysis is carried out at 100°C.¹ In order to investigate the effect of higher temperature hydrolysis on surface area, the hydrolysis was done at 200°C also. On increasing the temperature of hydrolysis to 200°C, the surface

area decreased noticeably. It would plausibly be due to agglomeration of titania particles.

3.2.3 Duration of thermal hydrolysis

Since the precipitation was incomplete on hydrolysis for 3 hrs, it was carried out for 5 hrs and 7 hrs. Duration of hydrolysis has also got a strong influence on surface area of TiO_2 formed. The samples prepared for 5 hrs duration under all conditions possess higher surface area than the ones prepared for 7 hrs. Decrease in surface area might be due to the growth of titania particles on increasing the duration of hydrolysis.

3.2.4 Calcination temperature

Out of the above samples, the one having highest surface area was prepared and calcined at different temperatures in order to investigate the changes in surface area. A drastic decrease in surface area on increasing the calcination temperature was observed, obviously due to the particle enlargement, taking place during higher temperature calcinations. A sudden decrease was observed till 550°C and there after a gradual decrease on increasing the temperature of calcination. So at temperatures less than 550°C , each and every degree rise in temperature has marked influence on surface area. The results are shown in Fig. 3.2.

For comparing with the properties of various metal oxide loaded TiO_2 , prepared though co-precipitation using hydrazine hydrate, which will be discussed in the following Chapters, pure TiO_2 was also prepared by precipitation using hydrazine hydrate. For this purpose, pure hydrated TiO_2 containing 82 % TiO_2 (1.22g) was dissolved in conc.

H_2SO_4 and $(\text{NH}_4)_2\text{SO}_4$, cooled and diluted four times with distilled water. Hydrazine hydrate was added slowly with stirring to this solution and the precipitate was oven dried at 110°C for 8 hrs and finally calcined at 350°C , 450°C , 550°C , 600°C , 700°C , 800°C and 1200°C for 6 hrs each. Surface area of these samples was measured and the results are shown in Fig. 3.2. Here also a drastic decrease was observed in surface area on increasing calcination temperature.

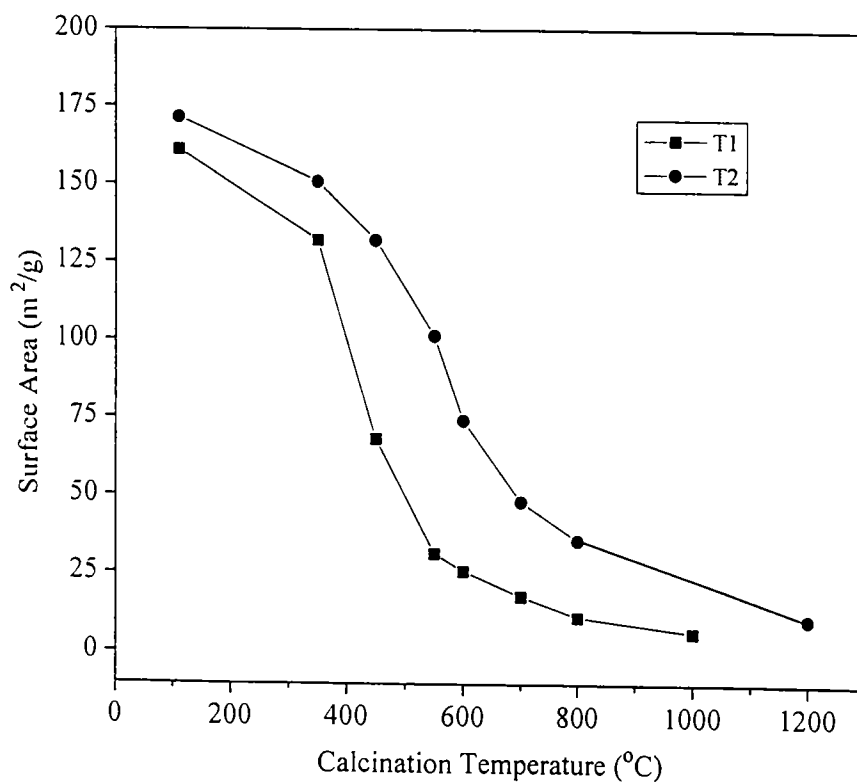


Fig.3.2. Effect of calcination temperature on surface area of TiO_2 prepared by T1) Thermal hydrolysis and T2) Hydrazine precipitation

3.3 XRD studies

The sample having highest surface area was prepared and calcined at different temperatures to carry out XRD analyses for investigating the phase changes occurring during high temperature calcinations. The patterns are shown in Fig.3.3. The pattern of oven dried sample is not given, since the crystallization has not taken place and

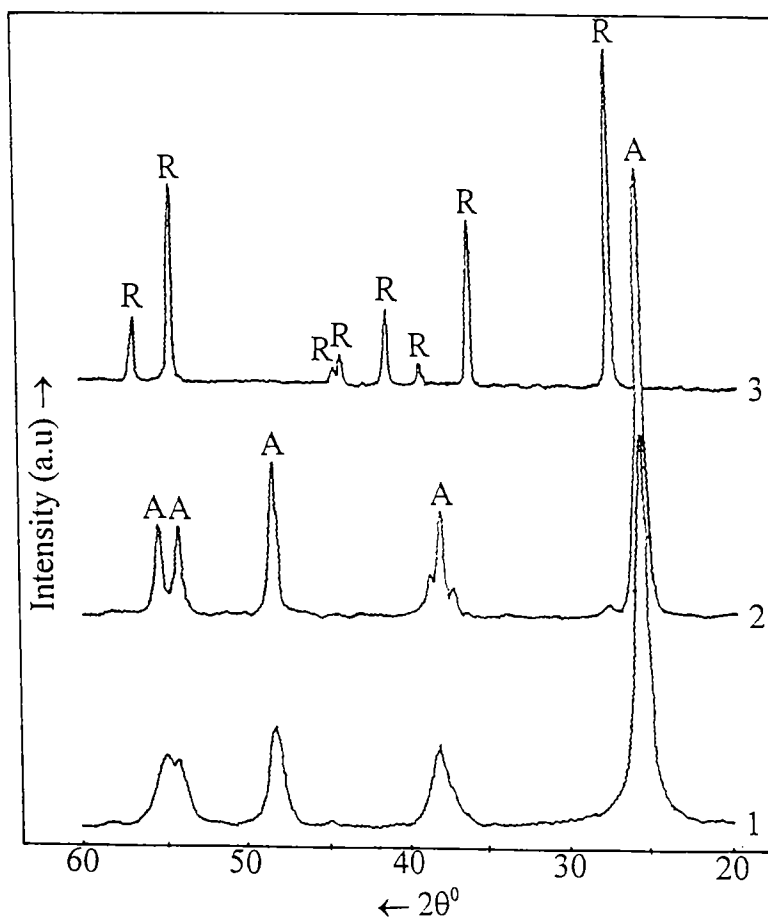


Fig. 3.3. XRD patterns of TiO₂ prepared by thermal hydrolysis - calcined at 1) 350, 2) 700 and 3) 1000°C for 6 hrs. (A = anatase and R = rutile).

hence the peaks were broad and were not sharp. This would be due to the presence of hydroxyl groups on the surface and it is in agreement with chemical analysis results. Upon calcination at 350⁰C for 6 hrs, well-defined sharp peaks of anatase were obtained. So, it is obvious that the calcination at 350⁰C for 6 hrs is enough for preparing highly pure crystalline TiO₂ anatase by this method. On increasing the calcination temperature to 550⁰C and 600⁰C, no phase changes were observed. When the calcination temperature was increased further to 700⁰C, the characteristic peak of rutile appeared at 3.23nm in the pattern. This is clear from Fig.3.3. The intensity of the rutile peaks increased on further calcinations and finally at 1000⁰C, all the anatase peaks disappeared from the pattern and well defined and intense rutile peaks appeared. Hence it can be concluded that, the rutilation started at 700⁰C and was complete at 1000⁰C. So, the drastic decrease in surface area of these samples as mentioned above could be due to the crystallographic changes occurring prior to rutilation.

The percentage of rutile and anatase were calculated in these samples and the results are shown in Table 3.2. As the calcination temperature was increased, the rutile percentage also increased.

The crystallite size of anatase calculated from XRD data is also given in Table 3.2. The crystallite size increased on increasing calcination temperature. In the sample calcined at 600⁰C, the crystallite size was 17.1nm, but on increasing the calcination temperature further to 700⁰C and 800⁰C, no change in crystallite size was seen, but the

Table 3.2 Anatase, rutile percentages and crystallite size of TiO₂ prepared by thermal hydrolysis.

Calcination temp. (°C)	Phases of TiO ₂ present (%)		Crystallite size (nm)
	Anatase	Rutile	
350	100	0	9.07
550	100	0	13.96
600	100	0	17.1
700	97.22	2.78	17.1
800	71.15	28.85	17.1
1000	0	100	---

percentage of rutile was increased. Hence, it can be concluded that, in pure titania, prepared through thermal hydrolysis, the anatase to rutile transformation takes place only after the enlargement of anatase crystallites and it is not a simultaneous process along with rutile phase formation.

XRD studies of the titania samples prepared by hydrazine precipitation method was also carried out and the patterns are shown in Fig.3.4. Here the anatase crystallized only at 450°C. Unlike that of thermally hydrolyzed one, here the rutilation started at 800°C and completed at 1200°C.

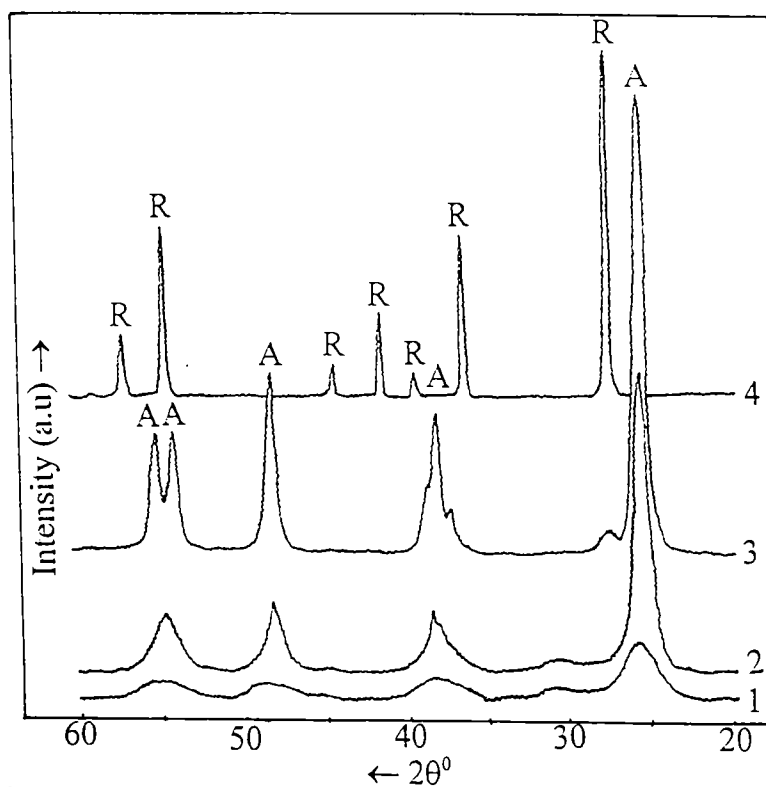


Fig. 3.4. XRD patterns of TiO_2 prepared by hydrazine precipitation - calcined at 1) 350, 2) 450, 3) 800 and 4) 1200°C for 6 hrs. (A = anatase and R = rutile).

Like TiO_2 prepared through thermal hydrolysis, the crystallite size was increased on increasing calcination temperature, but at the onset of rutilation, here the crystallite size of anatase was only 12.8nm and it increased to 13.96nm, when calcined at 900°C. The crystallite size of anatase, anatase and rutile percentages are given in Table 3.3. It is obvious that, the rutilation, in pure TiO_2 prepared by hydrazine precipitation, started and completed at higher temperatures compared to that prepared by thermal hydrolysis.

Table 3.3 Anatase, rutile percentages and crystallite size of TiO₂ prepared by hydrazine precipitation.

Calcination temperature (°C)	Phases of TiO ₂ present (%)		Crystallite size (nm)
	Anatase	Rutile	
350	Amorphous	Amorphous	---
450	100	0	9.07
700	100	0	11.00
800	97.71	2.29	12.80
900	67.40	32.60	13.96
1200	0	100	---

3.4 TGA and DTA studies

Thermo gravimetric pattern of oven dried sample is given in Fig.3.5. On heating the weight loss took place in two stages and a total weight loss of 18.62% at 821⁰C was observed. The total weight loss confirms the presence of meta titanic acid (i.e. TiO₂.H₂O), in oven dried sample, which is consistent with chemical analysis results. But in chemical analysis 99.34 % TiO₂ was obtained in the sample calcined at 350⁰C for 6hrs, which suggests complete removal of water molecule present in hydrated titania. XRD pattern also supports the crystallization of the sample calcined at 350⁰C for 6 hrs. However in TGA, the weight loss was seen up to 821⁰C.

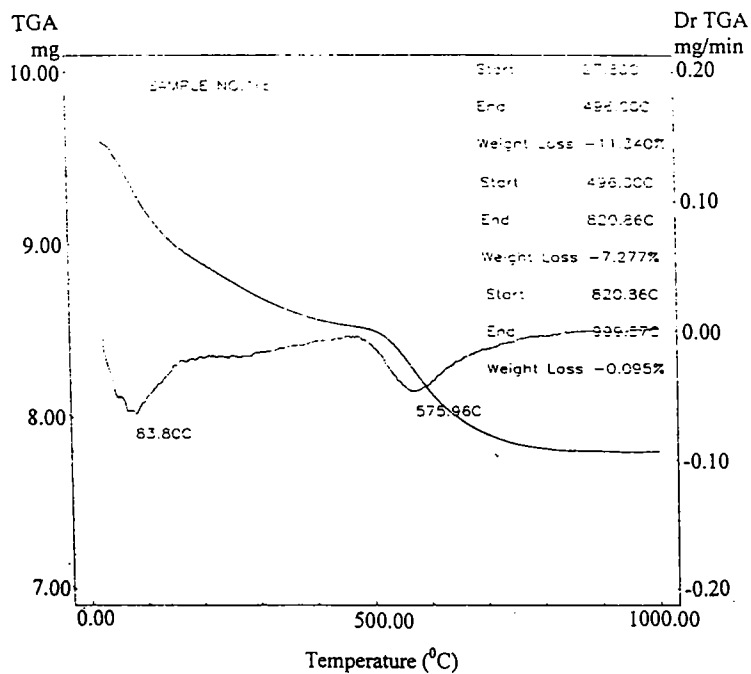


Fig. 3.5. TGA curve of TiO_2 prepared through thermal hydrolysis.

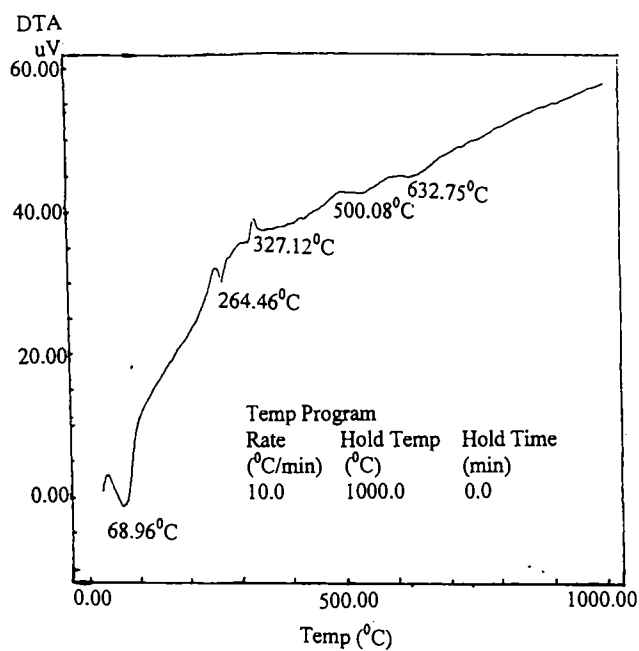


Fig. 3.6 DTA curve of TiO_2 prepared through thermal hydrolysis.

Fig. 3.6 represents the DTA of oven dried TiO_2 . It consists of four endothermic peaks and one exothermic peak. The two endothermic peaks at 68.96°C and 264.46°C could be attributed to the removal of adsorbed and coordinated water molecules. The sharp well-defined exothermic peak at 327.12°C could be due to anatase phase formation. XRD studies also supports this, where the anatase crystallization took place at around 350°C . Two more endothermic peaks at 500.08 and 632.7°C are found in the figure. The one at 500.08°C would be due to some crystallographic rearrangements taking place before rutilation and the other at 632.75°C would be due to rutilation, where as in XRD pattern, a well-defined small peak of rutile was observed in the sample calcined at 700°C for 6 hrs.

3.7 Conclusions

From all these experiments and data the following conclusions can be arrived at

- ☐ Conditions of thermal hydrolysis have significant role on the physical properties of TiO_2 formed.
- ☐ Phase pure TiO_2 anatase having high surface area can be prepared by thermal hydrolysis of titanyl sulfate solution.
- ☐ Optimum conditions for obtaining high surface area titania – 35gpl TiO_2 , 66.5gpl acid, thermal hydrolysis at $100^\circ\text{C}/5$ hrs and calcination at $350^\circ\text{C}/6$ hrs.
- ☐ Marked decrease in surface area was observed upon rutile phase formation. Rutilation started at 700°C and completed at 1000°C .

- ☐ Rutilation started at 800⁰C and completed at 1200⁰C in TiO₂ prepared by hydrazine precipitation method.
- ☐ Rutile % increased with calcination temperature.
- ☐ Crystallite size enlargement took place during rutilation.

Chapter 4

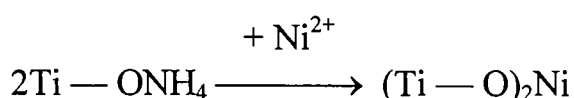
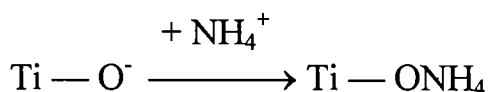
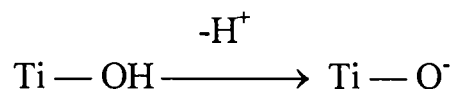
STUDIES ON NiO/TiO₂ CATALYST

Group VIII metals, especially nickel, are excellent catalysts for hydrogenation of olefins and CO to synthesize saturated hydrocarbons. SiO₂ and Al₂O₃ are the commonly used support materials for Ni catalyst, since they possess high surface area.²⁷⁹ Extensive work has been reported recently on Ni supported on TiO₂ as a catalyst for CO hydrogenation with better activity compared to the other supports. But limited methods are only reported for the preparation of this catalyst. Traditional methods like, wet-impregnation and ion-exchange on crystalline TiO₂ were found to be employed in most of the investigations. In both the above methods, Ni atoms are introduced in to the TiO₂ crystal lattice by heating crystalline TiO₂ in presence of nickel salt solution at different temperatures, These methods would obviously reduce the surface area of TiO₂, enhance the phase transformation and affect adversely on the homogeneous dispersion of the active metal on it. This may cause much greater diffusion of active metal particles towards the bulk of titania during reduction¹⁰⁰ and thus reduce the number of surface exposed active metal atoms.

Hydrazine hydrate precipitation is a new method described in literature for the preparation of nano sized metal oxides used for electronic applications. The preparation of catalysts by this method is yet to be reported. Hydrazine hydrate can quantitatively precipitate certain

metals by complexing with them. These complexes undergo decomposition upon calcination resulting in high surface area metal oxides.

Titania, in the amorphous state possesses high surface area and hence can incorporate large quantities of other metal oxides. Also, while loading metal oxides on crystalline titania, there is an increased chance for rutilation. Hence, amorphous titania was used for ion-exchange and wet-impregnation methods. The ion-exchange method is based on zero point charge of titania, which is reported to be pH 5-5.6^{57&78} and above which cations can be exchanged as reported. The negative charge is built up on the aqueous dispersion of hydrated TiO₂ due to proton transfer from hydrated TiO₂ to the water. On increasing the pH above zero point charge, this proton transfer would also be increased leaving behind the electrons in the partially bonded oxygen atoms.²⁸⁰ NH₄⁺ ions get attached to this negatively charged oxygen atoms and while refluxing in presence of Ni²⁺ solution, the NH₄⁺ ions get exchanged by nickel atoms. Schematic representation for ion exchange is given below:



The samples prepared by co-precipitation were labeled as CN1, CN2 and CN3. Like wise IN1, IN2 and IN3 for ion exchanged and WN1, WN2 and WN3 for wet-impregnated ones. The percentage of NiO in each sample is shown in Table 4.1.

4.1 XRD studies

XRD patterns are shown in Figs 4.1 – 4.6. Well-defined and sharp peaks were obtained for ion-exchanged and wet-impregnated

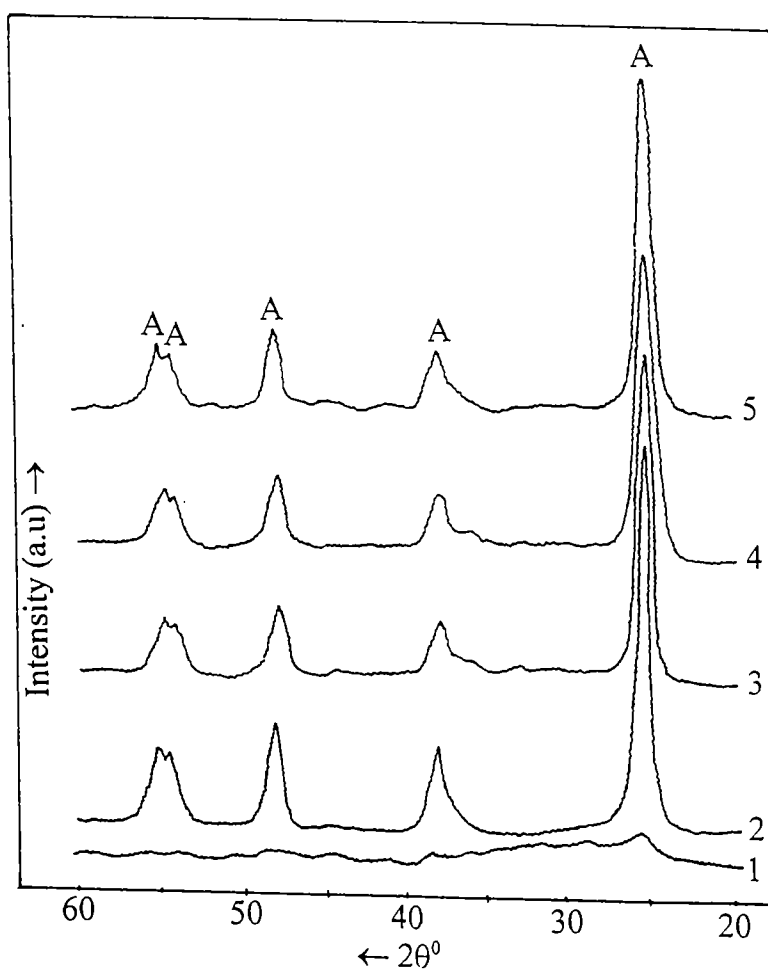


Fig. 4.1. XRD pattern of NiO/ TiO₂ samples prepared by co-precipitation method 1) CN3 calcined at 350°C / 6hrs., 2) CN1, 3) CN2, 4) CN3 calcined at 450°C / 6hrs. and 5) CN3 after catalysis. (A = anatase).

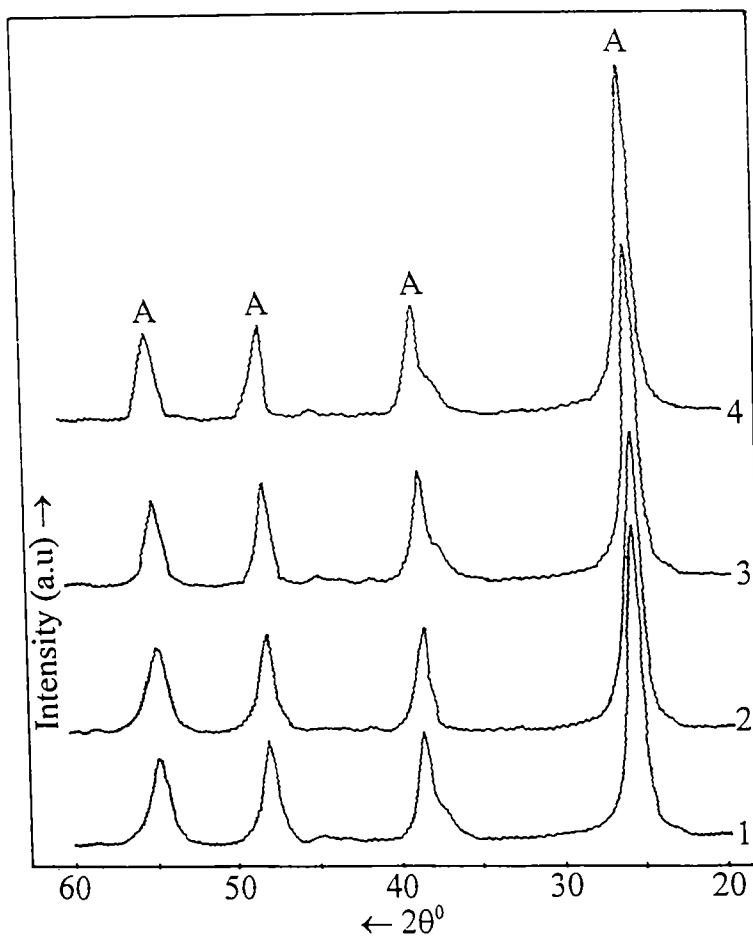


Fig. 4.2. XRD pattern of NiO/TiO_2 samples prepared by ion-exchange method - calcined at 350°C / 6hrs. 1) IN1, 2) IN2, 3) IN3 and 4) IN3 after catalysis. (A = anatase).

samples calcined at 350°C for 6 hrs, but co-precipitated one was amorphous at this temperature. It has become crystalline only at 450°C . All the peaks were those of anatase in all the samples, except in WN3, where a small peak of NiO was observed. There were no peaks due to rutile or NiTiO_3 in any of the sample. The absence of NiO peaks clearly discloses the fine nature of NiO, which can not be detected using XRD

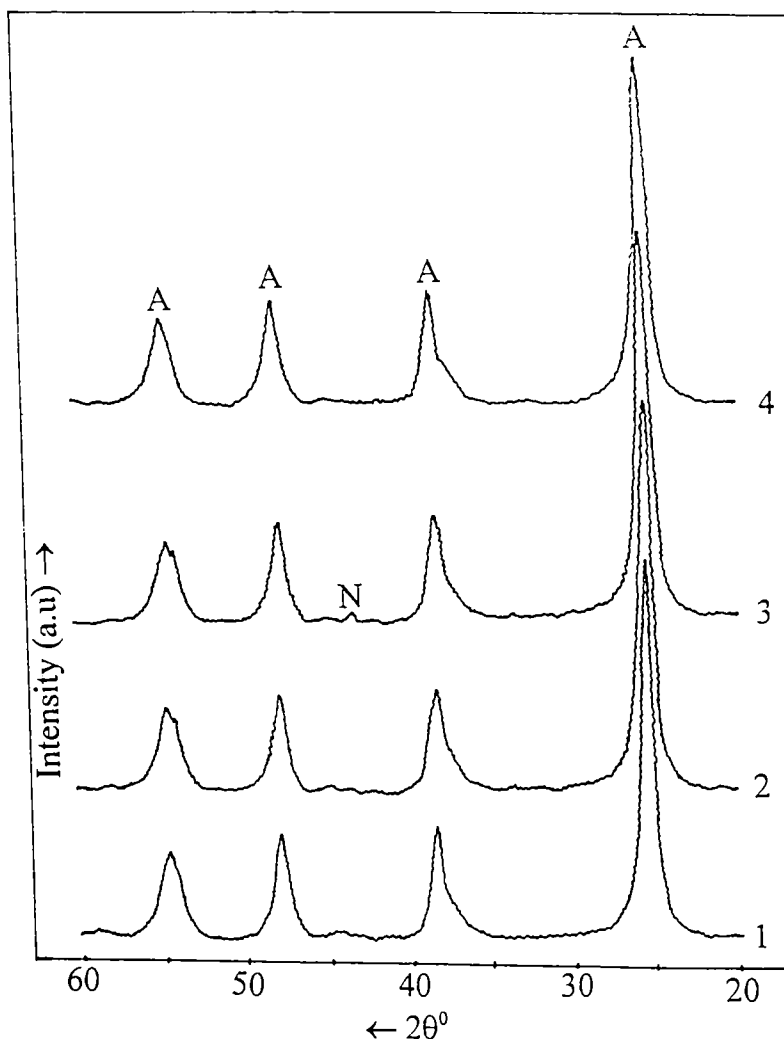


Fig. 4.3. XRD pattern of NiO/ TiO₂ samples prepared by wet-impregnation method - calcined at 350°C / 6hrs. 1) WN1, 2) WN2, 3) WN3 and 4) WN3 after catalysis. (A = anatase and N = NiO).

technique as has been reported in the case of ZnO and Fe₂O₃ doped titania and V₂O₅/TiO₂.^{124&268} On comparing with crystallization temperatures of bare TiO₂ prepared by hydrazine precipitation and thermal hydrolysis, no change was observed in crystallization temperature in presence of NiO.

In order to investigate clearly the effect of NiO on rutilation, the XRD analysis of all the samples calcined at different temperatures were carried out. Well-defined rutile peaks were obtained in the sample CN3 calcined at 600°C (Fig. 4.4), but in IN3 and WN3, the rutile peaks appeared only after calcination at 700°C (Figs 4.5 and 4.6). So, it is apparent from the XRD data that the onset temperature of rutilation was

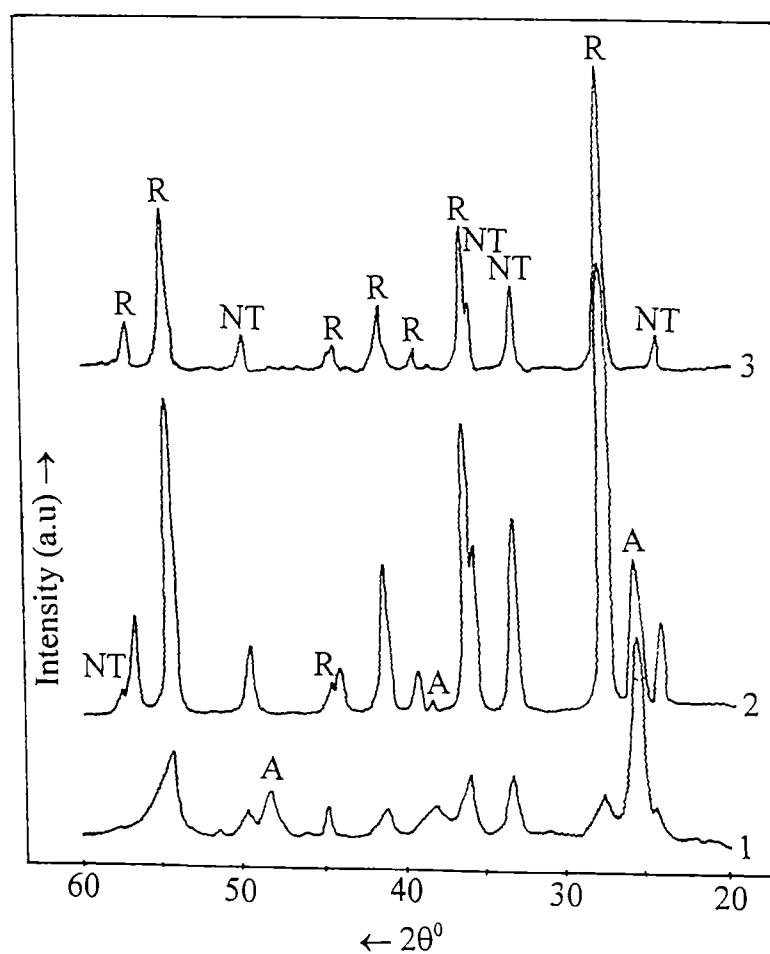


Fig. 4.4. XRD patterns of CN3 calcined at 1) 600, 2) 800 and 3) 900°C / 6hrs. (A = anatase, R = rutile and NT = NiTiO₃).

lower in co-precipitated ones. When the calcination temperature was increased to 800°C, the intensity of rutile peaks increased and that of anatase decreased. On increasing further to 900°C in CN3 and 1000°C in IN3 and WN3, all the anatase peaks disappeared and rutile peaks became

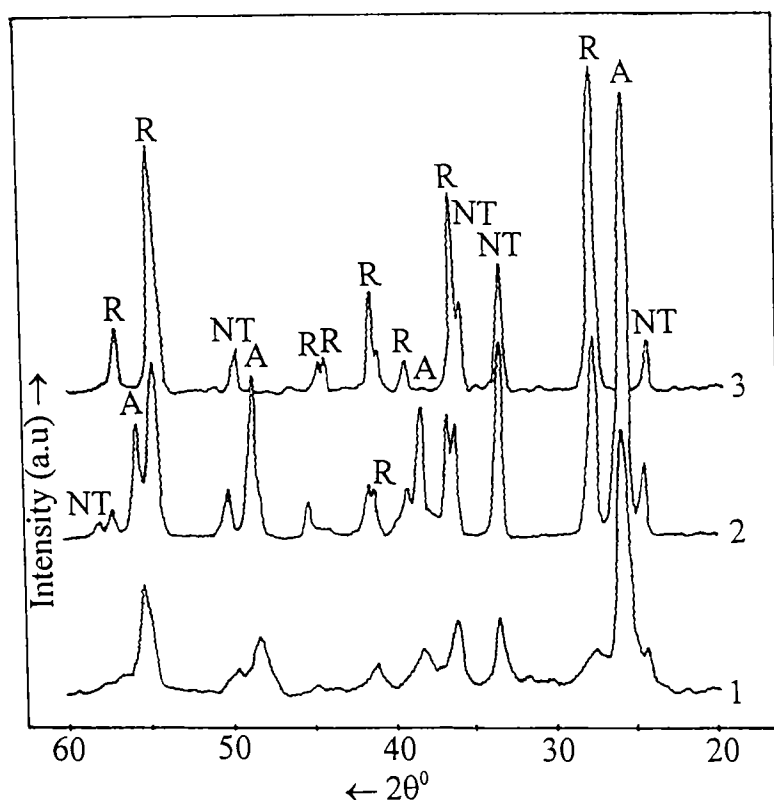


Fig. 4.5. XRD patterns of IN3 calcined at 1) 700, 2) 800 and 3) 1000°C / 6hrs. (A = anatase, R = rutile & NT = NiTiO₃).

more predominant. Marked changes could be seen in the characteristic peaks of anatase at d-value 3.52Å⁰ and that of rutile at d-value 3.23Å⁰. The percentage of rutile in CN3, IN3 and WN3 was calculated and the

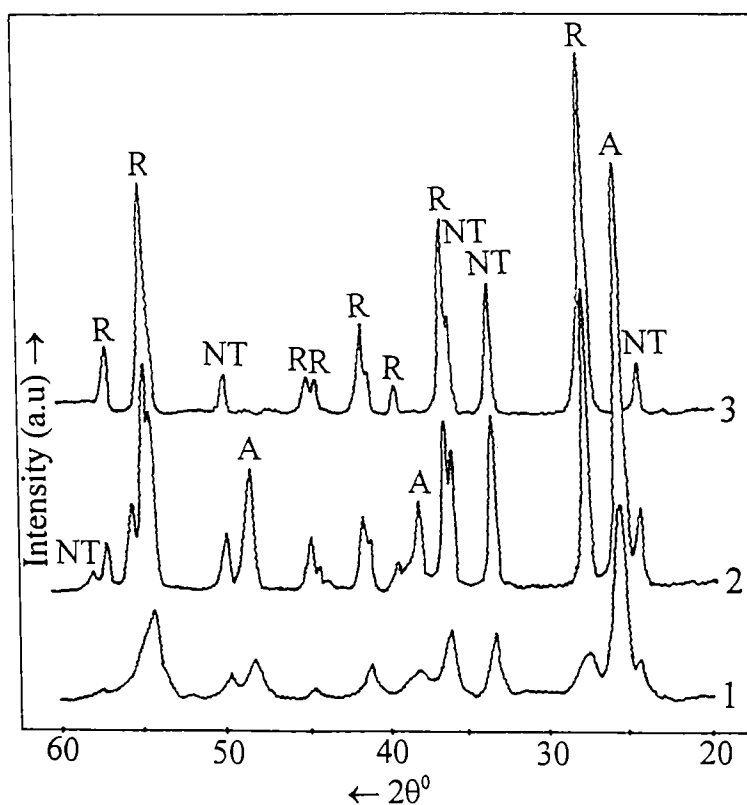


Fig. 4.6. XRD patterns of WN_3 calcined at 1) 700, 2) 800 and 3) 1000°C / 6hrs. (A = anatase, R = rutile & NT = NiTiO_3).

results are shown in Fig. 4.7. Among all the samples, the co-precipitated one has highest rutile percentage at any temperature and lowest for ion-exchanged one. So, the preparation method and NiO percentage have marked influence on rutile phase formation.

On comparing with bare TiO_2 , where the onset and completion temperatures of rutilation were 700°C and 1000°C in TiO_2 prepared by thermal hydrolysis and 800°C and 1200°C in TiO_2 prepared

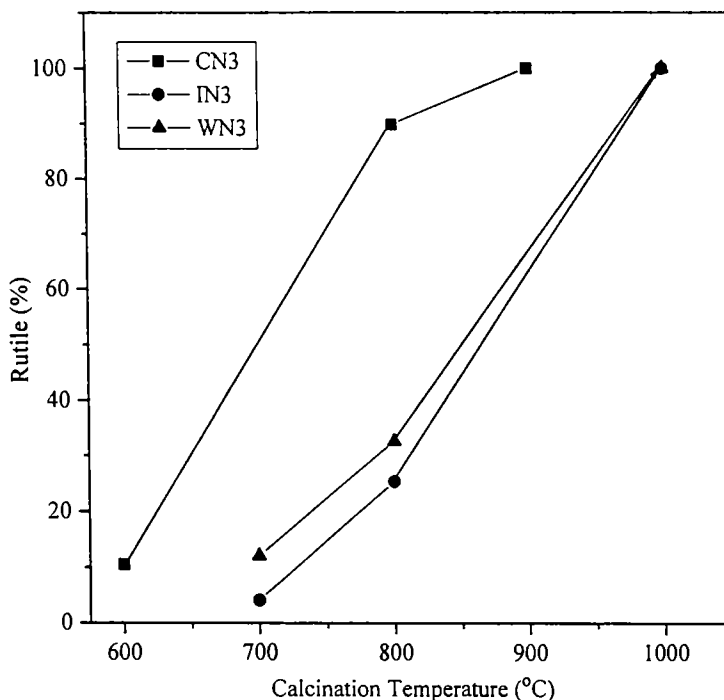


Fig.4.7. Variation in rutile (%) with calcination temperature of NiO/TiO₂ catalyst prepared by different methods

by hydrazine precipitation, it is very clear that in ion exchanged and wet-impregnated ones there were no changes in these temperatures, whereas in co-precipitated one, both the onset and completion temperatures were reduced much.

It is noteworthy that, at the onset of rutilation, some peaks due to NiTiO₃ were also present in the pattern. On increasing the calcination temperature, the intensity of these peaks also increased.

The XRD pattern of CN3, IN3 and WN3 after catalysis is given in Figs 4.1 – 4.3. No phase changes could be observed in any of the sample. This reflects the thermal stability of these catalysts under the conditions adopted.

The crystallite size of anatase (not particle size) calculated from XRD data are given in Table 4.1. Crystallite size calculations were

Table 4.1 Variation in crystallite size of anatase with calcination temperature of NiO/TiO₂ samples.

Method of preparation	NiO (%)	Sample label	Crystallite size (nm)				
			350 ^o C	450 ^o C	600 ^o C	700 ^o C	800 ^o C
Co-ppion	4.98	CN1	Amorphous	10.98	11.82	---	---
	9.93	CN2		10.26	11.82	---	---
	14.96	CN3		9.63	11.82	---	31.6
I.E	4.96	IN1	10.26	---	---	15.37	---
	9.98	IN2	10.26	---	---	15.37	---
	14.94	IN3	10.26	---	13.97	15.37	19.3
W.I	4.92	WN1	10.26	---	---	13.97	---
	9.95	WN2	10.26	---	---	15.37	---
	14.97	WN3	10.26	---	13.97	17.1	22.18

done only at certain calcination temperatures at which drastic changes occurred. No change in crystallite size was observed in ion-exchanged and wet-impregnated samples on increasing NiO percentage, while in co-precipitated ones, the crystallite size decreased on increasing NiO percentage. It would be due to the suppression of titania grain growth by extremely fine NiO particles uniformly dispersed on TiO₂. On increasing the calcination temperature, the crystallite size was also increased in all the samples, but to different extent. In co-precipitated ones, at the onset of rutilation, the crystallite size was 11.82nm, while in ion-exchanged one it was 15.37nm and in wet-impregnated one 17.1nm. So, the rutilation takes place after the enlargement of anatase crystallites and the growth in crystallite size is highly dependent on method of preparation. The anatase crystallites are larger in NiO loaded samples than that in bare titania.

4.2 Surface area studies

The results are shown in Figs 4.8 – 4.10. The co-precipitated samples have got largest surface area even though prepared at 450⁰C. The surface area increased in co-precipitated and ion-exchanged ones and decreased in wet-impregnated samples on increasing the percentage of NiO, which is in agreement with crystallite size results given in Table 4.1. In sample CN1 the surface area was 94.39 m²/g and it increased to 119.06 m²/g in CN2 and 130.2 m²/g in CN3. Similarly, in sample IN1 the surface area was 78.4 m²/g, in IN2 it became 87.2 m²/g and in IN3 it again increased to 90.3 m²/g. While in sample WN1, it was 91.8 m²/g, but it decreased in WN2 to 80.5 m²/g and to 65.26 m²/g in WN3. Hence the

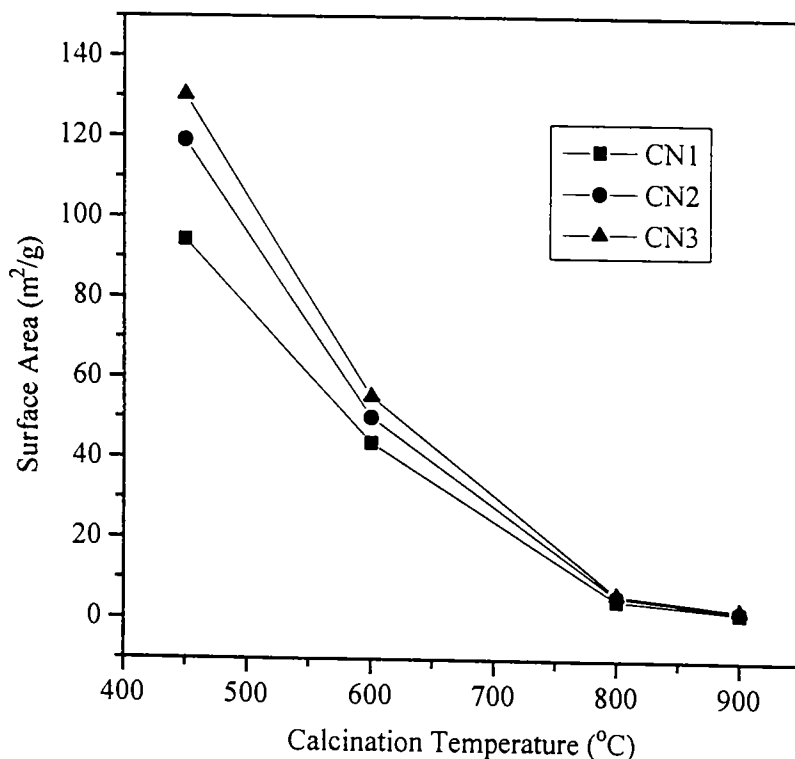


Fig 4.8. Effect of calcination temperature on surface area of NiO/TiO₂ catalysts prepared by co-precipitation method

change in surface area with increase in NiO percentage is highly influenced by preparation method.

On increasing calcination temperature, there occurred a marked decrease in surface area in all the samples. When the calcination temperature was increased to 600⁰C, in sample CN1, the surface area became nearly half of the earlier value, i.e. 43.8 m²/g, like wise, in the case of CN2 and CN3, it became 50.12 m²/g and 55.28 m²/g respectively. In ion exchanged and wet-impregnated samples, the surface area became

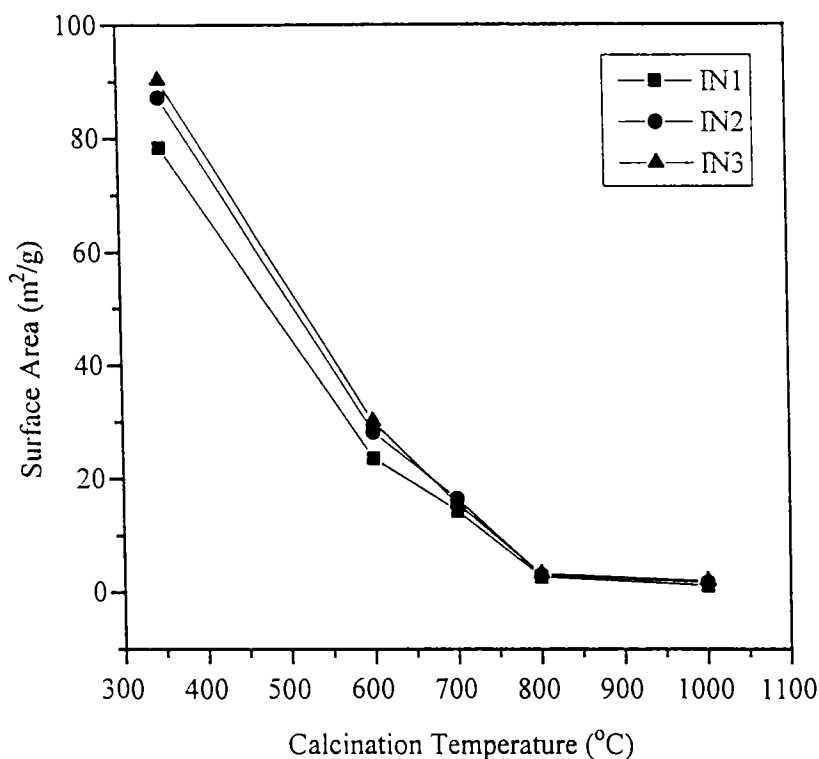


Fig.4.9. Effect of calcination temperature on surface area of NiO/TiO₂ catalysts prepared by ion-exchange method

one third when the calcination temperature was increased to 600⁰C and it again decreased at 700⁰C at which the rutilation was started. On increasing the temperature further to 800⁰C, the surface area was reduced very much in all the samples. At 900⁰C, when the TiO₂ was fully converted to rutile in co-precipitated samples, the surface area of CN1, CN2 and CN3 became 2.01 m²/g, 2.32 m²/g and 2.74 m²/g respectively. Similarly at 1000⁰C the surface area was reduced to 1.12 m²/g, 1.71 m²/g and 1.97 m²/g in samples IN1, IN2 and IN3 respectively and 1.8 m²/g,

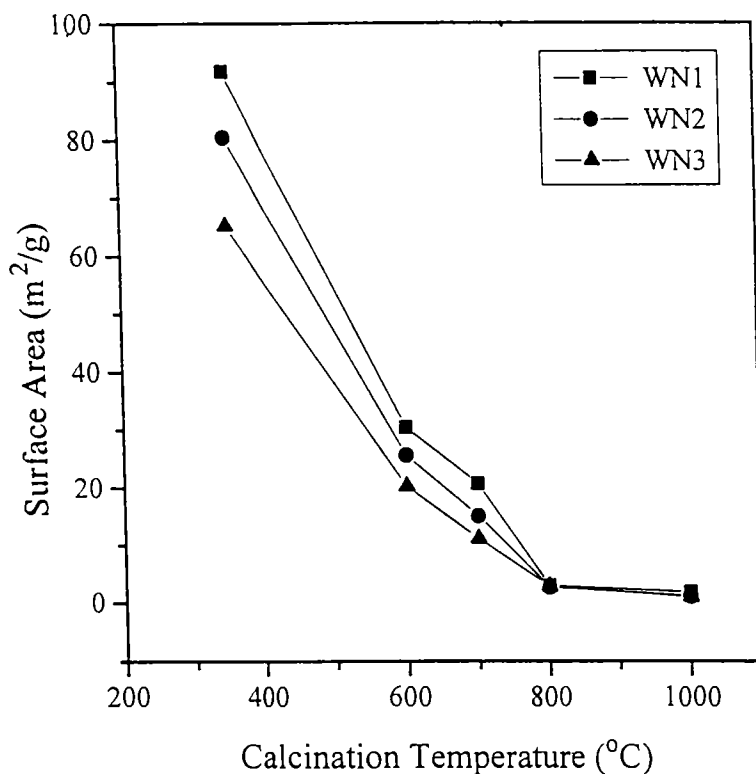


Fig 4.10. Effect of calcination temperature on surface area of NiO/TiO₂ catalysts prepared by wet-impregnation method

1.12 m²/g and 0.98 m²/g in samples WN1, WN2 and WN3 samples respectively. Even though no direct relation between crystallite size and surface area could be made, surface area decreased significantly along with marked increase in crystallite size. It is also evident that a very smaller change in crystallite size does not always necessarily involve a change in surface area. There was a decrease in surface area at the onset and completion of rutilation due to sintering and fusion of TiO₂ and NiO, to form NiTiO₃, which is in agreement with XRD data.

On comparing with surface area of bare TiO_2 , (vide Fig3.1) surface area decreased on loading NiO. It is obvious from the above observations that the surface area decreased drastically during rutilation, which in turn is dependent on method of preparation, calcination temperature and NiO percentage. The decrease in surface area during rutilation was also greater in presence of NiO compared to bare TiO_2 .

4.3 Dispersion studies

The results are shown in Table 4.2. Determination of dispersion of the catalytically active component on the surface of the support is one of the best ways to characterize supported catalysts. The dispersion was carried out at room temperature after reducing the sample at 390°C for 1hr. Comparatively better dispersion was obtained for co-precipitated samples, since they are precipitated from a homogeneous solution. As the NiO percentage was increased the dispersion decreased in all the samples. This reflects that a slight diffusion of Ni particles towards the bulk of the pellets would have occurred during reduction and the chance for such diffusion is obviously higher on increasing the percentage of NiO. Dispersion of 22.18% was obtained in sample CN1 and it decreased to 19.33% in CN2 and 16.64% in CN3. Similarly it decreased from 13.28% to 10.07% in ion exchanged ones and from 21.16% to 13.18% in wet-impregnated ones on increasing the NiO%

The surface average crystallite size of Ni calculated from dispersion data showed that it increased on increasing NiO percentage and nickel is present as very fine particles on the surface with size range

in nanometers. These results are in line with XRD data. No peaks due to NiO were seen, since the NiO particles were present in very fine form.

Table 4.2. Results of dispersion studies

Method of preparation	Sample label	Oxygen chemisorbed ($\mu\text{mol} / \text{g}$)	Dispersion (%)	Surface average crystallite size of Ni (nm)
Co-ppion	CN1	147.88	22.18	3.61
	CN2	256.99	19.33	4.14
	CN3	333.28	16.64	4.81
I.E	IN1	88.19	13.28	6.02
	IN2	144.44	10.81	7.40
	IN3	201.43	10.07	7.94
W.I	WN1	139.39	21.16	3.78
	WN2	203.02	15.24	5.25
	WN3	264.17	13.18	6.06

4.4 SEM analysis

SEM analysis of CN3, IN3 and WN3 samples before rutilation and CN3 after rutilation were carried out and the micrographs are shown in Figs 4.11 and 4.12. Only titania particles could be seen, which mirrors the presence of NiO as very fine particles, as supported by XRD and dispersion studies. The particles were all in a shapeless nature and were aggregated. The aggregation of particles is an evidence for the

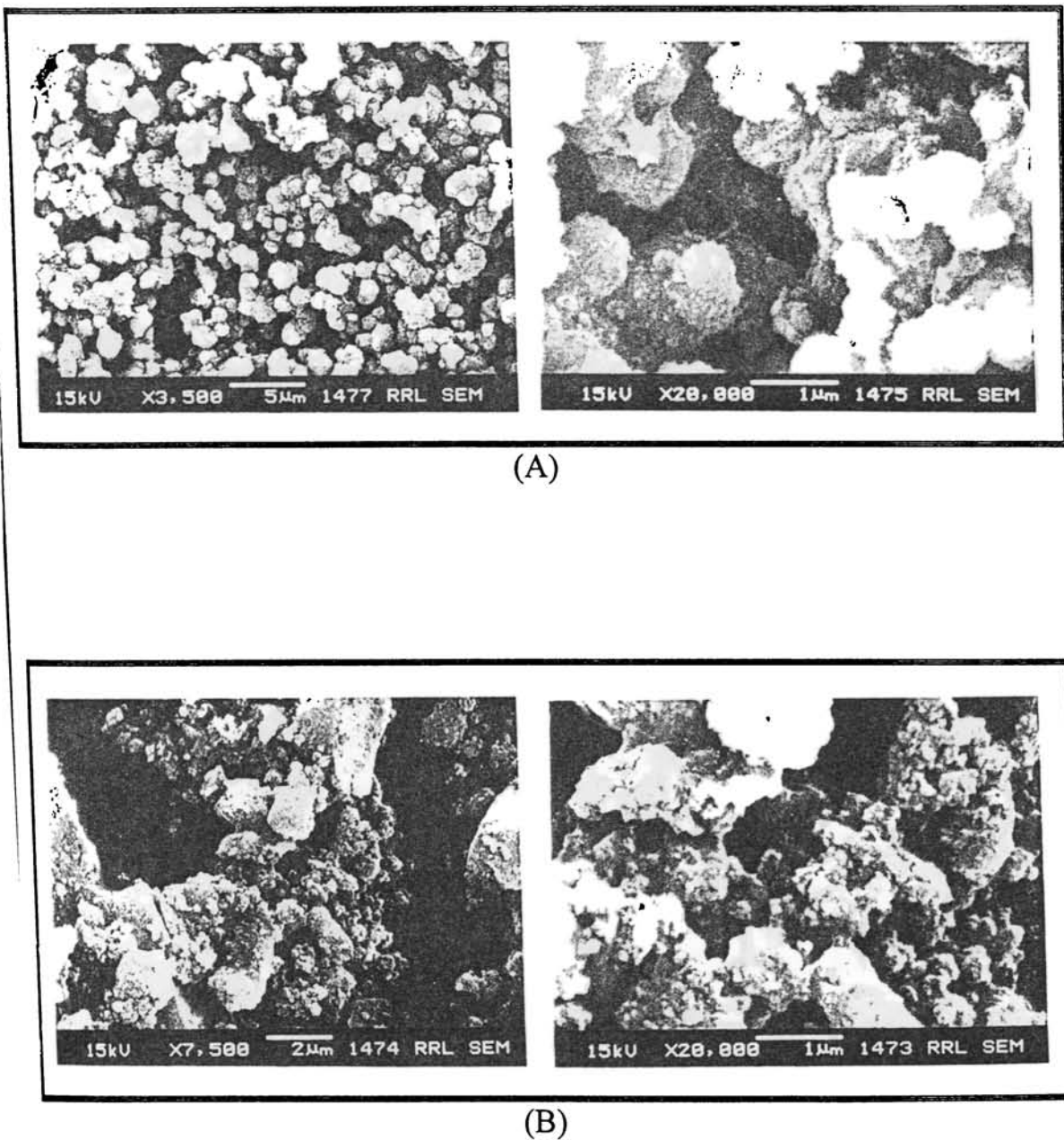
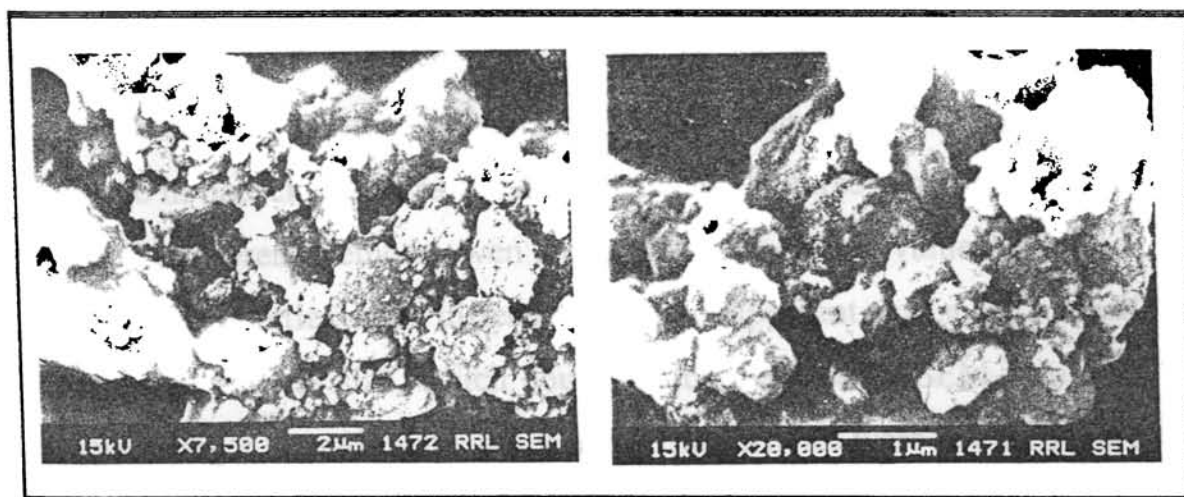
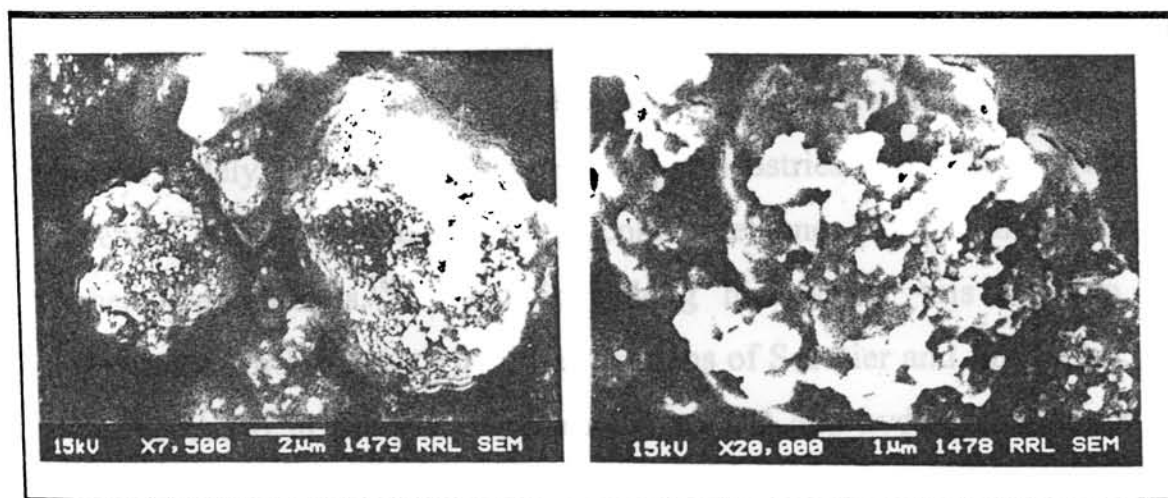


Fig. 4.11 Scanning electron micrographs of NiO/TiO₂ catalysts

A) IN3 and B) WN3 (calcined at 350⁰C)



(A)



(B)

Fig. 4.12 Scanning electron micrographs of NiO/TiO₂ catalysts

A) CN3 (calcined at 450⁰C and B) CN3 (calcined at 900⁰C)

fineness of the sample, because it has been reported that²⁸¹ the individual particles in a fine powder would be in an aggregated form (i.e. assemblages of particles which are loosely coherent). No appreciable change in particle size was observed between the three samples prepared through different methods, even though the surface area values and other physical properties were different. So, it is apparent that a very small change in particle size, which could not be detected in SEM, can also cause a larger alteration in surface area. The particles were in much more agglomerated state (i.e. assemblages of particles which are rigidly joined) when the TiO_2 was fully converted to rutile, which would be due to cementation and sintering of individual particles, which is in agreement with XRD and surface area studies.

4.5 Methanation activity studies

Carbon monoxide hydrogenation is a profoundly important process widely exploited by many chemical industries to produce a wide variety of organic compounds like, alcohol, methane, gasoline and other higher hydrocarbons.¹⁶⁰ There is a long history for this reaction, beginning from 1902, with the investigations of Sebatier and Senderens, who succeeded in producing methane from CO and hydrogen mixture over Ni catalyst. For this contribution and his work on catalytic hydrogenation, Sebatier won the Nobel Prize in Chemistry in 1912.¹⁶⁰ One year later, the German, Badische- Anilin- und Soda Fanrik (BASF) started to fabricate longer chain hydrocarbons and oxygenated hydrocarbons with the aid of Co-Os catalyst promoted with alkali metals. In 1923, BASF performed the first successful exclusive methanol

synthesis and three years later, Fischer and Tropsch described the formation of longer chain hydrocarbons from CO and hydrogen at 200^oC and at atmospheric pressure using Fe-Co catalysts doped with K and Cu as promoters.¹⁶⁰ It is a highly efficient method for producing fuels with high heating value from coal. By means of suitable choices of catalyst materials, one can control and direct the reaction to obtain the desired product. Hence it is an intensely pursued reaction even today. Methane is reported to form selectively over Ni catalyst.¹⁶⁰

The results of methanation activity studies are shown in Figs 4.13- 4.16. To optimize the reaction temperature the activity studies were

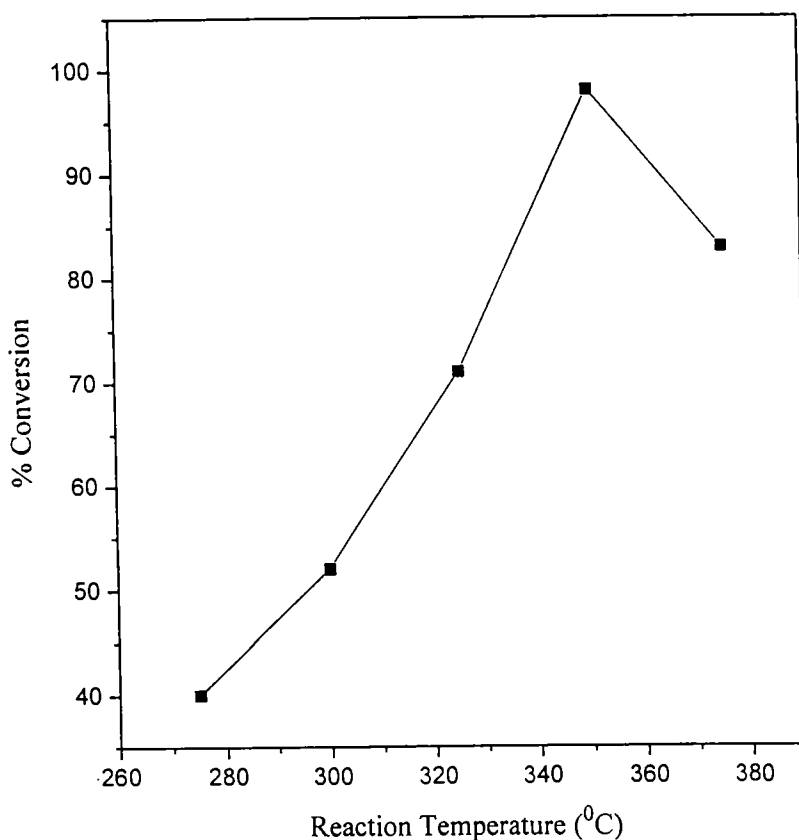


Fig.4.13. Variation in methanation activity of CN3 with reaction temperature

carried out at different temperatures ranging between 275⁰C and 375⁰C using the sample CN3, which is shown in Fig 4.13. Only 40% conversion was obtained at 275⁰C and the percentage conversion increased with increasing temperature of reaction. At 350⁰C, 98% conversion was obtained and on further increasing the reaction temperature the percentage conversion decreased to 83%. So, the activities of all the other samples were tested at 350⁰C. The percentage conversion was strongly influenced by temperature of reaction and maximum conversion was obtained at 350⁰C (vide Fig 4.13).

The methanation activity of co-precipitated and ion-exchanged catalysts increased much on increasing the NiO percentage due to the increase in surface area and increase in number of surface exposed nickel atoms. With sample CN1 90.8% conversion was obtained and it increased to 98% in CN2 and on further increase in NiO% there was no change in activity, i.e. with sample CN3 also 98% conversion was obtained. Much lower percentage conversion was observed with ion-exchanged samples; with IN1 63.8%, with IN2 66.2% and 68.1% with IN3. Whereas in wet-impregnated samples the percentage conversion decreased with increasing NiO%. 73.8% conversion of was obtained with the sample WN1, 71.8% with WN2 and 64.1% using WN3. So, it is very important to note that this reaction is highly influenced by the quantity of nickel atom present on the surface of the catalyst and the surface area of the sample. It has been reported²⁸² that a significant variation occurs in methanation activity with change in dispersion and metal concentration. But, the activity of wet-impregnated ones decreased

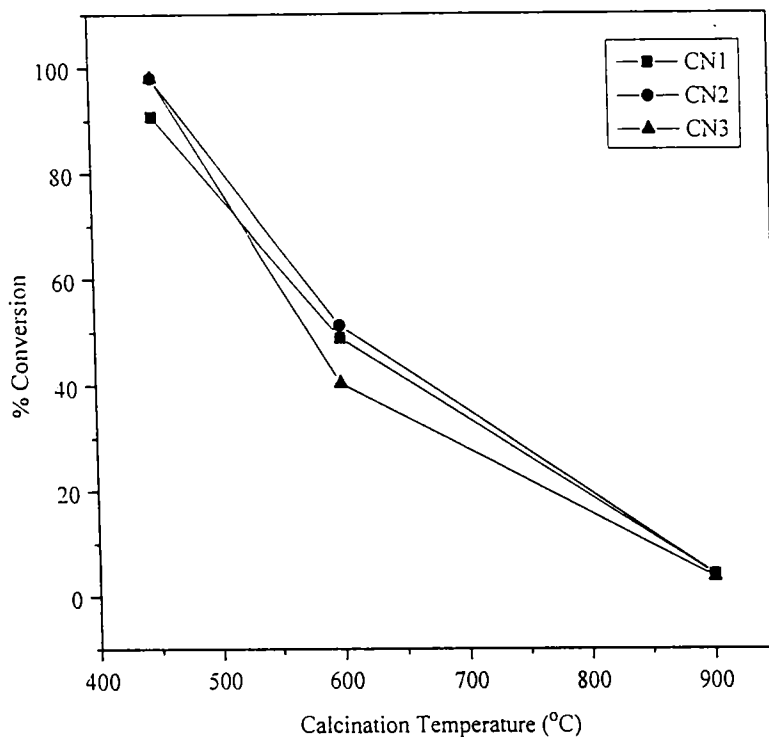


Fig.4.14. Variation in methanation activity with calcination temperature of NiO/TiO₂ catalysts prepared by co-precipitation method

on increasing percentage of NiO due to a noticeable decrease in surface area in these samples on increasing the percentage of NiO. So, it is evident that, the surface area of the catalyst is also equally important as dispersion to enhance the activity. No solid relation could be made between surface average crystallite size of nickel and activity of the catalyst. Hence this reaction can be considered as a structure in sensitive one. This is in line with the literature data.²⁸³

In order to investigate the effect of rutilation and changes in physical properties on the activity of these catalysts, the activity studies

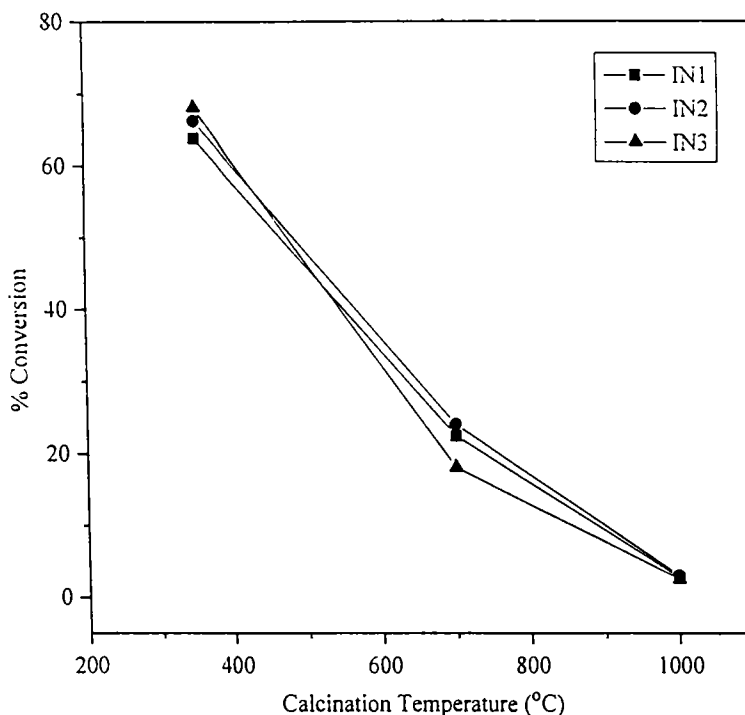


Fig.4.15. Variation in methanation activity with calcination temperature of NiO/TiO₂ catalysts prepared by ion-exchange method

were carried out after calcination of these samples at temperatures, when drastic changes in physical properties have occurred. The activity of these catalysts was altered on increasing the calcination temperature. The percentage conversion was nearly halved in co-precipitated ones and it became one third or less in ion-exchanged and wet-impregnated ones at the onset of rutilation. When the samples were fully rutilated the percentage conversion became very much lowered to less than 5% in all the samples as evidenced by Figs 4.14 – 4.16. The severe reduction observed in activity upon rutilation could be due to the following reasons,

R
546.821:66.097
AHM.

G8299

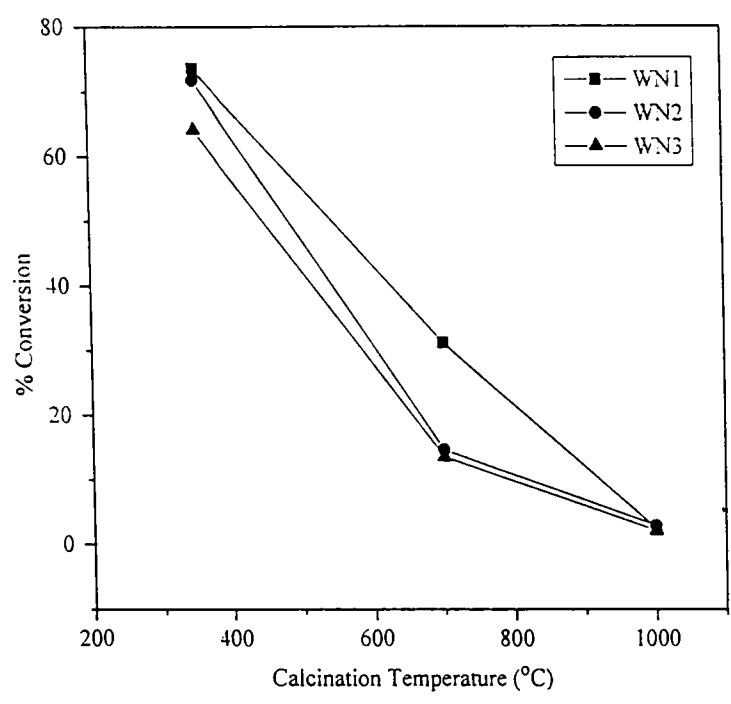
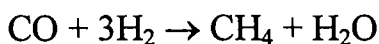


Fig. 4.16. Variation in methanation activity with calcination temperature of NiO/TiO₂ catalysts prepared by wet-impregnation method

i) the shortage of enough free Ni atoms on the surface due to sintering and NiTiO₃ phase formation, ii) the incompleteness of reduction of NiTiO₃ in to Ni and TiO₂ under the conditions adopted iii) the increased possibility for strong-metal-support-interaction in the reduced state during the reduction of NiTiO₃, iv) the irreversible conversion of the support to rutile and v) the much lower surface area of these samples. It has been reported that the strong-metal-support-interaction (SMSI) is drastically changing the properties of Ni/TiO₂ catalyst²⁸⁴ and it has also been reported that this reaction is significantly influenced by support material.^{43&285-287}

The product formed was selectively methane. Hence the reaction would have proceeded through dissociative addition mechanism with carbidic carbon intermediate.¹⁶⁰ The proposed reaction is:



Hence, the presence of even a very low percentage of rutile on the support can affect badly the activity of this catalyst. The co-precipitated ones are the best among these catalysts for methanation, even though they have lower onset temperature of rutilation, which is well above the optimum temperature of methanation. So, it is worth to note that, only by using pure anatase as a support, the effect of rutile phase, on activity could be investigated. Most or almost all investigations on this catalyst prepared through other methods described in literature, were found to be carried out on TiO₂ having both anatase and rutile phases.

In this investigation, since the 'CO pulse method' was adopted to study the methanation activity (of the samples prepared through different methods and the changes occurring in activity upon rutile phase formation), the percentage conversion was studied instead of the rate of the reaction. For the same reason it was not possible to compare with other studies reported in literature, where the rate and turn over frequency are only mentioned instead of percentage conversion. However, it is apparent from this study that the methanation activity has been reduced much upon rutilation and the activity was strongly influenced by quantity of nickel present on the surface and surface area of the sample, which in turn is dependent on method of preparation. But most of the studies reported in literature do not consider or account for

the presence of rutile phase in TiO_2 support. However, in the case of samples prepared in this study, it is very clear that rutile phase formation take place only at very high temperature, which is well above the optimum temperature of methanation and hence should be superior to the catalysts reported in literature as the properties deteriorate on rutilation.

4.6 Conclusions

- ☐ The co-precipitated samples crystallize at 450°C , while ion-exchanged and wet-impregnated ones crystallize at 350°C .
- ☐ Onset and completion temperatures of rutilation were found to vary with method of preparation.
- ☐ At the onset of rutilation NiTiO_3 phase is also formed.
- ☐ Better surface area, dispersion and activity are obtained with co-precipitated ones. Ion-exchange and wet-impregnation methods also gave better properties compared to conventional methods.
- ☐ Method of preparation, calcination temperature, rutilation and NiO percentage have greater role in determining surface area.
- ☐ Enhancement of rutilation by same metal oxide varies with method of preparation.
- ☐ Crystallite size enlargement takes place during rutile phase formation.
- ☐ Methanation activity significantly reduces at the onset of rutilation and drastically when the TiO_2 is fully converted to rutile.

- ☐ All these samples were found to be thermally stable under the conditions adopted for methanation.
- ☐ The order of methanation activity is: co-precipitated > wet-impregnated > ion exchanged samples.

Chapter 5

STUDIES ON Fe₂O₃/TiO₂ CATALYSTS

Iron is an important catalyst in various commercially exploited processes, like ammonia synthesis, F-T synthesis, water gas shift reactions, etc. The products obtained in F-T synthesis using Fe catalyst are reported to be highly olefinic in nature.²⁸⁸ But, the unsupported catalysts have poor attrition resistance²⁸⁸ and in F-T synthesis, the major operational problem is separation of catalyst and wax in a slurry reactor.²⁸⁸ Hence, there have been extensive investigations on supported Fe catalysts. Iron supported on TiO₂ is reported to be highly active in Koebel – Engelhardt synthesis of hydrocarbon,²⁸⁹ ammonia synthesis,⁵⁹ reaction between carbon monoxide and hydrogen,¹⁶² while iron oxide supported on TiO₂ in presence of Sb₂O₃ is reported to be an excellent catalyst for oxidation of propylene to acrolein.²²⁰

Many efforts have been made for preparing highly dispersed Fe catalysts on high surface area TiO₂. But, unfortunately, only a few methods for the preparation of these catalysts are available in literature (see section 1.6.2.).

Fe₂O₃/TiO₂ catalyst with different percentages of Fe₂O₃ was prepared using the three methods, which are described in Chapter 2. The samples prepared by co-precipitation were labeled as CF1, CF2 and CF3. The ion-exchanged ones were labeled as IF1, IF2 and IF3 and wet-impregnated ones as WF1, WF2 and WF3. The percentage of Fe₂O₃ in

each sample is given in Table 5.1. This catalyst can be used as Fe/TiO₂ by reducing at 400°C in hydrogen stream.

5.1 XRD studies

XRD pattern of ion exchanged and wet-impregnated samples calcined at 350°C/6hrs showed that these samples are crystalline at 350°C, where as the co-precipitated one, unlike NiO/TiO₂, was not crystalline even at 450°C (vide Figs 5.1- 5.3). The co-precipitated ones became crystalline only by calcination at 550°C/6hrs. All the peaks were due to the anatase phase of TiO₂ and no peaks due to Fe₂O₃ appeared in the pattern, obviously due to the fineness of iron oxide particles. While

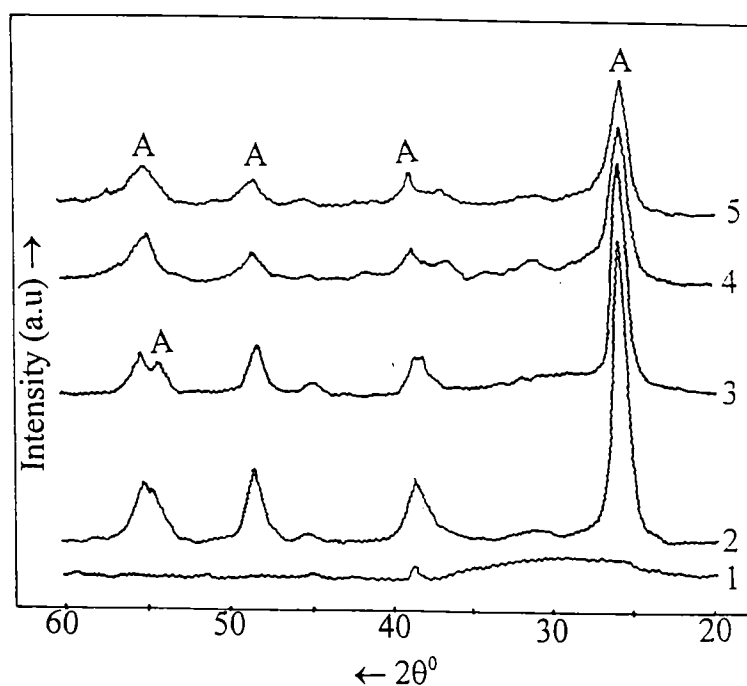


Fig. 5.1. XRD pattern of Fe₂O₃/TiO₂ samples prepared by co-precipitation method 1) CF3 calcined at 450°C / 6hrs., 2) CF1, 3) CF2, 4) CF3 calcined at 550°C / 6hrs. & 5) CF3 after catalysis. (A = anatase).

comparing the crystallization temperature of pure TiO_2 prepared by both the methods, a change has been observed in Fe_2O_3 loaded sample prepared by co-precipitation. Pure TiO_2 prepared by hydrazine precipitation was found to crystallize at 450°C , whereas in presence of

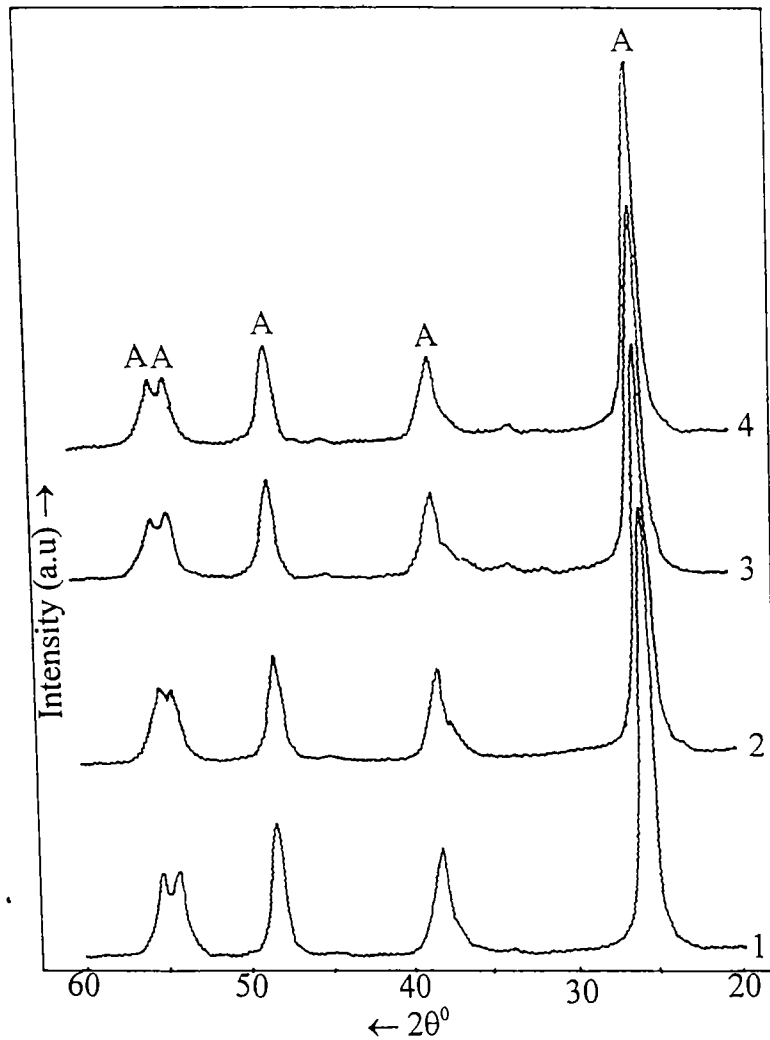


Fig. 5.2. XRD pattern of $\text{Fe}_2\text{O}_3/\text{TiO}_2$ samples prepared by ion-exchange method - calcined at 350°C / 6hrs. 1) IF1, 2) IF2, 3) IF3 and 4) IF3 after catalysis (A = anatase).

Fe_2O_3 , the crystallization temperature has been altered to 550°C . So, the presence of Fe_2O_3 has a strong influence on the crystallization of the co-precipitated sample.

On increasing the calcination temperature up to 650°C in sample CF3, peaks of rutile appeared in the pattern and on further increase, the rutile peaks became more intense and anatase peaks

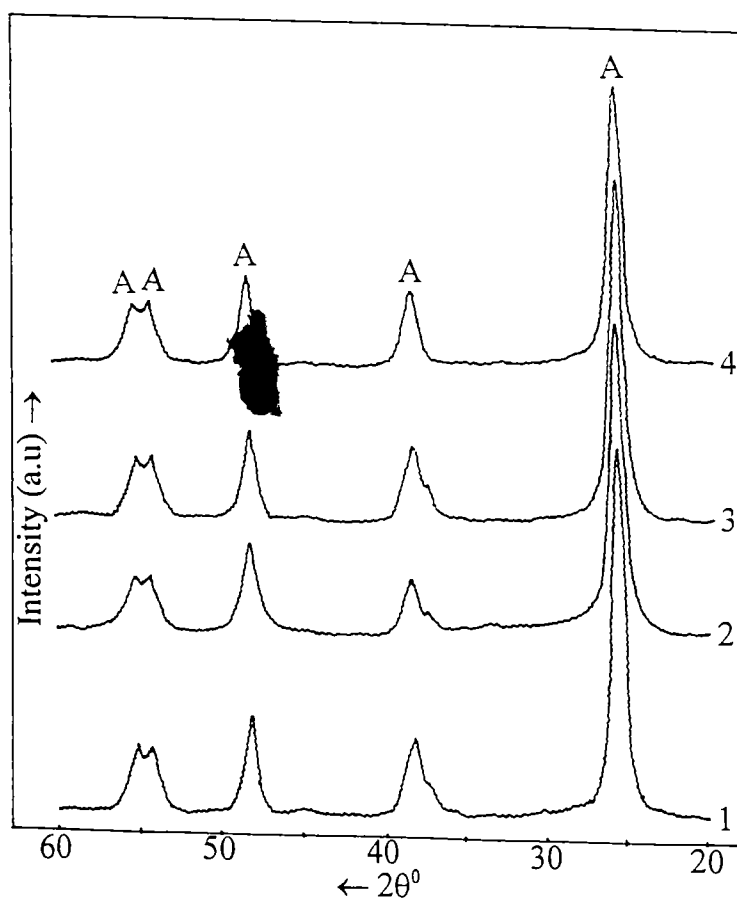


Fig. 5.3. XRD pattern of $\text{Fe}_2\text{O}_3/\text{TiO}_2$ samples prepared by wet-impregnation method- calcined at 350°C / 6hrs. 1) WF1, 2) WF2, 3) WF3 & 4) WF3 after catalysis (A = anatase).

disappeared from the pattern, similar to that of NiO/TiO₂. The patterns are given in Figs 5.4 – 5.6. The sample CF3 got rutiled completely at 800^oC itself, where as in the sample IF3, the rutilation started only at 800^oC and completed at 1000^oC, while in WF3, rutile phase appeared in the pattern at 700^oC and the rutilation was complete at 900^oC. So, it is obvious from all these observations that Fe₂O₃ influences the rutile phase formation to different extents in samples prepared through different routes. The rutile percentage against calcination temperature of samples CF3, IF3 and WF3 is given in Fig 5.7. Here also, like NiO/TiO₂ samples,

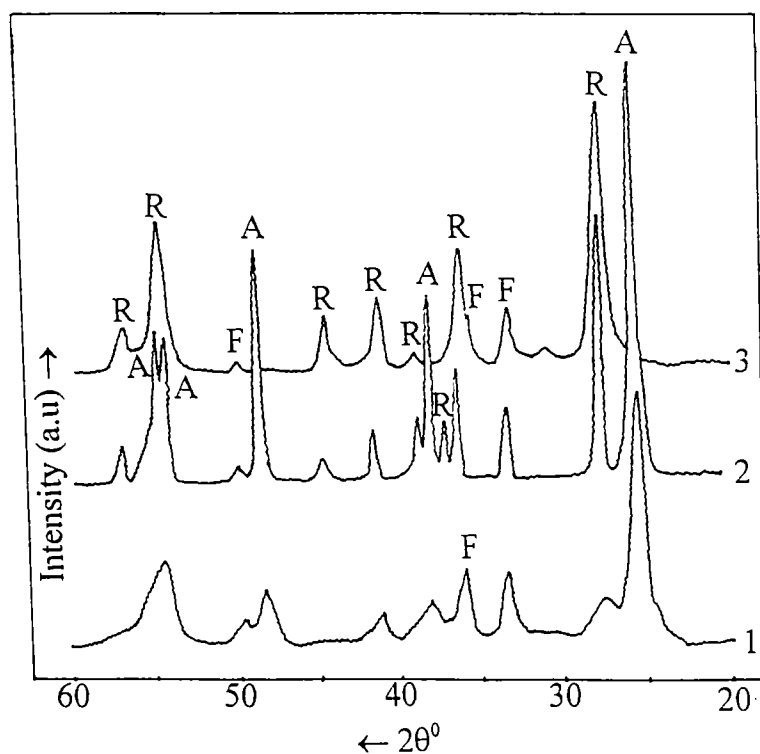


Fig. 5.4. XRD patterns of CF3 calcined at 1) 650, 2) 700 and 3) 800^oC / 6hrs. (A = anatase, R = rutile and F = α Fe₂O₃).

the onset and completion temperatures of rutilation were much lower in co-precipitated ones. The Fe_2O_3 influences noticeably the rutilation temperature in co-precipitated samples. Hence it can be inferred that the presence of Fe_2O_3 during the crystallization of TiO_2 would enhance the formation of rutile, to different extent depending on the method of preparation. If the distribution of Fe_2O_3 were more uniform, the chance for rutilation would also be higher.

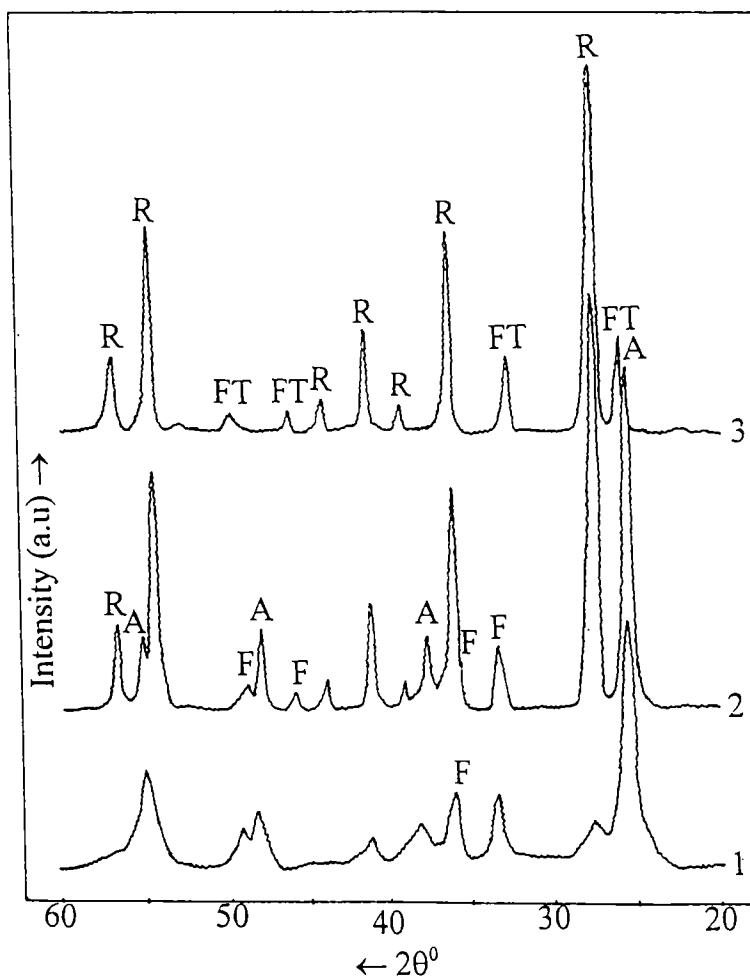


Fig. 5.5. XRD patterns of IF3 calcined at 1) 800, 2) 900 and 3) 1000°C / 6hrs. (A = anatase, R = rutile, F = $\alpha\text{-Fe}_2\text{O}_3$ and FT = Fe_2TiO_5).

The peaks of α -Fe₂O₃ appeared only when the rutilation was started in all the samples, which might be due to the growth of Fe₂O₃ particles during rutilation. α -Fe₂O₃ particles reacts with TiO₂ to form pseudo brookite (Fe₂TiO₅) and the remaining TiO₂ transforms irreversibly to rutile in the case of samples IF3 and WF3, while in the case of CF3, the intensity of α -Fe₂O₃ peaks increases at this stage and no pseudo brookite peaks were formed.

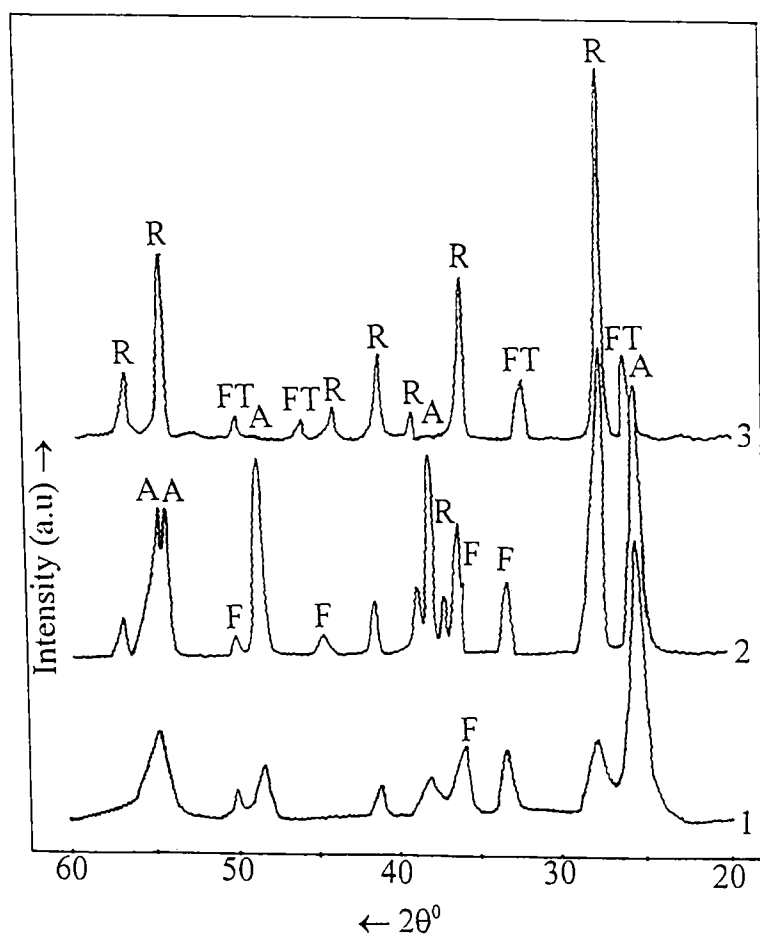


Fig. 5.6. XRD patterns of WF3 calcined at 1) 700, 2) 800 and 3) 900°C / 6hrs. (A = anatase, R = rutile, F = α Fe₂O₃ and FT = Fe₂TiO₅).

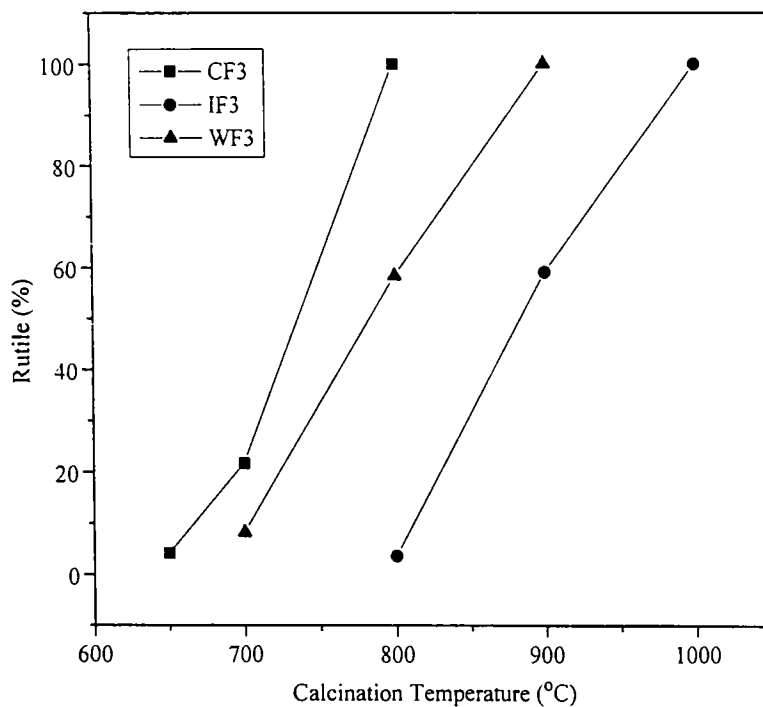


Fig. 5.7. Variation in rutile (%) with calcination temperature of $\text{Fe}_2\text{O}_3/\text{TiO}_2$ catalyst prepared by different methods

The XRD patterns of CF3, IF3 and WF3 samples after catalytic activity studies are shown in Figs 5.1 – 5.3. There is no change in the patterns when compared to that of the samples prior to the activity studies. This suggests that the samples are thermally stable under the conditions adopted for toluene oxidation.

The crystallite size of anatase calculated from XRD data is given in Table 5.1. The crystallite size was calculated only at temperatures at which major changes occurred in the samples so that the

rest of the columns are kept vacant in Table 5.1. Crystallite size decrease was found on increasing percentage of Fe_2O_3 in co-precipitated and ion-exchanged samples, while it increased in wet-impregnated ones. The crystallite size was reduced more than that of pure TiO_2 in sample CF3 and It increased with increasing temperature, but to different degree, depending on the method of preparation. The rutilation starts in co-precipitated samples when the anatase crystallites grow to a size of 12.8nm, while in the case of ion-exchanged and wet-impregnated ones the transformation happens at 15.37nm.

Table 5.1 Variation in crystallite size of anatase with calcination temperature of $\text{Fe}_2\text{O}_3/\text{TiO}_2$ samples

Prepn method	Sample label	Fe_2O_3 (%)	Crystallite size (nm)					
			350 ^o C	550 ^o C	650 ^o C	700 ^o C	800 ^o C	900 ^o C
Co-ppn	CF1	4.98	Amorphous	9.63	10.98	---	---	---
	CF2	9.97		9.63	10.98	---	---	---
	CF3	14.95		7.37	12.79	17.1	---	---
I.E	IF1	4.95	12.79	---	---	---	13.97	---
	IF2	9.98	11.82	---	---	---	13.97	---
	IF3	14.99	10.98	---	---	---	15.37	17.1
W.I	WF1	4.99	9.63	---	---	12.79	---	---
	WF2	9.94	10.26	---	---	13.97	---	---
	WF3	14.97	10.98	---	---	15.37	---	22.18

5.2 Surface area studies

The surface area values plotted against calcination temperature are given in Figs 5.8 – 5.10. The values increased on increasing Fe_2O_3 percentage in co-precipitated and ion-exchanged samples. In the case of co-precipitated samples, surface area was $101.4 \text{ m}^2/\text{g}$, $118.7 \text{ m}^2/\text{g}$ and $141.1 \text{ m}^2/\text{g}$ in CF1, CF2 and in CF3 respectively. Similarly, for IF1 it was $85.3 \text{ m}^2/\text{g}$, for IF2 it became $95.3 \text{ m}^2/\text{g}$ and for

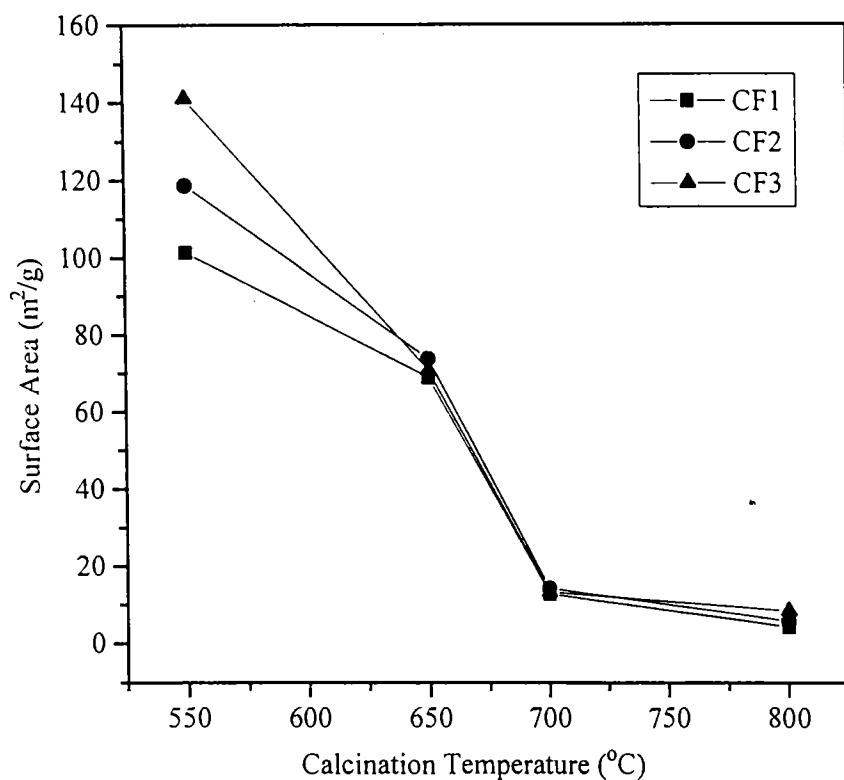


Fig. 5.8. Effect of calcination temperature on surface area of $\text{Fe}_2\text{O}_3/\text{TiO}_2$ catalysts prepared by co-precipitation method

IF3 the surface area again increased to 108.3 m²/g. In the case of wet-impregnated ones, the surface area decreased on increasing the percentage of Fe₂O₃ (For WF1 the surface area was 118.0 m²/g and it decreased to 113.0 m²/g in WF2 and 106.3 m²/g in WF3). More predominant change was observed in co-precipitated ones. This is in agreement with crystallite size of anatase, which is found to decrease on increasing Fe₂O₃ percentage. At this point, it would be noteworthy that the co-precipitated samples are prepared at 550^o C and even then they

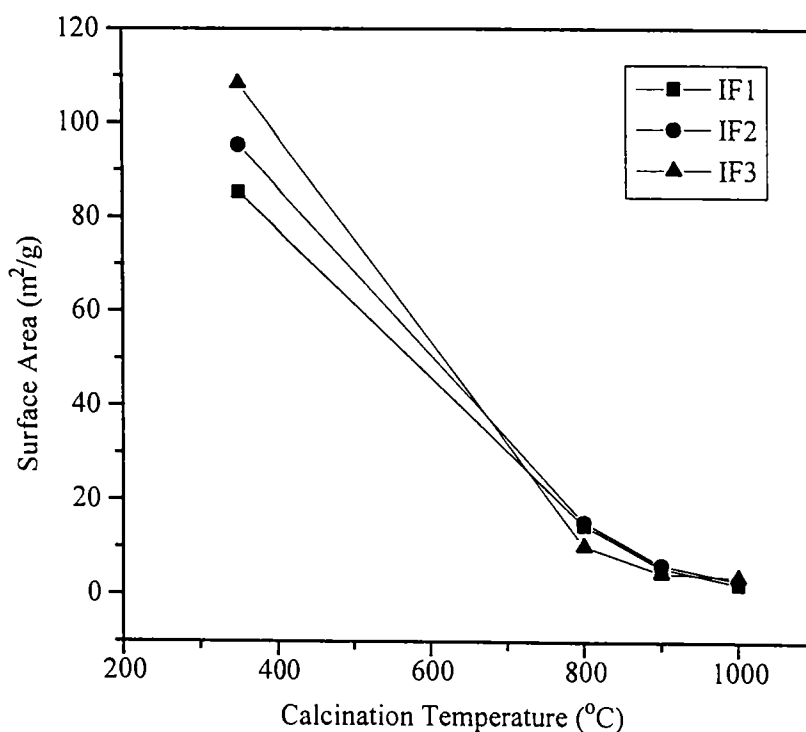


Fig. 5.9. Effect of calcination temperature on surface area of Fe₂O₃/TiO₂ catalysts prepared by ion-exchange method

possess comparatively larger surface area, even better than pure TiO_2 .

On further increasing the calcination temperature to 650°C in co-precipitated ones, the surface area became $68.9 \text{ m}^2/\text{g}$ in CF1, $73.7 \text{ m}^2/\text{g}$ in CF2 and $70.8 \text{ m}^2/\text{g}$ in CF3. The decrease was much greater for CF3, which would be due to the presence of 4.2 % rutile in this sample. On increasing the temperature further the decrease in surface area was drastic. At 800°C , when rutilation was complete, the surface area became $4.2 \text{ m}^2/\text{g}$ in CF1, $5.7 \text{ m}^2/\text{g}$ in CF2 and $8.3 \text{ m}^2/\text{g}$ in CF3. These changes are evident from Fig. 5.8.

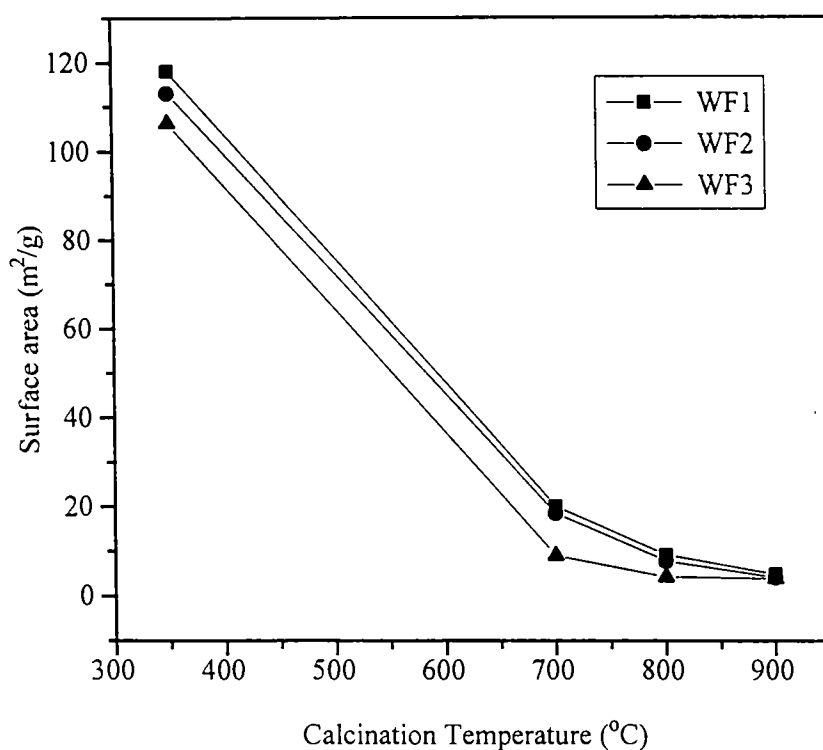


Fig. 5.10. Effect of calcination temperature on surface area of $\text{Fe}_2\text{O}_3/\text{TiO}_2$ catalysts prepared by wet-impregnation method

In the case of ion-exchanged samples, when the calcination temperature was raised to 800⁰C, the surface area decreased to 14.6 m²/g in IF1, 15.3 m²/g in IF2 and 10.2 m²/g in IF3. The much higher decrease in surface area observed in IF3 would be due to the presence of 3.59 % rutile. On further rise in calcination temperature, the surface area decreased markedly in all the samples and at 1000⁰C, it became 2.2 m²/g in IF1, 2.9 m²/g in IF2 and 3.7 m²/g in IF3 (vide Fig. 5.9).

Similarly, in wet-impregnated samples calcined at 700⁰C, (at which the rutilation was started in WF3) the surface area became 20.1 m²/g in WF1, 18.5 m²/g in WF2 and 8.98 m²/g in WF3. Significant decrease in surface area was observed when the calcination temperature was increased to 900⁰C (at which rutilation was complete in WF3). The values were 4.87 m²/g, 4.21 m²/g and 3.91 m²/g in WF1, WF2 and WF3 samples respectively. These changes in surface area are shown in Fig 5.10.

Here, in these samples, crystallite size of anatase seems to have some relation with surface area, unlike in the case of NiO/TiO₂ samples. It decreased on increasing surface area in all the samples depending on the method of preparation. So, Fe₂O₃ has a significant influence on the surface area of these samples. The decrease in surface area with increase in rutile percentage was also larger in presence of Fe₂O₃.

5.3 Dispersion studies

The Fe₂O₃ exposed on the surface of Fe₂O₃/TiO₂ catalyst is normally determined by CO chemisorption. Carbon monoxide is reported

to be more effectively associated with Fe particles at 0°C.^{59&125} As the percentage of Fe₂O₃ was increased, the quantity of the chemisorbed CO increased and hence the percentage dispersion also increased.

Since, the surface average crystallite size was inversely proportional to CO chemisorbed, it decreased on increasing the percentage of Fe₂O₃ in all the samples. These results are shown in Table 5.2. Maximum percentage dispersion was obtained in sample CF3 and minimum in WF1. Out of all these samples the co-precipitated ones

Table 5.2. Results of dispersion studies.

Prepn method	Sample label	CO chemisorbed (μmol / g)	Dispersion (%)	Surface average crystallite size of Fe (nm)
Co-ppn	CF1	9.98	3.2	25.00
	CF2	27.47	4.4	18.18
	CF3	57.11	6.1	13.11
I.E	IF1	9.24	2.98	26.85
	IF2	20.75	3.32	24.10
	IF3	36.23	3.86	20.72
W.I	WF1	8.22	2.63	30.42
	WF2	18.11	2.91	27.49
	WF3	30.28	3.23	24.77

showed much higher dispersion and the wet-impregnated ones exhibited the lowest. The surface average crystallite size of iron, calculated from dispersion data, seems to be much larger. It ranged between 13.11 nm and 30.42 nm, but it is not correlated with XRD data, where no peaks due to Fe_2O_3 were obtained in any of the patterns, showing the fineness of Fe_2O_3 particles. However, similar observations can be seen in other studies,^{164,290&291} where the authors argued that the surface average crystallite size calculated from CO chemisorption often disagrees with XRD results.

Like NiO/TiO₂ samples, here also, better dispersion was obtained for co-precipitated ones, but the percentage dispersion was much lower compared to NiO/TiO₂. However, by using CO chemisorption method, similar or much lower values are reported in literature with these catalysts prepared through wet-impregnation on TiO₂ (Degussa p-25).^{162&164} A plausible explanation for this would be the diffusion of reduced iron particles towards the bulk of the pellet during the course of reduction, thereby reducing the number of iron atoms on the surface to chemisorb carbon monoxide.

5.4 Studies on toluene oxidation to benzoic acid (Gas phase)

The first change in benzoic acid preparation came in the 1850s when hippuric acid ($\text{C}_6\text{H}_5\text{CONHCH}_2\text{COOH}$), from the urine of horses and cattle, replaced gum benzoin as the starting material. Hippuric acid was used extensively until 1870, when coal tar raw materials were utilized for the first time.^{270&292} Phthalic acid was also used as the raw material until 1890, when the hydrolysis of benzo trichloride took over the bulk production. This route and the route employing chlorination of

toluene to benzyl chloride and subsequent oxidation with HNO_3 to benzoic acid remained as the major production route until after World War I.^{270&292} After World War II, started another change in manufacturing technique of benzoic acid, as the air oxidation of toluene took hold in Germany and after the war, this method was carried over to US. The air oxidation in liquid phase using cobalt catalysts has now become the main manufacturing method in US. Considering the present and future petrochemical economic factors, it is difficult to fore see any commercial raw material other than toluene for benzoic acid production.^{270&292} The benzoic acid has got many industrial applications such as, in medicines, veterinary medicines, food and industrial preservatives, dye stuffs, synthetic fiber, etc.²⁷⁰

Air oxidation of toluene in gas phase in presence of $\text{Fe}_2\text{O}_3/\text{TiO}_2$ catalysts is yet to be reported. The Figs 5.11 - 5.13 show the results of benzoic acid formed. The activity studies were done after calcination of the samples at temperatures, when severe alteration in properties occurred. Hence the activity of co-precipitated ones calcined at 550°C , 650°C and 800°C are given in Fig 6.11. Similarly, the activity studies of ion exchanged ones calcined at 350°C , 800°C and 1000°C and that of wet-impregnated ones calcined at 350°C , 700°C and 900°C were only shown in Figs 6.12 & 6.13 respectively.

The conversion obtained with CF1 was 58.9%, with CF2 it was 61.3% and with CF3 the conversion obtained was 65.45%. Similarly with IF1 the conversion was 49.25%, with IF2 50.8% and with IF3 55.7%. In the case of wet-impregnated ones the conversion was 58.6%,

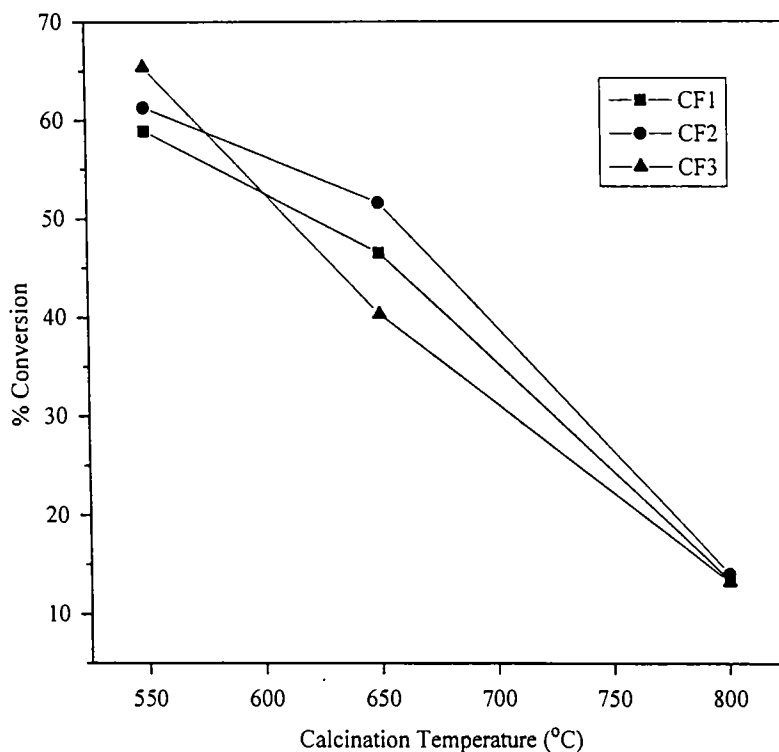


Fig. 5.11. Variation in toluene oxidation activity with calcination temperature of $\text{Fe}_2\text{O}_3/\text{TiO}_2$ catalysts prepared by co-precipitation method

56.5% and 57.3% by WF1, WF2 and WF3 respectively. The percentage conversion was very low with ion exchanged and wet-impregnated ones due to their much lower dispersion and lower surface area compared to co-precipitated ones. In co-precipitated and ion-exchanged samples, the percentage of benzoic acid formed increased on increasing Fe_2O_3 percentage, whereas in wet-impregnated ones the activity decreased. It can be ascribed to the decrease in surface area of these samples on

increasing Fe_2O_3 percentage. Co-precipitated ones have got better activity, as expected, due to their enhanced properties.

A sudden decrease in activity was seen with co-precipitated ones calcined at 650°C , ion exchanged ones calcined at 800°C and wet-impregnated ones calcined at 700°C , which would be due to the onset of rutilation. The percentage conversions were 46.5, 51.6 and 40.3 with CF1, CF2 and CF3; 17.55, 19.4 and 14.25 with IF1, IF2 and IF3; 28.2, 25.5 and 16.4 with WF1, WF2 and WF3 respectively. On further rise in

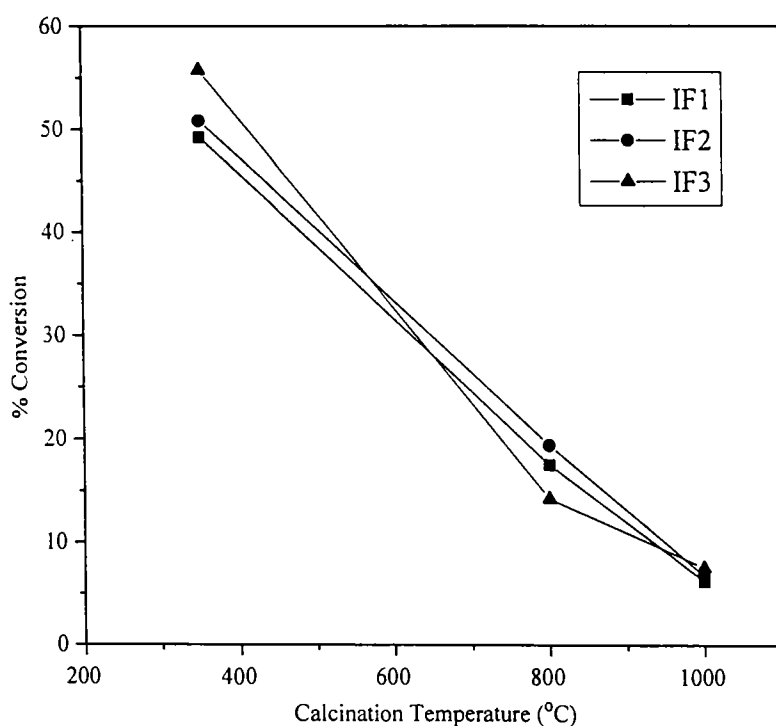


Fig. 5.12. Variation in toluene oxidation activity with calcination temperature of $\text{Fe}_2\text{O}_3/\text{TiO}_2$ catalysts prepared by ion-exchange method

calcination temperature to 800°C, at which the TiO₂ was fully converted to rutile in co-precipitated samples, the percentage conversion reduced to 13.4, 14.0 and 13.2 in CF1, CF2 and CF3 respectively, while in ion exchanged ones calcined at 1000°C, the percentage conversion decreased to 6.2, 6.7 and 7.5 respectively for IF1, IF2 and IF3. With wet-impregnated ones calcined at 900°C, the percentage conversion became 8.6, 8.2 and 7.8 with WF1, WF2 and WF3 samples respectively. All these observations are evident from Figs 5.11 – 5.13.

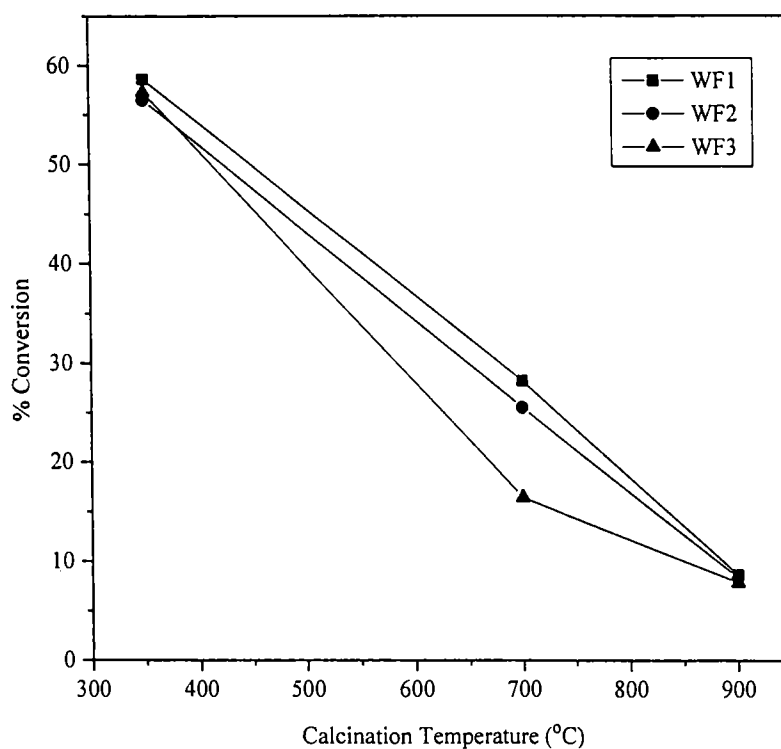


Fig. 5.13. Variation in toluene oxidation activity with calcination temperature of Fe₂O₃/TiO₂ catalysts prepared by wet-impregnation method

The reduction in activity at high temperature calcination would obviously be due to rutilation and a drastic change at the completion of rutilation due to the lack of free active Fe_2O_3 particles (vide Fig. 5.4) on the surface. Instead, pseudo brookite phase is only present along with rutile in these samples. It is very noticeable that in co-precipitated samples, even though, there exists free Fe_2O_3 particles on the surface at the completion of rutilation, the activity was drastically decreased. This decrease in activity can be attributed to the lower surface area, presence of rutile phase instead of anatase and much agglomerated individual particles. So, this reaction is influenced by the phase changes occurring in the support material in addition to method of preparation and other physical properties.

5.5 Conclusions

The following conclusion can be arrived at from the results of the above investigations.

- ☐ Co-precipitated samples are amorphous at 350°C and 450°C .
- ☐ On increasing percentage of Fe_2O_3 the surface area increases in co-precipitated and ion-exchanged samples.
- ☐ The percentage of Fe_2O_3 and method of preparation have major role on surface area.
- ☐ Comparatively better surface area, dispersion and activity were obtained with co-precipitated ones.
- ☐ Pseudobrookite phase was formed when all the TiO_2 was transformed to rutile in ion-exchanged and wet-impregnated ones.

- ☐ Crystallite size of anatase increases markedly upon Fe_2O_3 loading and rutilation.
- ☐ Severe decrease in activity was observed at the onset and completion of rutilation.
- ☐ Order of activity for toluene oxidation is: co-precipitated > wet-impregnated > ion-exchanged samples.
- ☐ All these catalysts were highly stable thermally.

Chapter 6

STUDIES ON CeO₂/TiO₂ CATALYSTS

Rare earth metal oxides alone as well as supported on other transition metal oxides are profoundly important catalyst materials. Ceria in particular is increasingly considered to be an effective catalyst in several processes and has become the focus of increasing interest among rare earth metal oxides, despite the label 'rare' applied to it. The most important use of it is in three-way catalyst used in automobile emission control. Its ability to shift between Ce⁴⁺ and Ce³⁺ is solely responsible for its high activity in emission control.²⁹³ Many other oxidation reactions are also reported using ceria.²⁹³ CeO₂/TiO₂ is also reported for degradation of chloro fluoro carbons.⁵⁶

Only a few methods are available in literature for preparing this catalyst. CeO₂/TiO₂ catalyst with three different percentages of CeO₂ was prepared using the three methods described in Chapter 2. The samples prepared by co-precipitation method were labeled as CC1, CC2 and CC3, the ion-exchanged ones were labeled as IC1, IC2 and IC3 and the wet-impregnated ones were labeled as WC1, WC2 and WC3. The percentage of CeO₂ present in each sample is given in Table 6.1.

6.1 XRD studies

Figs 6.1 – 6.6 exhibit the XRD pattern of all the samples calcined at different temperatures. The pattern 1 in Fig 6.1 reveals the amorphous nature of co-precipitated sample CC3 calcined at 350⁰C. Five peaks were seen in all the other patterns calcined at 450⁰C and all were

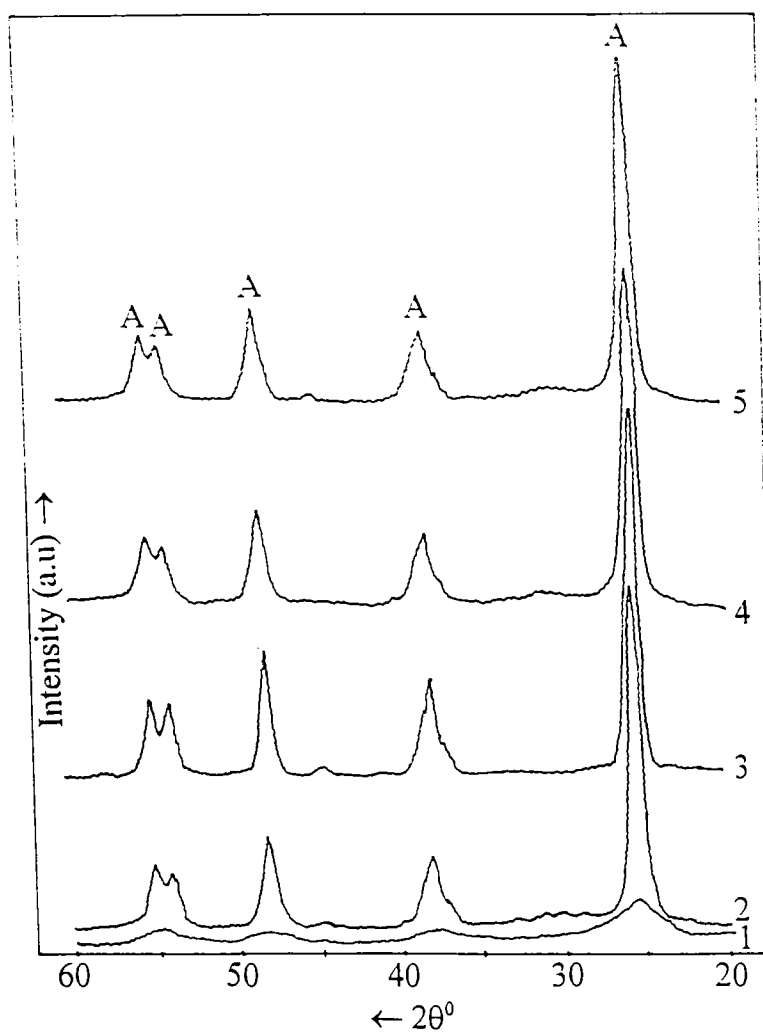


Fig. 6.1. XRD pattern of $\text{CeO}_2/\text{TiO}_2$ samples prepared by co-precipitation method 1) CC3 calcined at 350°C / 6hrs., 2) CC1, 3) CC2, 4) CC3 calcined at 450°C / 6hrs. and 5) CC3 after catalysis. (A = anatase).

that of anatase TiO_2 . Similarly, in ion-exchanged and wet-impregnated ones, peaks of anatase were only present. No peaks corresponding to CeO_2 or CeTiO_4 were observed.

The rutilation started at 800°C in co-precipitated one and at 900°C in ion exchanged and wet-impregnated samples. Along with rutile, CeO₂ peaks also appeared in the patterns. On increasing the temperature further, the rutile percentage increased significantly (vide Fig. 6.7). Here, unlike the other catalysts, even when all the TiO₂ was transformed into rutile, no reaction between CeO₂ and TiO₂ did take place to form CeTiO₄.

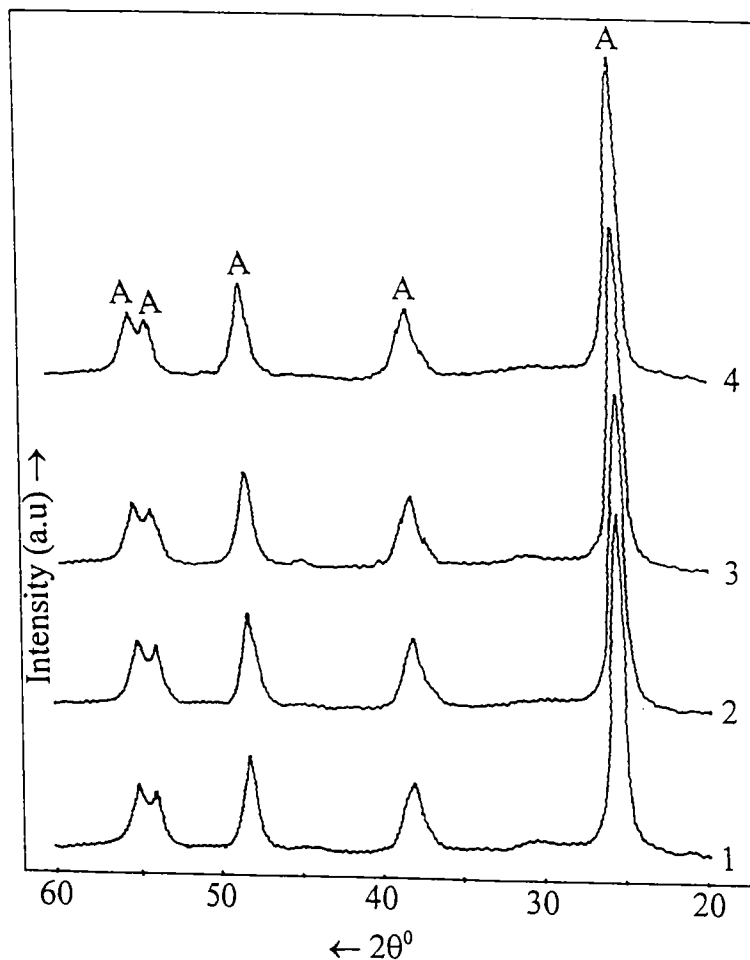


Fig. 6.2. XRD pattern of CeO₂/TiO₂ samples prepared by ion-exchange method - calcined at 350°C / 6hrs. 1) IC1, 2) IC2, 3) IC3 and 4) IC3 after catalysis. (A = anatase).

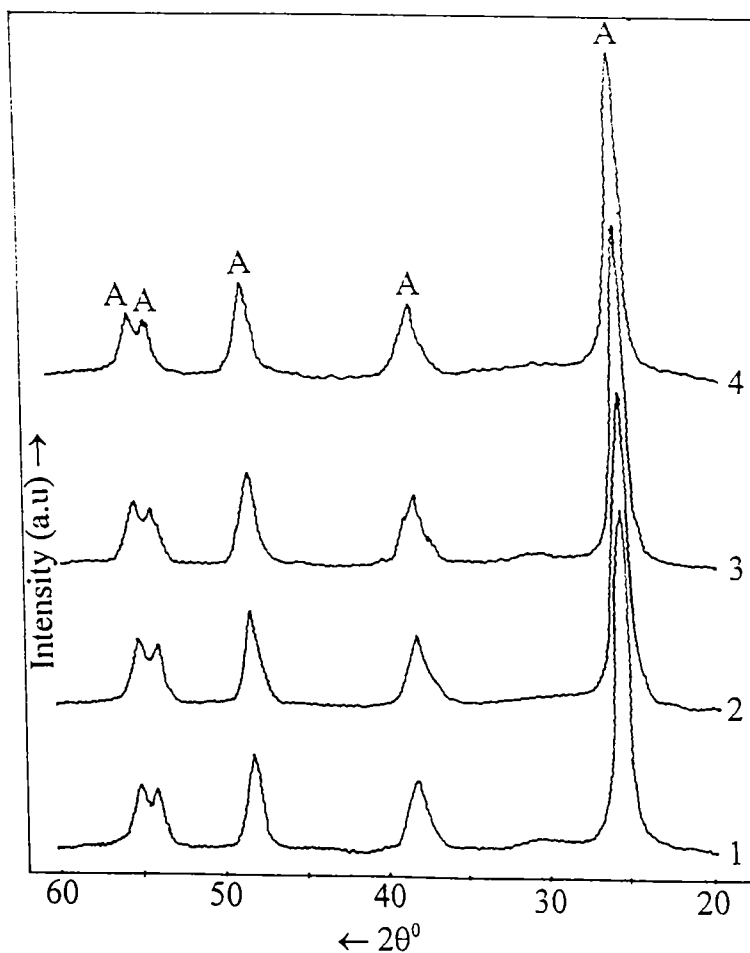


Fig. 6.3. XRD pattern of $\text{CeO}_2/\text{TiO}_2$ samples prepared by wet-impregnation method - calcined at 350°C / 6hrs. 1) WC1, 2) WC2, 3) WC3 & 4) WC3 after catalysis (A = anatase)

On comparing with bare TiO_2 , CeO_2 has no influence on crystallization temperature. The onset temperature of rutilation was also not affected by CeO_2 in co-precipitated samples, while in ion-exchanged and wet-impregnated ones, the rutilation started only at higher temperature compared to bare TiO_2 . But the completion temperature of rutilation was much lower in co-precipitated ones, whereas in ion-exchanged and wet-impregnated ones, the rutilation was completed only

at higher temperature compared to bare TiO_2 . So, it can be concluded that, the CeO_2 has no noticeable effect on rutile phase formation in co-precipitated ones and it suppresses rutilation in ion-exchanged and wet-impregnated ones. The enhancement or suppression of rutilation by a metal oxide is strongly dependent on how that particular sample was prepared regardless of the nature of the loaded metal oxides.

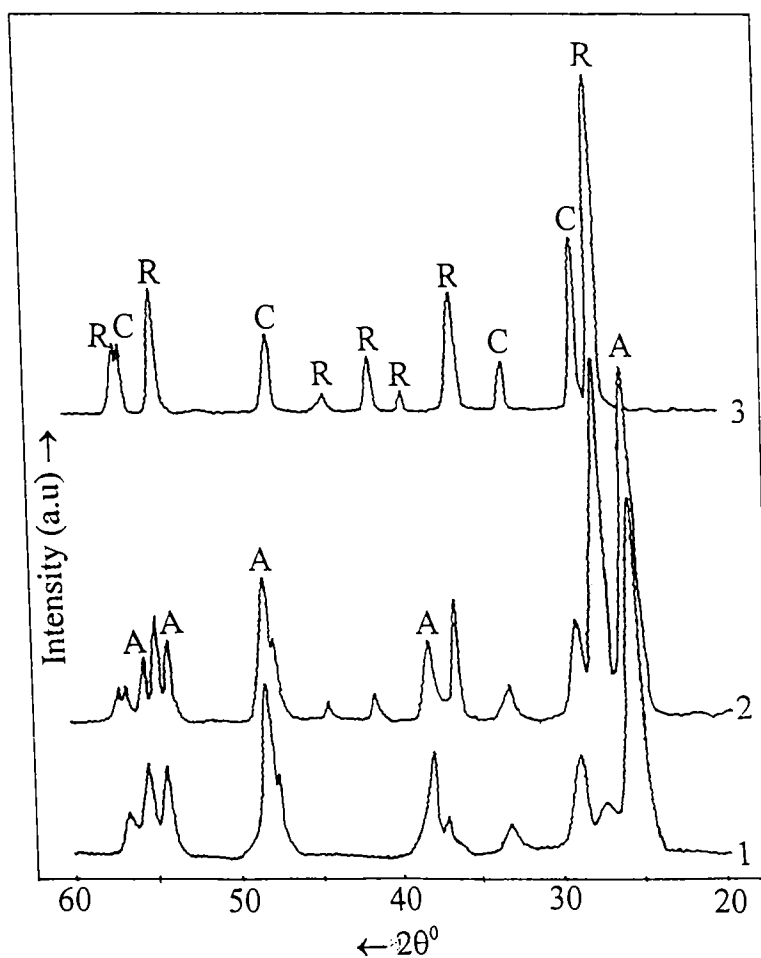


Fig. 6.4. XRD patterns of CC3 calcined at 1) 800, 2) 900 and 3) 1000°C / 6hrs. (A = anatase, R = rutile and C = CeO_2).

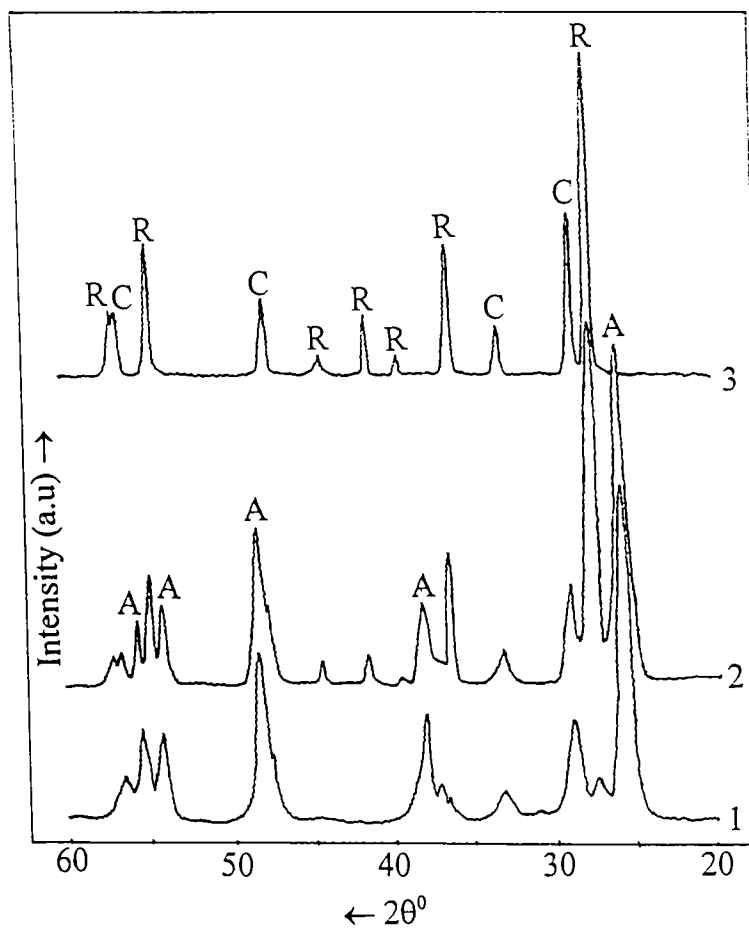


Fig. 6.5. XRD patterns of IC3 calcined at 1) 900, 2) 1000 and 3) 1100°C / 6hrs. (A = anatase, R = rutile and C = CeO₂).

Figs 6.1 – 6.3 also contain the pattern of these samples after toluene oxidation studies. These patterns reveal that these samples were thermally stable, because no phase transformation or compound formation took place during the course of catalytic activity studies.

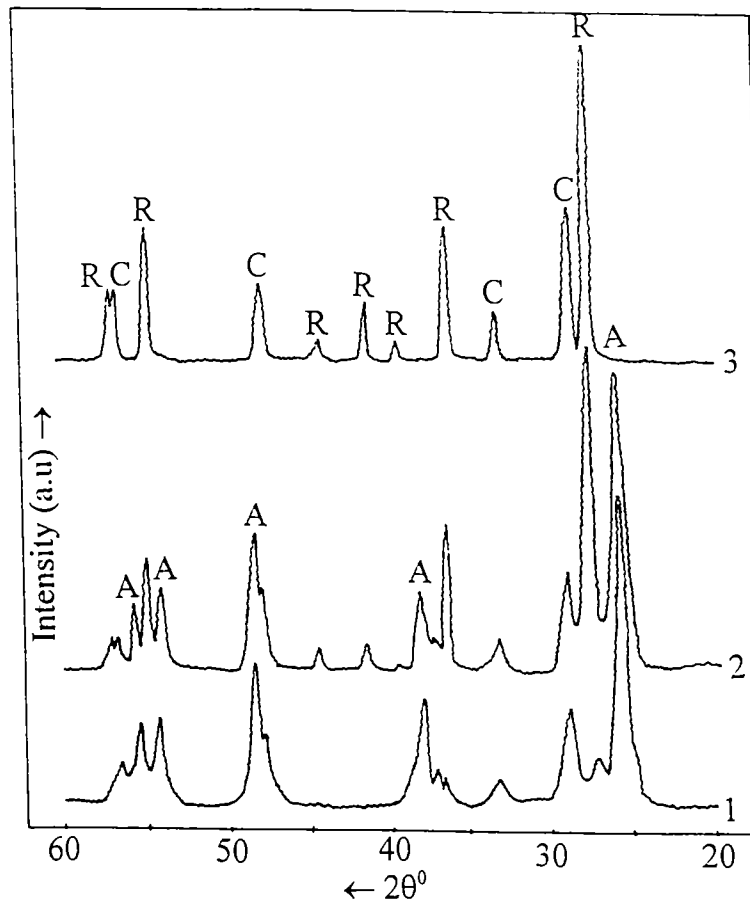


Fig. 6.6. XRD patterns of WC₃ calcined at 1) 900, 2) 1000 and 3) 1100°C / 6hrs. (A = anatase, R = rutile & C = CeO₂).

Table 6.1 shows the crystallite size of anatase at different calcination temperatures, when major changes in physical properties occurred. No marked change was seen on increasing the CeO₂ percentage, but it increased with increase in temperature. When the rutilation was started, the crystallite size of anatase attained a size of

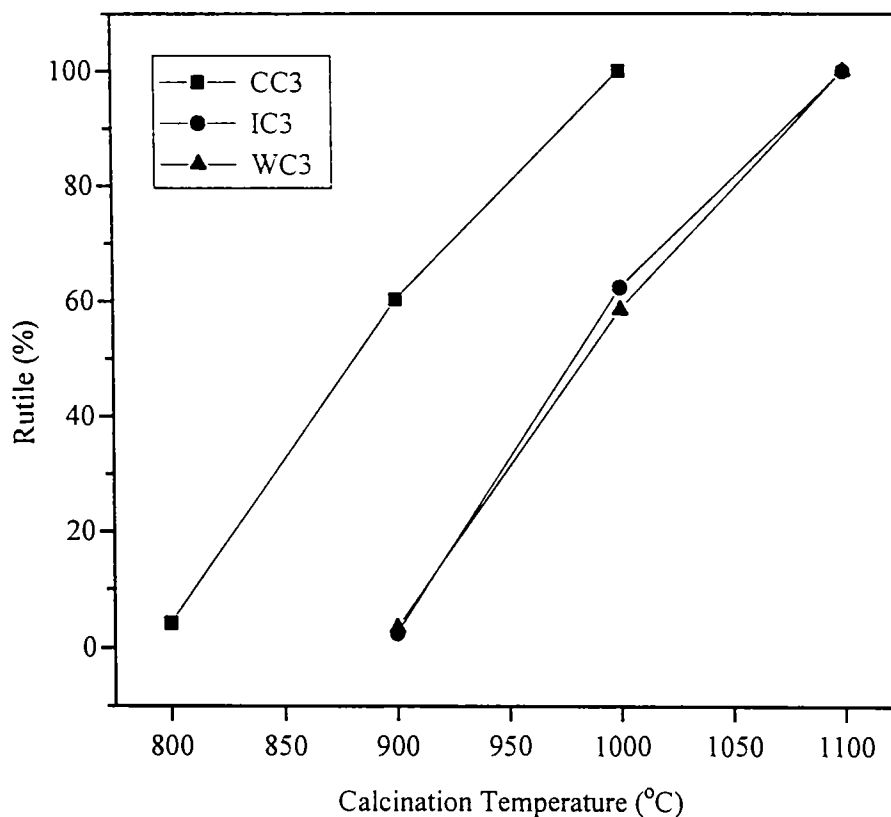


Fig. 6.7. Variation in rutile (%) with calcination temperature of $\text{CeO}_2/\text{TiO}_2$ catalyst prepared by different methods

13.97nm in co-precipitated ones and 22.18nm in ion-exchanged and wet-impregnated ones. Hence, depending on the method of preparation, the crystallite size may vary and the growth in crystallite size with temperature is also determined by method of preparation. The crystallite size was increased on loading CeO_2 compared to pure TiO_2 .

Table 6.1. Variation in crystallite size of anatase with calcination temperature of CeO₂/TiO₂ samples

Method of prepn	Sample label	CeO ₂ %	Crystallite size (nm)				
			350 ⁰ C	450 ⁰ C	800 ⁰ C	900 ⁰ C	1000 ⁰ C
Co-ppn	CC1	4.99	Amorphous	10.26	13.97	---	---
	CC2	9.96		10.26	13.97	---	---
	CC3	14.96		9.63	13.97	22.18	---
I.E	IC1	4.94	10.98	---	---	22.18	---
	IC2	9.97	10.98	---	---	22.18	---
	IC3	14.99	10.98	---	---	22.18	31.6
W.I	WC1	4.93	10.98	---	---	22.18	---
	WC2	9.96	10.98	---	---	22.18	---
	WC3	14.97	10.98	---	---	22.18	31.6

6.2 Surface area studies

Figs 6.8 - 6.10 show the variation in surface area with percentage of CeO₂ and calcination temperature. The surface area obtained for CC1 was 147.1 m²/g, for CC2, the surface area was 162.31 m²/g and for CC3 it was 184.61 m²/g. In the case of ion-exchanged ones, the surface area was 91.25 m²/g, 93.18 m²/g and 101.26 m²/g for IC1, IC2 and IC3 respectively, whereas in samples WC1, WC2 and WC3, the surface area obtained was 92.09 m²/g, 89.3 m²/g and 85.41 m²/g

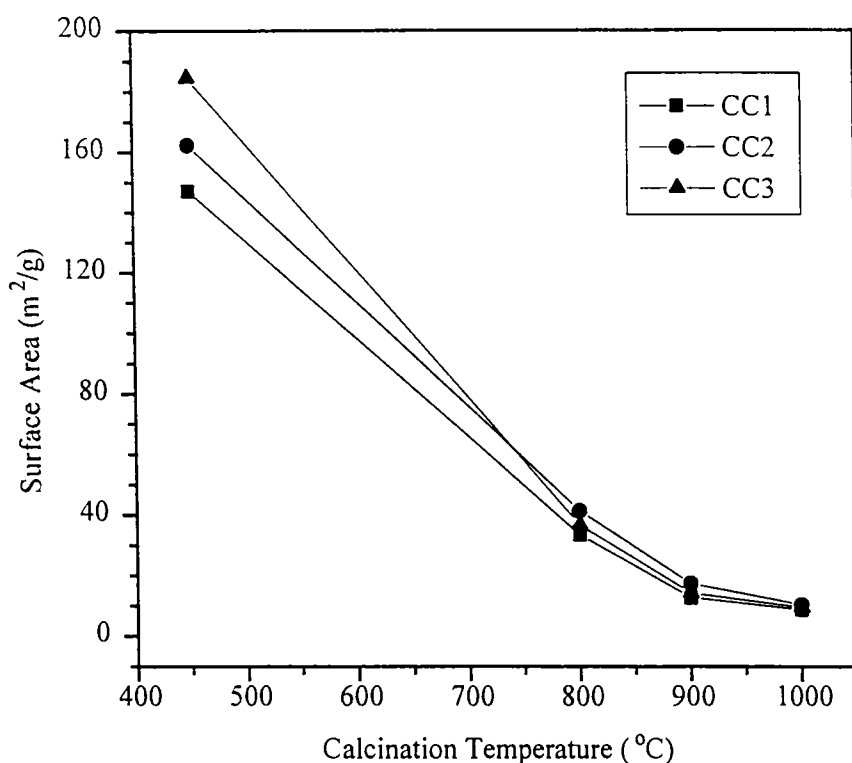


Fig. 6.8. Effect of calcination temperature on surface area of CeO₂/TiO₂ catalysts prepared by co-precipitation method

respectively. Like other samples, here also, co-precipitated ones have much higher surface area. Out of all the samples, maximum surface area was obtained in CC1, CC2 and CC3. The values are even higher than that for pure TiO₂. The surface area increased on increasing CeO₂ percentage in co-precipitated and ion exchanged ones and decreased in wet-impregnated ones as in the case of other samples discussed in earlier Chapters.

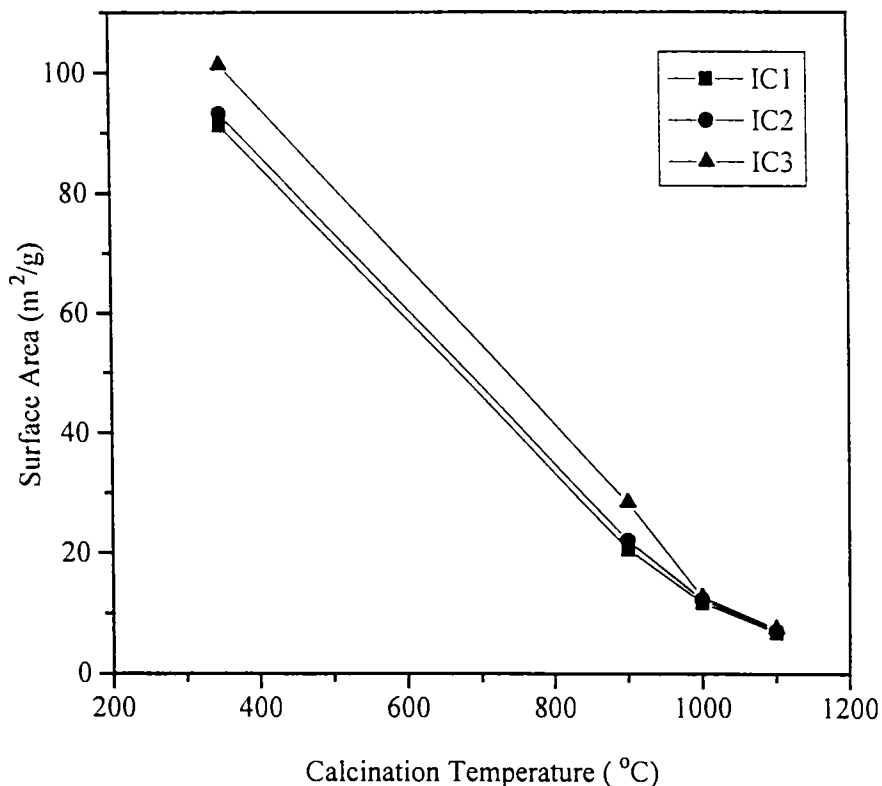


Fig. 6.9. Effect of calcination temperature on surface area of $\text{CeO}_2/\text{TiO}_2$ catalysts prepared by ion-exchange method

Here also a sudden decrease in surface area was observed in co-precipitated ones calcined at 800°C and in wet-impregnated and ion-exchanged ones calcined at 900°C due to the onset of rutilation and titania particle enlargement. The crystallite size results are also in parallel with these observations. At temperatures when the TiO_2 support was fully converted to rutile, the surface area became $8.72 \text{ m}^2/\text{g}$, $10.31 \text{ m}^2/\text{g}$ and $9.4 \text{ m}^2/\text{g}$ in CC1, CC2 and CC3; $6.8 \text{ m}^2/\text{g}$, $7.1 \text{ m}^2/\text{g}$ and $7.5 \text{ m}^2/\text{g}$ in IC1, IC2 and IC3; $8.3 \text{ m}^2/\text{g}$, $7.6 \text{ m}^2/\text{g}$ and $6.4 \text{ m}^2/\text{g}$ in WC1, WC2 and WC3

respectively, as reflected in Figs 6.8 – 6.10. The decrease in surface area was more severe in co-precipitated ones. So, like other samples discussed earlier, the method of preparation and percentage of CeO_2 have a greater role in deciding the surface area of these samples. The decrease in surface area with rutilation was also lower compared to bare TiO_2 . So, it is very clear that, CeO_2 is suppressing titania particle enlargement, which would otherwise occur on high temperature calcination.

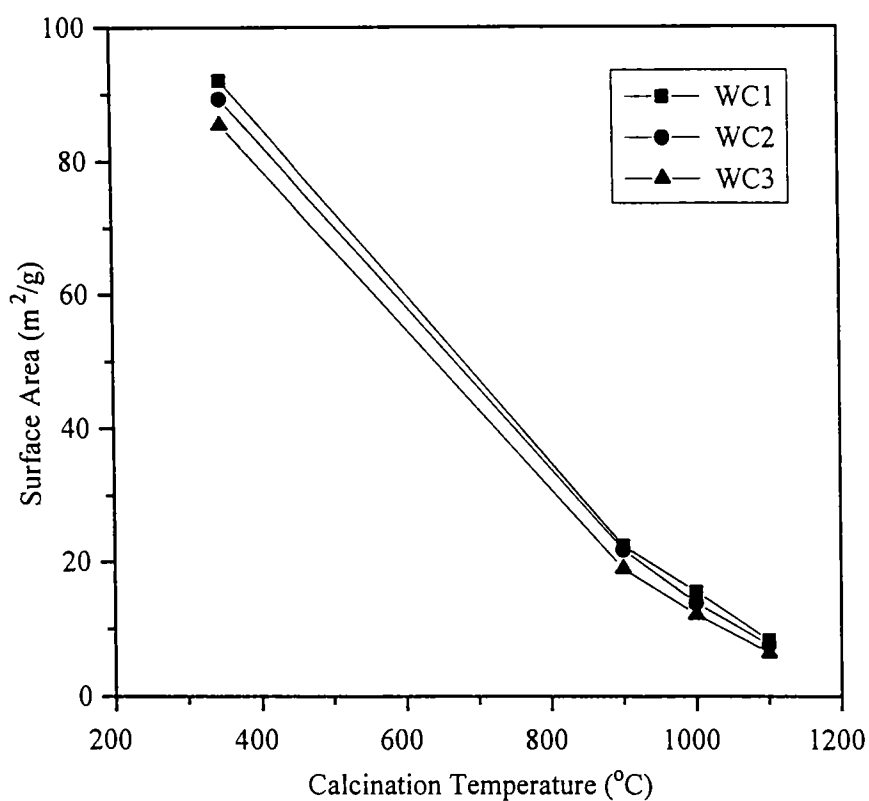


Fig. 6.10. Effect of calcination temperature on surface area of $\text{CeO}_2/\text{TiO}_2$ catalysts prepared by wet-impregnation method

6.3 Dispersion studies

The dispersion studies of CeO_2 on TiO_2 could not be determined by oxygen chemisorption after reduction, because both CeO_2 and TiO_2 get reduced at 500°C . Also CeO_2 itself chemisorbs some oxygen.²⁹³ All these would lead to overestimation of chemisorbed oxygen and thereby cause a higher value for dispersion.

6.4 Toluene oxidation studies

The air oxidation of toluene to produce benzoic acid by $\text{CeO}_2/\text{TiO}_2$ has not yet been reported. The percentage conversion plotted

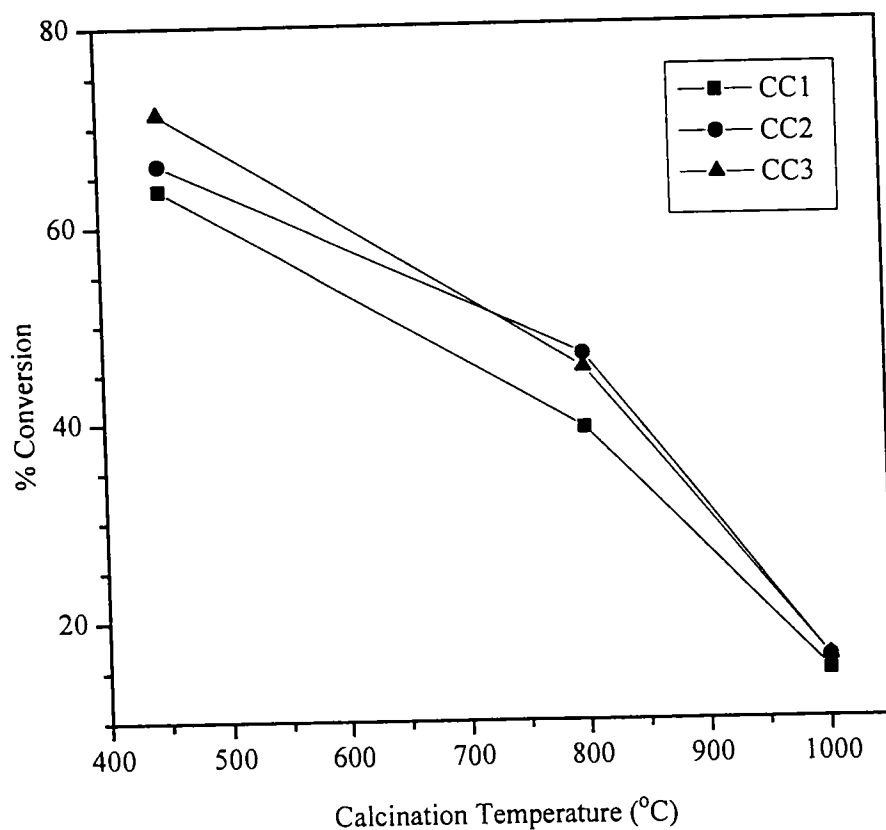


Fig. 6.11. Variation in toluene oxidation activity with calcination temperature of $\text{CeO}_2/\text{TiO}_2$ catalysts prepared by co-precipitation method

against calcination temperature of these catalysts is shown in Figs 6.11 – 6.13. The percentage conversion increased with increasing CeO_2 percentage. Conversion obtained with CC1 was 63.7%, with CC2 66.2% and with CC3 71.3%. Out of all the samples studied, the maximum conversion was obtained for the sample CC3. Much lower percentage conversions were observed for ion-exchanged and wet-impregnated ones, i.e. 53.3 %, 55.9 % and 59.7 % conversion with IC1, IC2 and IC3 and

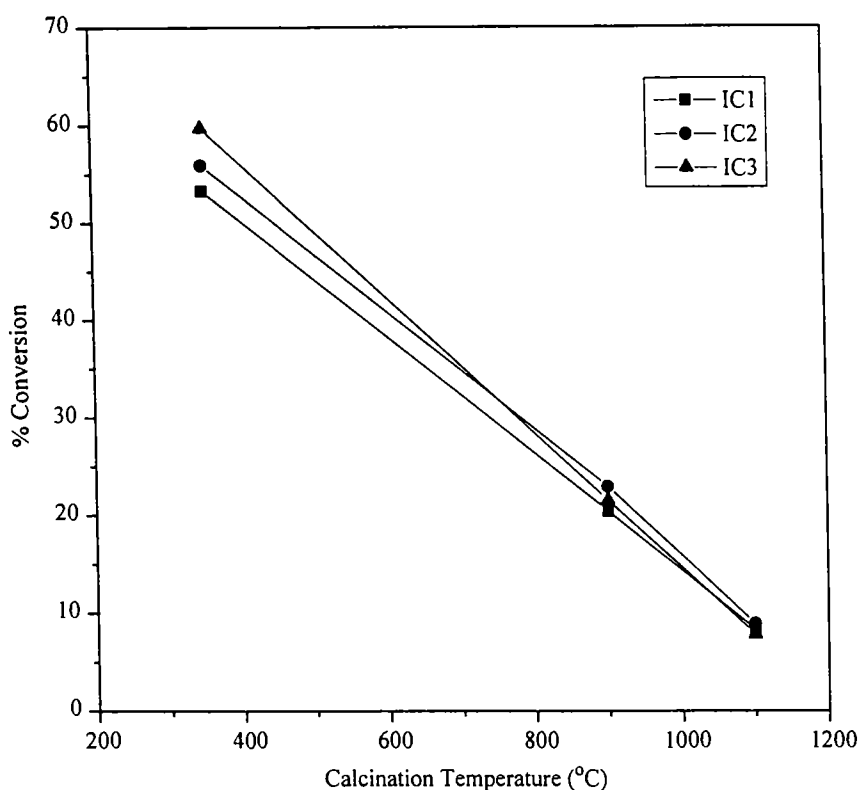


Fig. 6.12. Variation in toluene oxidation activity with calcination temperature of $\text{CeO}_2/\text{TiO}_2$ catalysts prepared by ion-exchange method

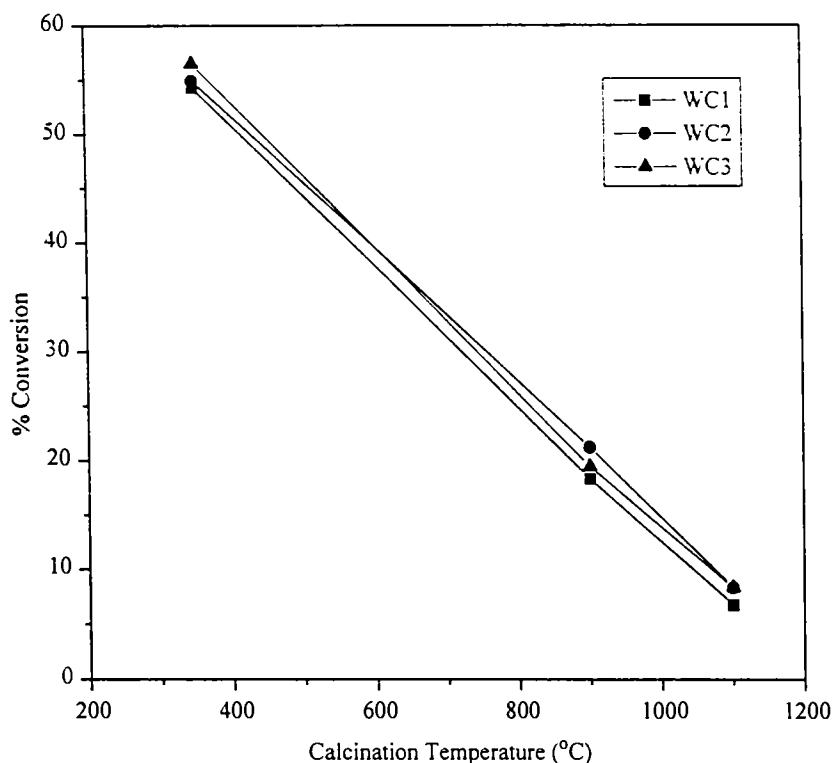


Fig. 6.13. Variation in toluene oxidation activity with calcination temperature of $\text{CeO}_2/\text{TiO}_2$ catalysts prepared by wet-impregnation method

54.3%, 54.9% and 56.5% conversion with WC1, WC2 and WC3 respectively. Like other samples, maximum conversion was obtained with co-precipitated ones. The much lower percentage conversion with ion-exchanged and wet-impregnated ones would be due to much lower surface area of these samples compared to co-precipitated ones. The activity studies were also carried out after calcination of these samples at temperatures when rutilation was started and completed. The percentage

conversion decreased suddenly at the onset of rutilation. It became 39.3%, 46.8% and 45.4% with CC1, CC2 and CC3; nearly halved or less than that in ion-exchanged and wet-impregnated ones, i.e. it was decreased to 20.4%, 22.9% and 21.5% with IC1, IC2 and IC3; 18.3%, 21.2% and 19.4% with WC1, WC2 and WC3 respectively. When the calcination temperature was raised further to transform all the TiO₂ support to rutile, i.e. when the co-precipitated ones calcined at 1000⁰C and wet-impregnated and ion-exchanged ones at 1100⁰C, the activity went very much downwards as can be seen from the Figs 6.11 – 6.13. The percentage conversion reached a value of 14.8, 16.1 and 16.1 with CC1, CC2 and CC3; 8.3, 8.9 and 7.8 with IC1, IC2 and IC3; 6.7, 8.3 and 8.3 with WC1, WC2 and WC3 respectively. Even though, there exist free CeO₂ in samples (vide Fig. 6.4 - 6.6), at the onset and completion of rutile phase formation, the activity was found to decrease markedly, showing the influence of surface area and nature of support on this reaction.

6.5 Conclusions

The following are the conclusions made out of the above studies.

- ☐ On loading CeO₂ noticeable change in surface area and no change in crystallization temperature were observed.
- ☐ The method of preparation, percentage of CeO₂ and calcination temperature have marked effect on surface area.

- ☐ The onset and completion temperatures of rutilation were far higher compared to all other samples and unlike in the case of other catalysts, here no enhancement of rutilation was observed.
- ☐ CeTiO_4 phase is not formed during rutilation.
- ☐ Crystallite size of anatase increases on loading CeO_2 and during rutilation.
- ☐ Maximum percentage conversion for toluene oxidation was observed with these samples.
- ☐ Order of activity for toluene oxidation is as follows: co-precipitated > ion exchanged > wet-impregnated ones.
- ☐ All these catalysts were thermally stable.
- ☐ Activity decreases markedly upon rutilation even though free CeO_2 are present at this stage.

Chapter 7

STUDIES ON V₂O₅/TiO₂ CATALYSTS

Vanadium oxide based catalysts are widely used for oxidation of hydrocarbons, SO₂, etc. Vanadia supported on TiO₂ was reported to have superior properties than that supported on other supports like SiO₂, Al₂O₃, etc.^{1&2} It is highly active and selective in oxidation processes of industrial importance.¹⁻⁴

Very few methods are described in literature for the preparation of V₂O₅/TiO₂ catalysts. In this Chapter our studies on the effect of preparation method on rutilation, physical properties and toluene oxidation activity are presented.

The samples prepared by co-precipitation are labeled as CV1, CV2 and CV3, those prepared by ion-exchange as IV1, IV2 and IV3 and those prepared by wet-impregnation as WV1, WV2 and WV3. The percentage of V₂O₅ in each sample is given in Table 7.1.

7.1 XRD studies

Figs 7.1 – 7.3 show the XRD pattern of co-precipitated, ion-exchanged and wet-impregnated ones respectively. Co-precipitated one calcined at 350⁰C was not crystalline, whereas ion-exchanged and wet-impregnated ones calcined at 350⁰C exhibit well-defined sharp peaks of anatase. The co-precipitated sample showed crystalline nature only by calcination at 450⁰C, like NiO/TiO₂ and CeO₂/TiO₂ samples. Here also there were no peaks due to V₂O₅. Any other phases of vanadium oxide were also not seen in any of the pattern.

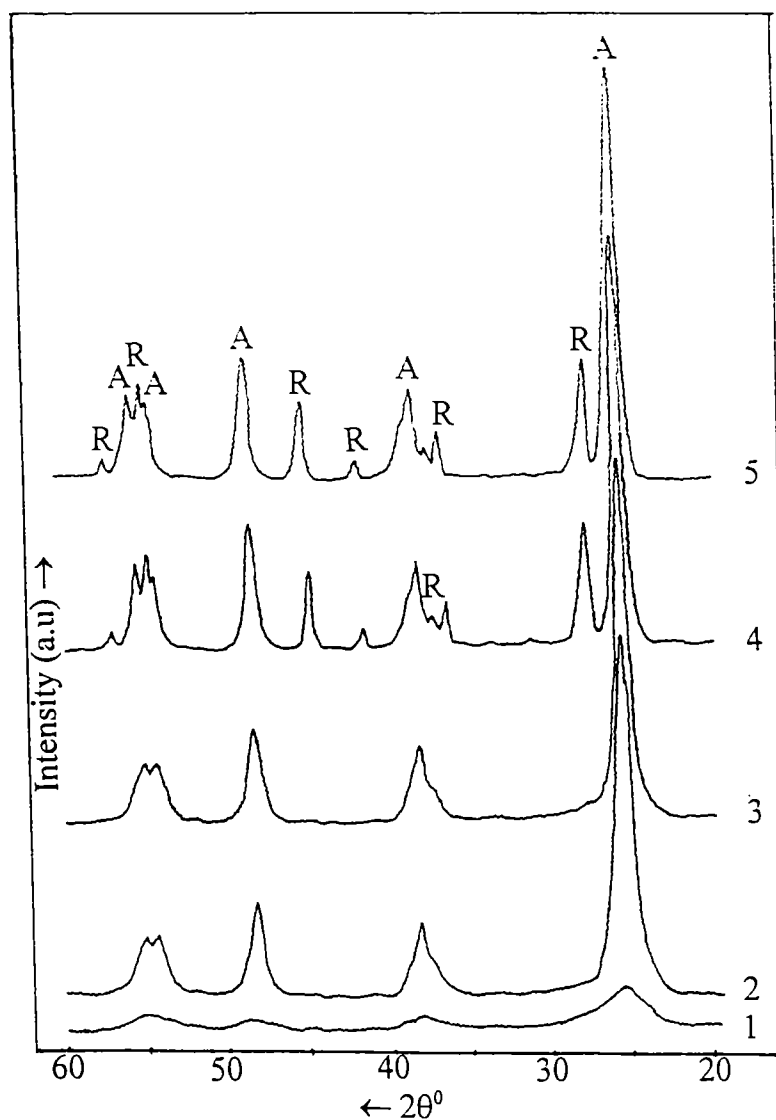


Fig. 7.1. XRD pattern of V_2O_5/TiO_2 samples prepared by co-precipitation method 1) CV3 calcined at $350^\circ C / 6hrs.$ 2) CV1, 3) CV2, 4) CV3 calcined at $450^\circ C / 6hrs.$ and 5) CV3 after catalysis. (A = anatase and R = rutile).

Interesting feature of these samples was that, the rutilation started at a very low temperature, i.e. at $450^\circ C$ in the samples CV3, IV3 and WV3, irrespective of the method of preparation. No peaks of rutile were observed in the samples containing lower percentages of V_2O_5 .

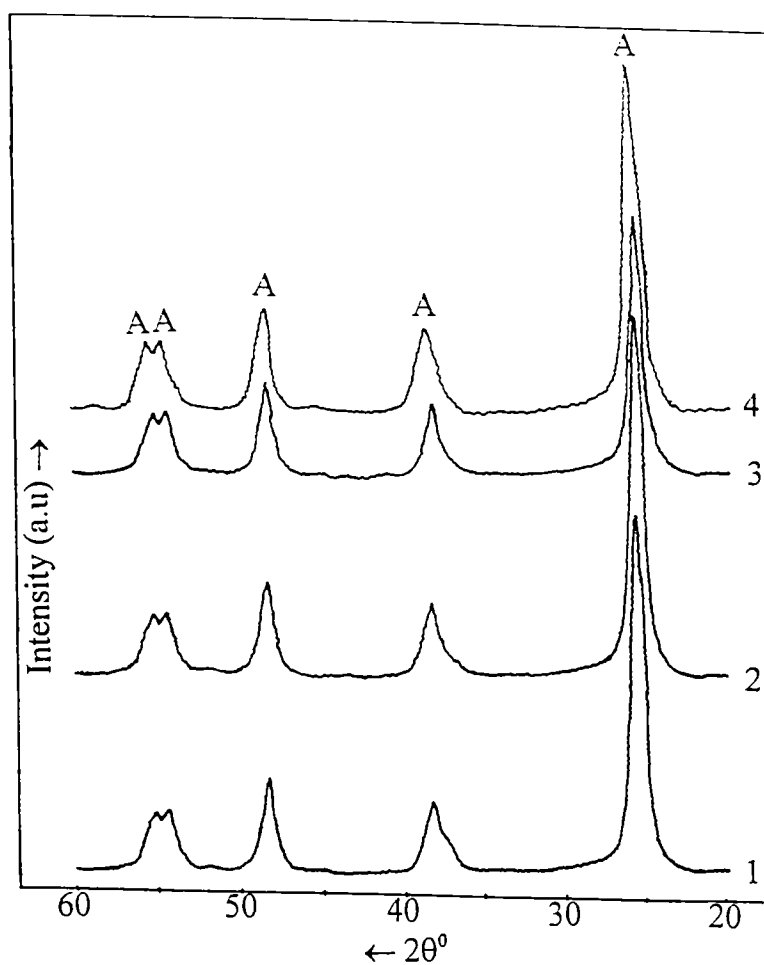


Fig. 7.2. XRD pattern of V_2O_5/TiO_2 samples prepared by ion-exchange method - calcined at $350^\circ C / 6hrs$. 1) I V1, 2) I V2, 3) I V3 & 4) I V3 after catalysis. (A = anatase).

Hence, for convenience, the XRD pattern of the samples, where rutilation started are only given in Figs 7.4 – 7.6. As the calcination temperature was increased to $600^\circ C$, the rutilation progressed. In co-precipitated sample CV3, calcined at $650^\circ C$, there were no anatase peaks seen in the pattern, whereas in IV3 and WV3, the anatase peaks disappeared

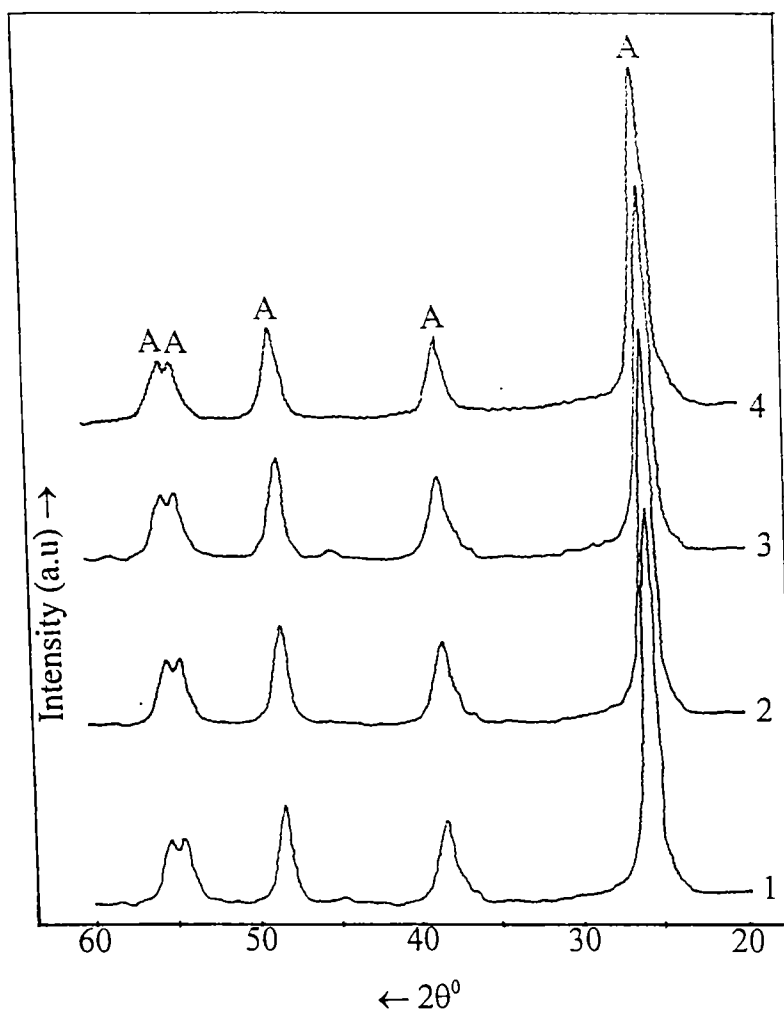


Fig. 7.3. XRD pattern of V_2O_5/TiO_2 samples prepared by wet-impregnation method - calcined at $350^\circ C / 6hrs$. 1) WV1, 2) WV2, 3) WV3 & 4) WV3 after catalysis (A = anatase)

completely only at $800^\circ C$ and $700^\circ C$ respectively. So, here also, the co-precipitated one was converted completely to rutile at a lower temperature. The rutilation was started and completed at a very low temperatures in all these samples compared to bare TiO_2 . Hence, it is

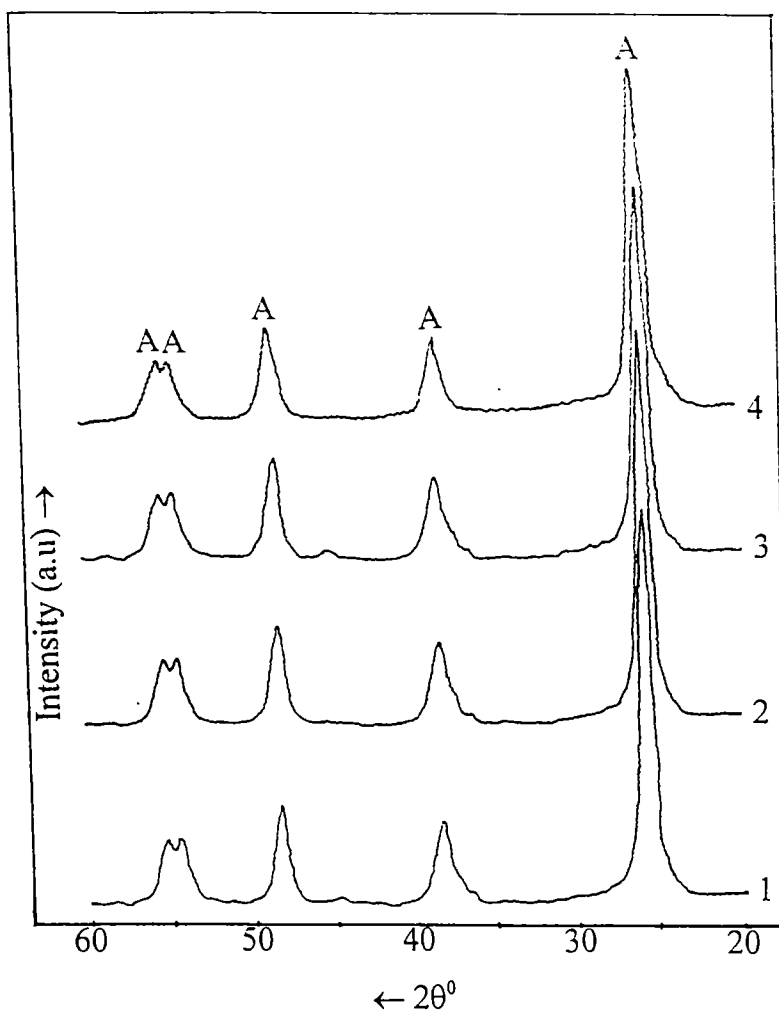


Fig. 7.3. XRD pattern of V_2O_5/TiO_2 samples prepared by wet-impregnation method - calcined at $350^\circ C / 6hrs$. 1) WV1, 2) WV2, 3) WV3 & 4) WV3 after catalysis (A = anatase)

completely only at $800^\circ C$ and $700^\circ C$ respectively. So, here also, the co-precipitated one was converted completely to rutile at a lower temperature. The rutilation was started and completed at a very low temperatures in all these samples compared to bare TiO_2 . Hence, it is

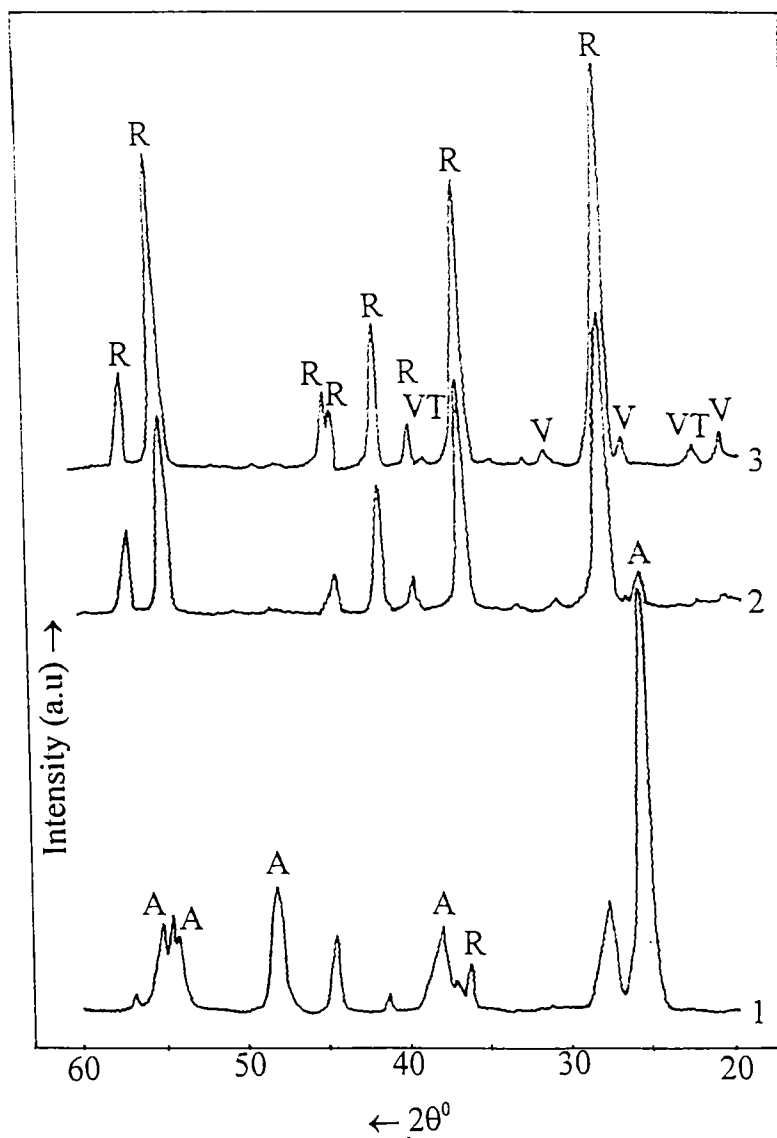


Fig. 7.4. XRD patterns of CV3 calcined at 1) 450, 2) 600 and 3) 650°C / 6hrs. (A = anatase, R = rutile, V = V_2O_5 and VT = $V_2Ti_3O_9$).

obvious that quantity of V_2O_5 has a marked effect on rutilation, in addition to method of preparation and calcination temperature. The rutile percentage plotted against calcination temperature is shown in Fig 7.7. It

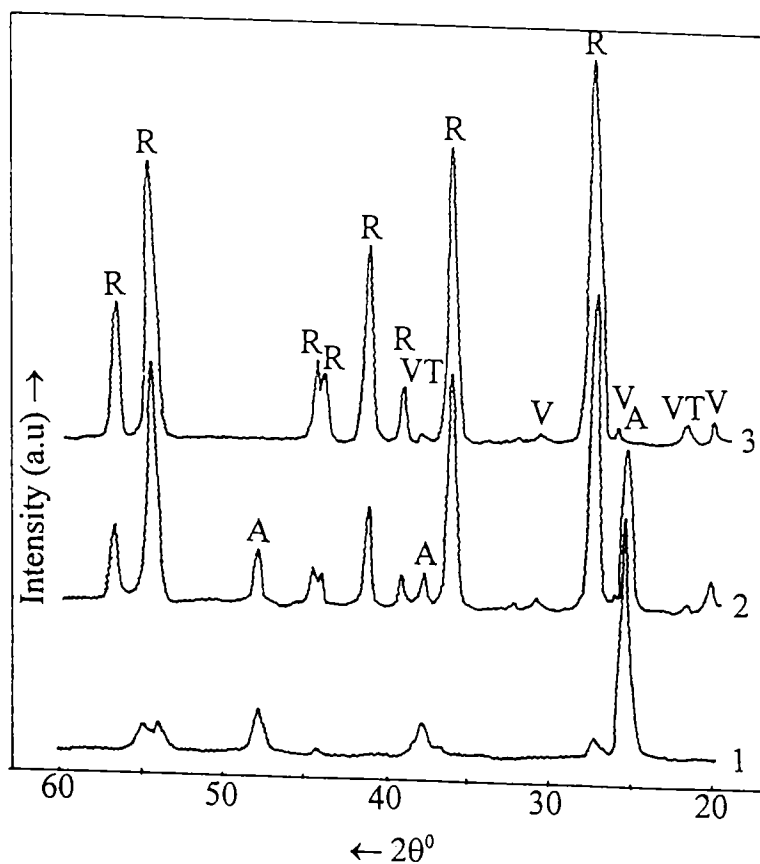


Fig. 7.5. XRD patterns of I V3 calcined at 1) 450, 2) 600 and 3) 800°C / 6hrs. (A = anatase, R = rutile, V = V_2O_5 and VT = $V_2Ti_3O_9$).

reflects clearly that, the co-precipitated one has highest rutile percentage at any temperature and the ion-exchanged one has the lowest rutile percentage.

In the samples calcined at 600°C and above, V_2O_5 peaks and some peaks of $V_2Ti_3O_9$ were also present along with peaks due to rutile.

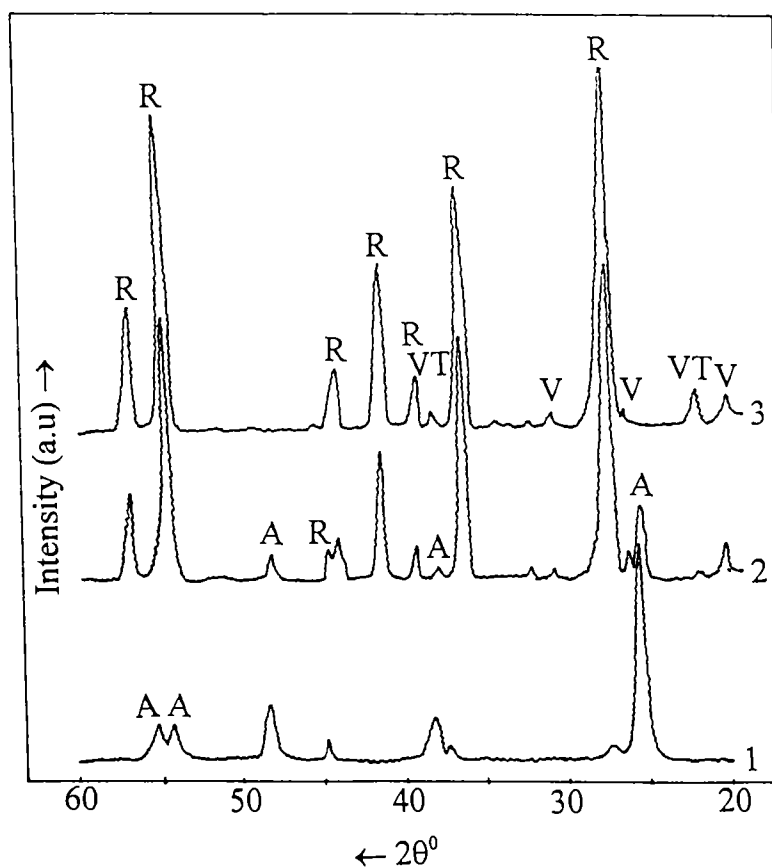


Fig. 7.6. XRD patterns of WV3 calcined at 1) 450, 2) 600 and 3) 700°C / 6hrs. (A = anatase, R = rutile, V = V_2O_5 and VT = $V_2Ti_3O_9$).

at the onset of rutilation, no peaks of V_2O_5 or $V_2Ti_3O_9$ were seen, but, as the intensity of rutile peaks increased on increasing calcination temperature, V_2O_5 and $V_2Ti_3O_9$ peaks also appeared in the pattern. On further calcination these peaks were seen to be more intense, revealing the growth of V_2O_5 crystals during high temperature calcination. The appearance of $V_2Ti_3O_9$ peaks (instead of V_2TiO_7 , by reacting V_2O_5 with

TiO₂) mirrored the fact that some non-stoichiometric titania (TiO_{1.33}) having some oxygen vacancies were formed on TiO₂ surface, when calcined in presence of V₂O₅. This might be the reason, for the easy rutilation of these samples. This is in accordance with the literature reports,⁵⁻⁷ which states that, the formation of oxygen vacancies are the basic reason for rutilation (as it enhances the rupture of Ti — O bonds of anatase).

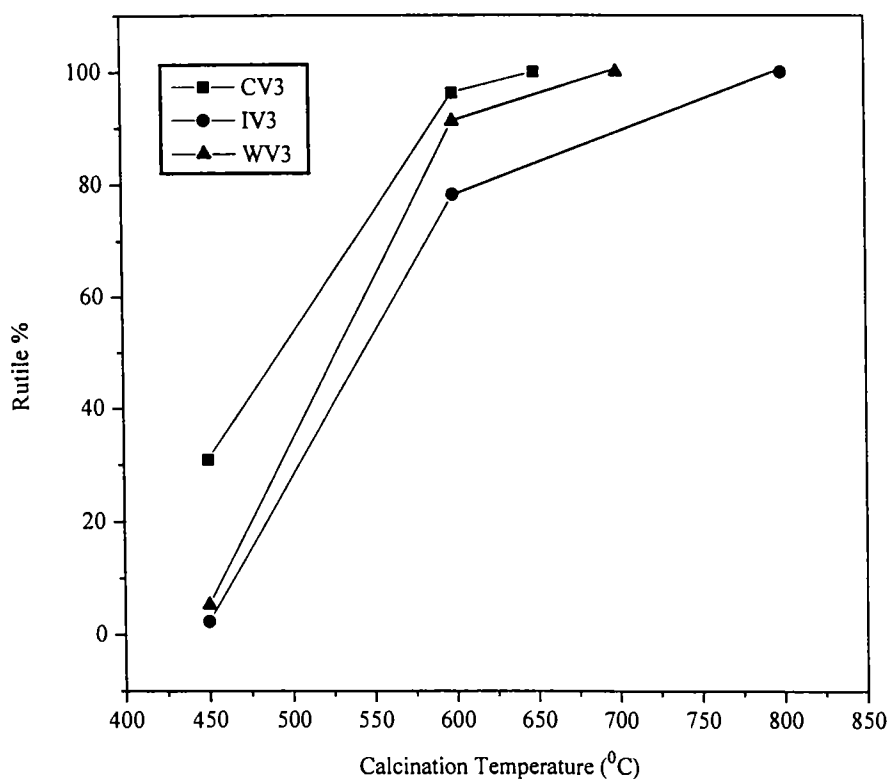


Fig. 7.7. Variation in rutile % with calcination temperature of V₂O₅/TiO₂ catalysts prepared by different methods.

The crystallite size of anatase was calculated after calcinations of these samples at temperatures when drastic changes in physical properties took place. The results are given in Table 7.1. No change was observed in crystallite size, on increasing the percentage of V_2O_5 in any of the samples, except in CV3, where the anatase crystallites were seen to grow to a size of 17.1nm (in this sample 30.9 % of anatase was irreversibly converted to rutile). So, it is noteworthy that, like NiO/TiO_2 , Fe_2O_3/TiO_2 and CeO_2/TiO_2 , as the rutile percentage increased, the anatase crystallite size also increased, but to different extent, depending on the method of preparation.

Table 7.1. Variation in crystallite size of anatase with calcination temperature of V_2O_5/TiO_2 samples

Method of prepn	Sample label	V_2O_5 (%)	Crystallite size (nm)		
			350 ⁰ C	450 ⁰ C	600 ⁰ C
Co-pptn	CV1	4.96	Amorphous	10.98	---
	CV2	9.95		10.98	---
	CV3	14.97		17.1	31.6
I.E	IV1	4.95	11.82	13.97	---
	IV2	9.96	11.82	13.97	---
	IV3	14.94	11.82	15.37	31.6
W.I	WV1	4.92	10.98	12.79	---
	WV2	9.91	10.98	13.97	---
	WV3	14.98	10.98	15.37	31.6

7.2 Surface area studies

Figs 7.8 – 7.10 show the surface area values plotted against calcination temperature. The surface area decreased with increasing V_2O_5 percentage and this decrease was more noticeable in co-precipitated and wet-impregnated ones. For CV1, CV2 and CV3, the values are $110.2 \text{ m}^2/\text{g}$, $102.7 \text{ m}^2/\text{g}$ and $56.4 \text{ m}^2/\text{g}$ respectively. In the case of ion-exchanged samples, IV1, IV2 and IV3, the values are $84.1 \text{ m}^2/\text{g}$, $83.5 \text{ m}^2/\text{g}$

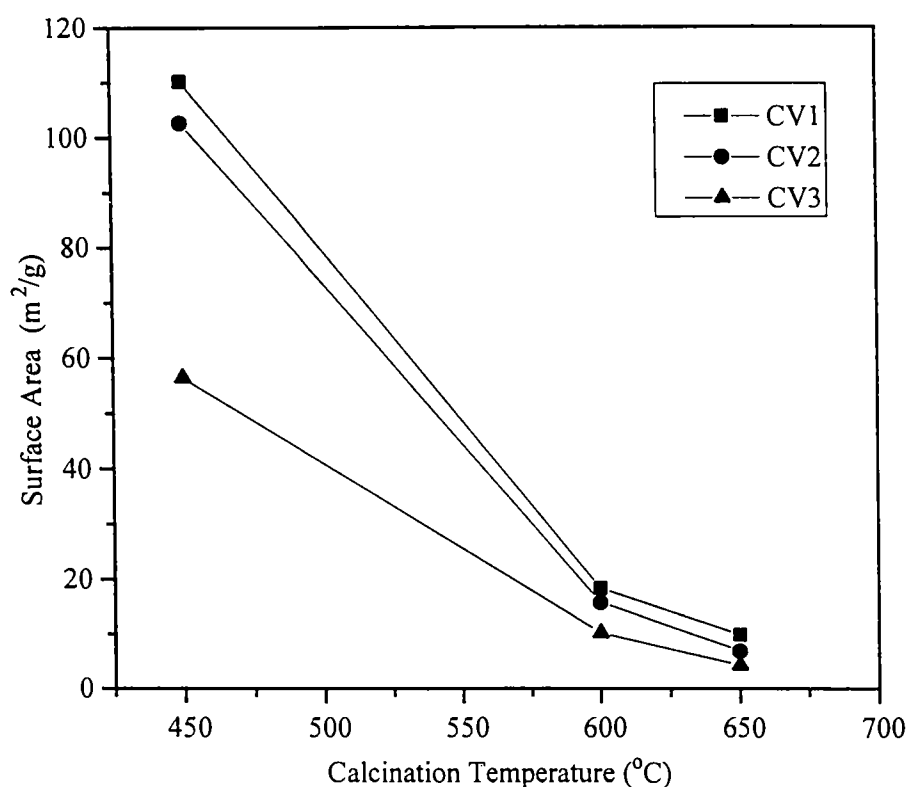


Fig. 7.8. Effect of calcination temperature on surface area of V_2O_5/TiO_2 catalysts prepared by co-precipitation method

and $82.1 \text{ m}^2/\text{g}$ respectively. Whereas in wet-impregnated samples, WV1, WV2 and WV3, the surface area values are $106.8 \text{ m}^2/\text{g}$, $84.8 \text{ m}^2/\text{g}$ and $71.2 \text{ m}^2/\text{g}$ respectively. The co-precipitated ones have the largest surface area and the ion-exchanged ones have the lowest values. On increasing further the calcination temperature to 600°C , the surface area decreased very much and it became $18.3 \text{ m}^2/\text{g}$, $15.7 \text{ m}^2/\text{g}$ and $10.12 \text{ m}^2/\text{g}$ in CV1, CV2 and CV3; $22.7 \text{ m}^2/\text{g}$, $19.45 \text{ m}^2/\text{g}$ and $17.8 \text{ m}^2/\text{g}$ in IV1, IV2 and IV3;

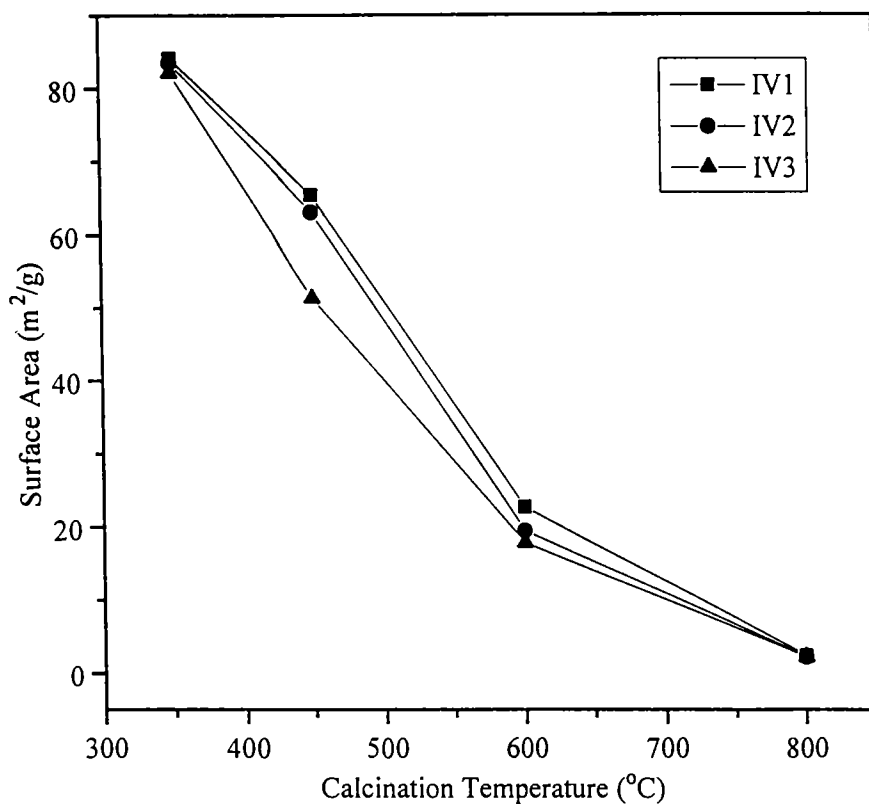


Fig. 7.9. Effect of calcination temperature on surface area of $\text{V}_2\text{O}_5/\text{TiO}_2$ catalysts prepared by ion-exchange method

18.4 m²/g, 16.51 m²/g and 13.7 m²/g in WV1, WV2 and WV3 respectively. These changes could be clearly seen in Figs 7.8 – 7.10.

When the TiO₂ support was fully transformed to rutile (at 650^oC in co-precipitated ones, at 800^oC in ion-exchanged ones and at 700^oC in wet-impregnated ones), the surface area was reduced markedly in all the samples. Surface area became 9.81 m²/g, 6.8 m²/g and 4.23 m²/g in CV1, CV2 and CV3 respectively; 2.32 m²/g, 2.21 m²/g and 2.17 m²/g in IV1, IV2 and IV3 and 4.83 m²/g, 4.35 m²/g and 4.1 m²/g in WV1, WV2 and WV3 respectively.

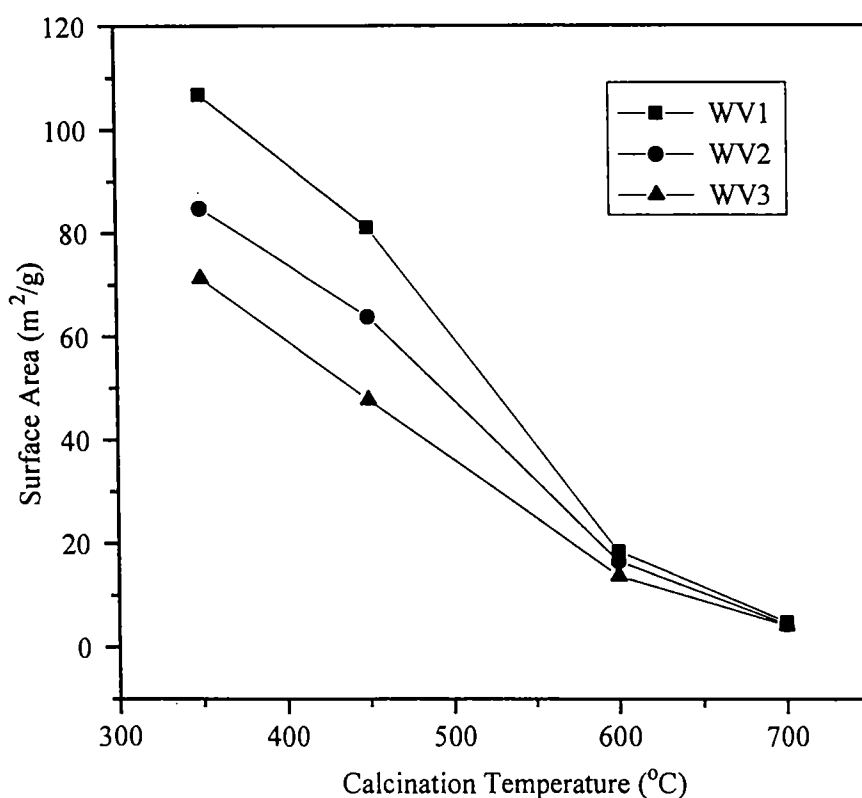
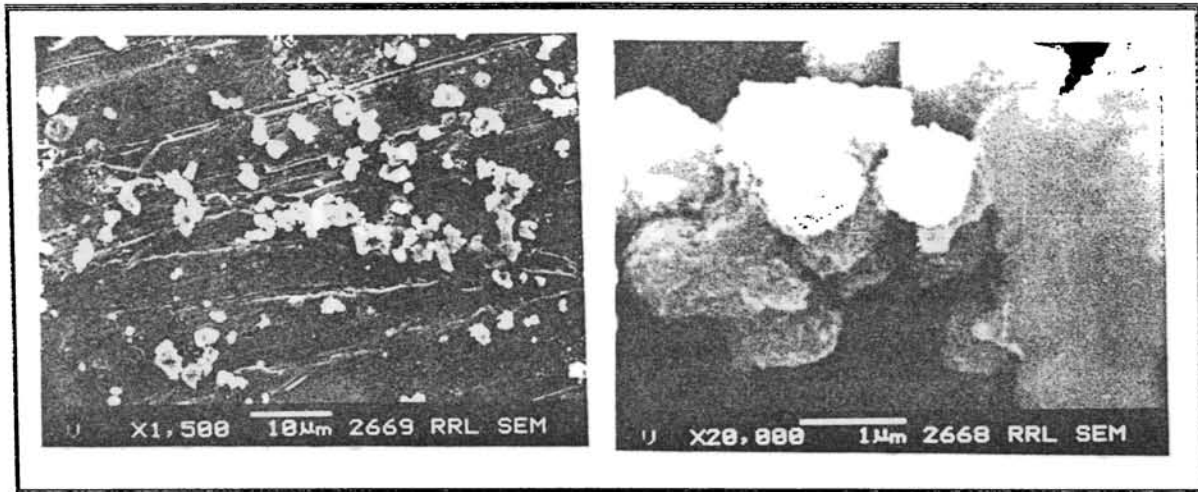


Fig. 7.10. Effect of calcination temperature on surface area of V₂O₅/TiO₂ catalysts prepared by wet-impregnation method

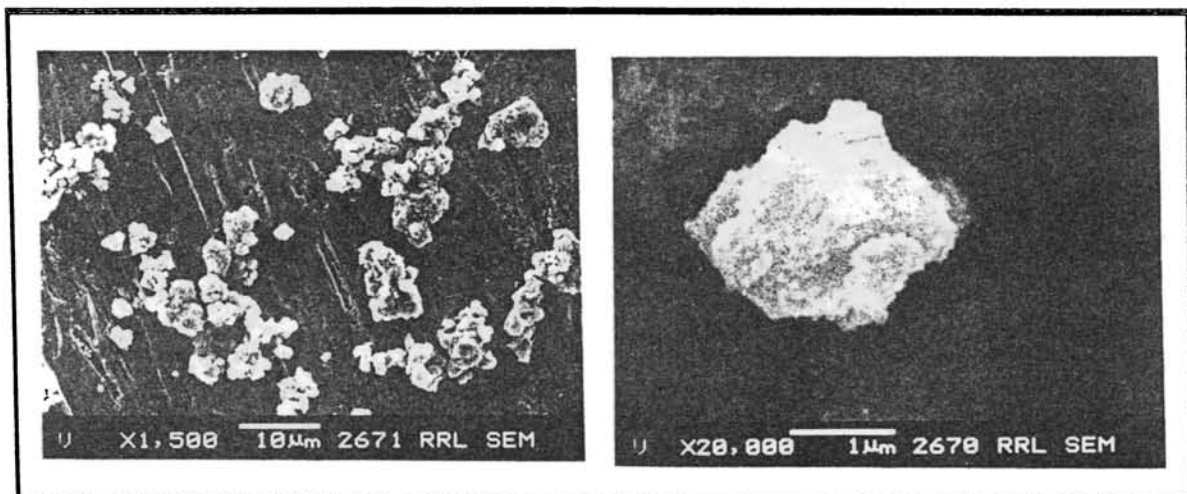
In all these samples, even though, no direct relation between crystallite size and surface area could be made, a marked decrease in surface area could be seen along with a significant increase in crystallite size. It was also noted that, a very small change in crystallite size does not necessarily involve a change in surface area. The surface area of sample CV3 was very low compared to its siblings IV3 and WV3, because of the presence of 30.9 % rutile in this sample. Figs 7.8 – 7.10 clearly show the decrease in surface area at the onset of rutilation and severe decrease when rutilation was complete, due to sintering. This is consistent with XRD data. On comparing with the surface area of pure TiO_2 , shown in Fig 3.1, the surface area decreased on loading V_2O_5 . It is very clear from all these observations that the surface area decreased noticeably during rutilation, which in turn is dependent on preparation method and calcination temperature. The decrease was greater compared to pure TiO_2 . So, V_2O_5 is enhancing the reduction in surface area during calcination.

7.3 SEM studies.

Figs 7.11A and 7.11B are the scanning electron micrographs of the samples IV3 and WV3 respectively. The micrographs of sample CV3 is shown in Fig. 7.12A. The individual particles were with a size ranging between 0.1 to $0.75\mu\text{m}$ in CV3 and IV3 samples and in WV3 the particle size was between 0.5 to $2\mu\text{m}$. All the particles were more or less spherical in shape in all the samples with much aggregation. In CV3, even though, there is 30.9 % rutile present, no appreciable change in particle size could be seen. In any of the micrographs, V_2O_5 particles

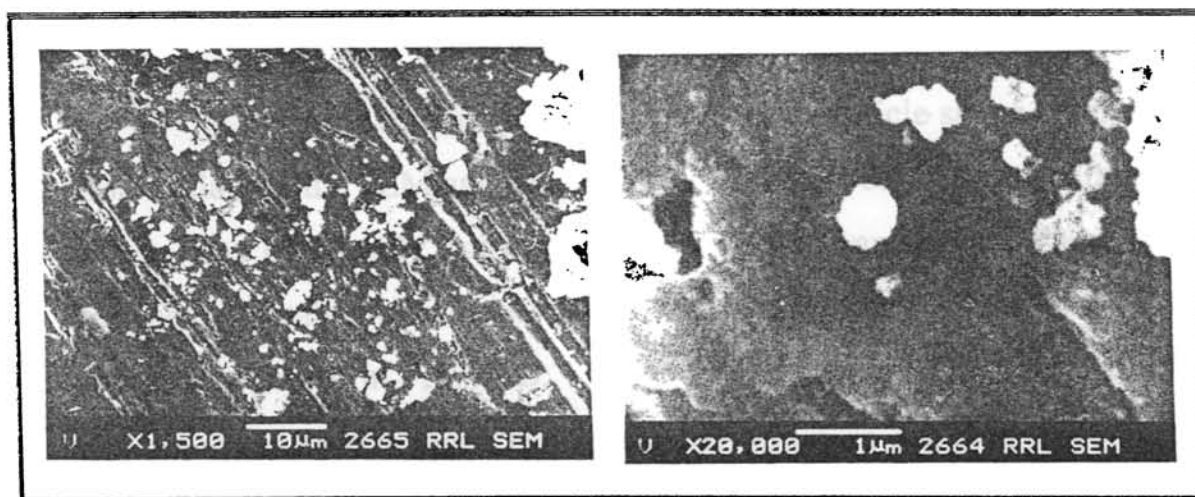


(A)

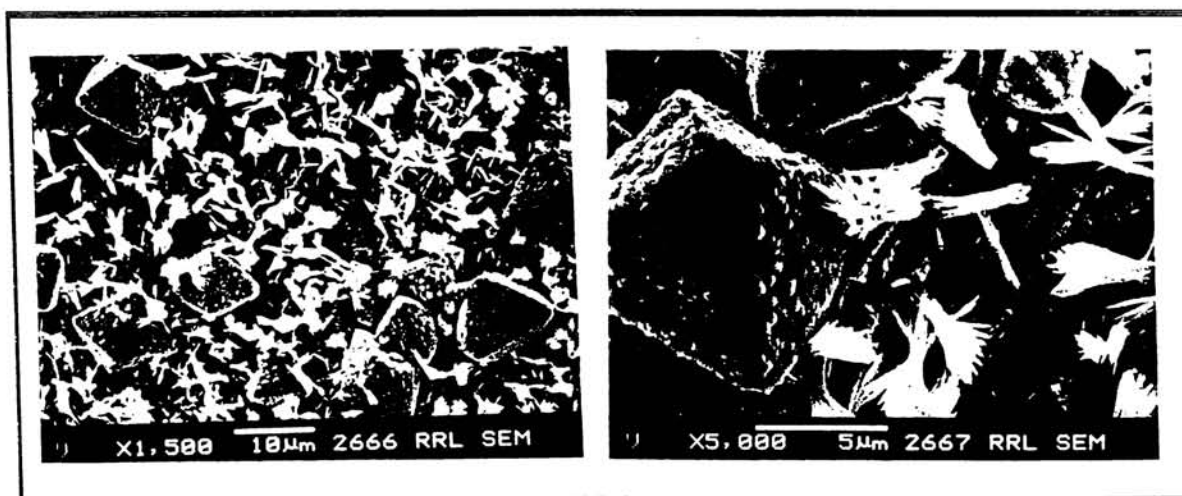


(B)

Fig. 7.11 Scanning electron micrographs of V_2O_5/TiO_2 catalystsA) IV3 and B) WV3 (calcined at $350^{\circ}C$)



(A)



(B)

Fig. 7.12 Scanning electron micrographs of V_2O_5/TiO_2 catalysts

A) CV3 (calcined at $450^\circ C$ and B) CV3 (calcined at $650^\circ C$)

could not be seen. This is in line with XRD data, where no peaks of V_2O_5 were seen due to the very fine nature of V_2O_5 .

In order to understand the changes in particle shape and size upon rutilation, the SEM analysis of CV3 calcined at 650°C (when all the anatase was completely converted to rutile), was carried out. Particles with sharp octahedral and needle like structures were present in the micrograph shown in Fig7.12B. The octahedral particles could be rutile with approximate size $8\mu\text{m}$. The needle like structure could be $V_2Ti_3O_9$, formed by the fusion between individual particles.

7.4 Dispersion studies

The dispersion was carried out at 370°C after reducing the catalyst samples at 370°C , because at this temperature V^{5+} species present on the surface of TiO_2 gets reduced to V^{3+} species and bulk phase reduction and the reduction of TiO_2 will not take place at this temperature.⁸⁻¹⁰ During oxygen chemisorption, the V^{3+} species chemisorbs one molecule of oxygen to regain V^{5+} state.⁸⁻¹⁰ The results are shown in Table 7.2. Comparatively better dispersion was obtained for co-precipitated samples. The dispersion of V_2O_5 was found to be increased on increasing V_2O_5 percentage, due to the increased chemisorption of oxygen (vide Table 7.2). The surface average crystallite size of vanadium atom calculated from chemisorption data is also included in Table7.2. In all samples the vanadium atoms have the size less than 7nm. Maximum size of 6.97nm was seen in WV1 and minimum size of 4.56nm was observed in CV3. It decreased on increasing V_2O_5 percentage. It is very interesting to note that as the anatase crystallite size increased, the surface

average crystallite size of vanadium atom was decreased. Because of the very smaller size of vanadium atom in all these samples, peaks due to V_2O_5 were not observed in XRD pattern.

Table 7.2. Results of dispersion studies

Method of prepn	Sample label	Oxygen chemisorbed ($\mu\text{mol} / \text{g}$)	Dispersion (%)	Surface average crystallite size of V atom (nm)
Co-ppn	CV1	76.84	14.1	5.67
	CV2	168.69	15.43	5.18
	CV3	288.51	17.54	4.56
I.E	IV1	64.18	11.8	6.78
	IV2	150.04	13.71	5.83
	IV3	233.1	14.2	5.63
W.I	WV1	62	11.47	6.97
	WV2	144.6	13.28	6.02
	WV3	254.46	15.46	5.17

7.5 Toluene oxidation studies

The results are shown in Figs 7.13 – 7.15. Air oxidation of toluene to form benzoic acid by V_2O_5/TiO_2 has not yet been reported in literature. The activity studies were carried out after calcination of these samples at temperatures when drastic change occurred in physical

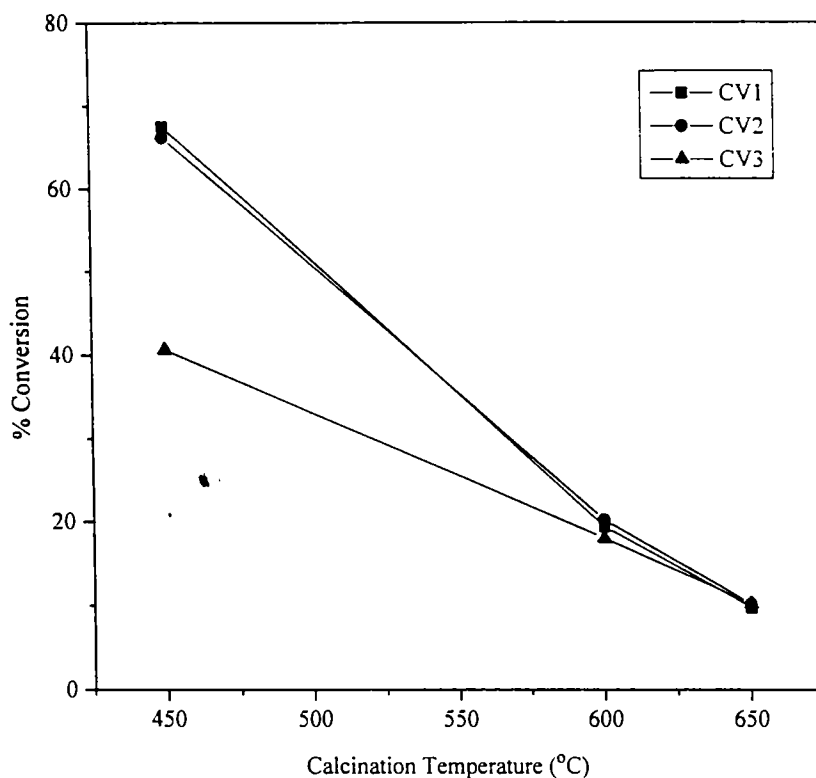


Fig. 7.13. Variation in toluene oxidation activity with calcination temperature of V_2O_5/TiO_2 catalysts prepared by co-precipitation method

properties. In ion-exchanged samples, the percentage conversion increased on increasing V_2O_5 percentage, while in co-precipitated and wet-impregnated ones, the percentage conversion decreased. Out of all these samples, better conversion was obtained with co-precipitated ones with low V_2O_5 loading. With sample CV1, percentage conversion was 67.5, while with CV2 and CV3 it was 66.2% and 40.6% respectively. The reduction in activity of CV3 to 40.6%, even though the dispersion of

V_2O_5 was very high, would be due to the presence of 30.9% rutile in this sample. The very low surface area of this sample would also affect the activity. With ion-exchanged ones IV1, IV2 and IV3 the percentage conversion was 63.2, 64.15 and 66.2 respectively and with WV1, WV2 and WV3 the percentage conversion was 65.1, 64.0 and 62.0 respectively.

In order to investigate the changes occurring in activity along with rutilation, the activity studies of co-precipitated ones calcined

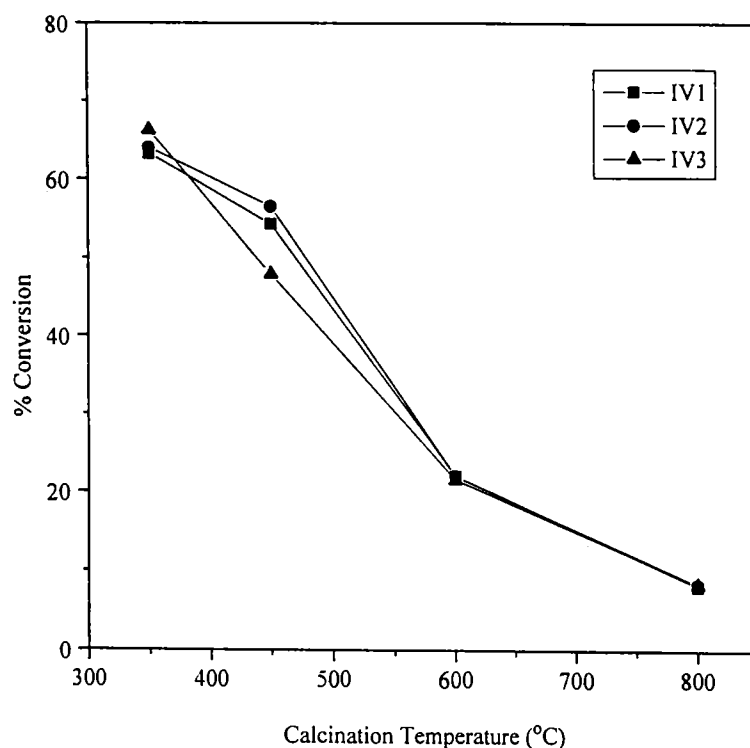


Fig. 7.14. Variation in toluene oxidation activity with calcination temperature of V_2O_5/TiO_2 catalysts prepared by ion-exchange method

at 600°C and 650°C were carried out. Similarly the activity studies of ion-exchanged ones calcined at 450°C, 600°C and 800°C and wet-impregnated ones calcined at 450°C, 600°C and 700°C were also carried out.

A severe decrease in activity was observed with these samples on increasing the calcination temperature. In co-precipitated ones CV1, CV2 and CV3 calcined at 600°C, the percentage conversion became 19.4, 20.1 and 18 respectively. On further calcination at 650°C at

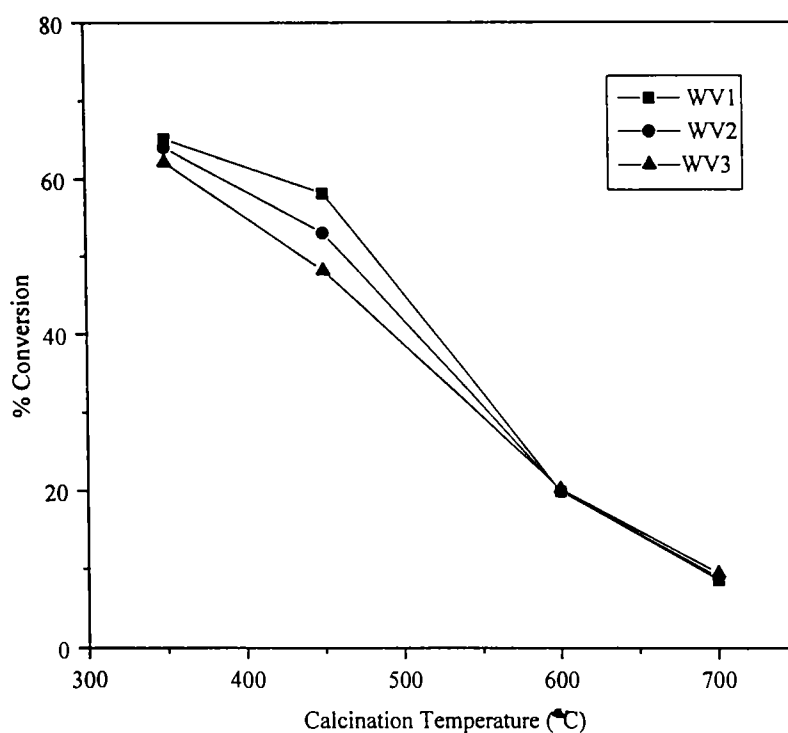


Fig. 7.15. Variation in toluene oxidation activity with calcination temperature of V_2O_5/TiO_2 catalysts prepared by wet-impregnation method

which the TiO_2 was fully transformed to rutile, the percentage conversion was reduced to 9.7, 10.1 and 10.1 respectively. With ion-exchanged ones IV1, IV2 and IV3 calcined at 450°C (which was the onset temperature of rutilation), the activity became 54.3%, 56.5% and 47.9% respectively and the activity reduced noticeably on every rise in calcination temperature. At calcination temperature when rutilation was complete, the percentage conversion became 8.1, 8.3 and 8.3 respectively. Similarly with wet-impregnated ones WV1, WV2 and WV3 calcined at 450°C , the percentage conversion was reduced to 58.1, 53 and 48.1 respectively and on further increasing the calcination temperature, the conversion became nearly 20% with all the samples. When these samples were calcined at 700°C (at which the TiO_2 support was fully converted to rutile), the percentage conversion became 8.6, 8.9 and 9.4 respectively. All these changes could be clearly seen in Figs 7.13 – 7.15.

Dramatic change in percentage conversion could be seen when the TiO_2 was fully converted to rutile. The lack of enough V_2O_5 sites, lower surface area, presence of rutile phase as the support and presence of $\text{V}_2\text{Ti}_3\text{O}_9$ would be the reason for the reduced activity.

7.6 Conclusions

From all the above observations the following conclusions can be made.

- ☐ On loading V_2O_5 and during rutilation significant reduction in surface area was observed.

- ☐ The onset and completion temperatures of rutilation were much lower compared to all other samples
- ☐ Quantity of V_2O_5 and percentage play a major role in rutilation.
- ☐ $V_2Ti_3O_9$ phase formed at above 600^0C , which indicate the presence of some non-stoichiometric titania.
- ☐ Crystallite size enlargement of anatase take place during rutilation and V_2O_5 loading.
- ☐ Better surface area, dispersion and activity were obtained with co-precipitated samples.
- ☐ Order of activity for toluene oxidation with these samples is: co-precipitated > ion exchanged > wet-impregnated ones.
- ☐ All of these samples were stable under the conditions adopted.
- ☐ The significant decrease in percentage conversion upon rutilation would be due to lower surface area and shortage of free V_2O_5 particles.

Chapter 8

SUMMARY AND CONCLUSION

TiO₂ supported catalysis is an emerging field and the development of new and better methods for the preparation is the need of the hour. TiO₂ (anatase) having high surface area, with better crystallinity and high onset temperature of rutilation can be prepared (without adding nuclei and anti rutilating agents) by thermal hydrolysis of titanyl sulfate solution under controlled conditions. The conditions of thermal hydrolysis have significant role in determining the physical properties. Thermal hydrolysis of titanyl sulfate solution containing 35gpl TiO₂, at 100⁰C for 5 hrs are the optimum conditions for obtaining TiO₂ with improved properties. Calcination at 350⁰C for 6 hrs was necessary to crystallize anatase. Various metals like Ni, Fe, V and Ce can be ion-exchanged onto this TiO₂ in the hydrous amorphous state.

Better surface area, dispersion and catalytic activity were obtained with co-precipitated samples, even though they are prepared at higher temperatures, than those of ion-exchanged and wet-impregnated ones. On loading metal oxides like NiO, V₂O₅, Fe₂O₃ and CeO₂, the surface area decreased in all the samples. Method of preparation and percentage of the loaded metal oxides have greater influence on surface area. Drastic decrease in surface area was observed upon rutilation.

No change in crystallization temperature occurred in presence of NiO, V₂O₅ and CeO₂, while the Fe₂O₃ loaded sample prepared through co-precipitation crystallized only at higher temperature

than pure TiO_2 , i.e. at 550°C . Hence Fe_2O_3 has a strong influence on the crystallization temperature. Rutilation started at different temperatures depending on the metal oxide and the method of preparation. Co-precipitated ones got rutilated at lower temperatures compared to ion-exchanged and wet-impregnated samples. In most of the cases, the onset temperatures of rutilation were lower in presence of the metal oxides used in this study, compared to pure TiO_2 , except in CeO_2 loaded samples prepared by ion-exchange and wet-impregnation methods, where the onset temperature of rutilation was 900°C against 700°C for pure TiO_2 . Out of all these samples, the onset temperature of rutilation was very low for V_2O_5 loaded ones irrespective of the method of preparation. In general, the enhancement of rutilation was in the order $\text{V}_2\text{O}_5 \gg \text{NiO} > \text{Fe}_2\text{O}_3$ and the CeO_2 has some suppressing effect rather than enhancement. All these metal oxides were present in a very fine nature at lower temperatures and during rutilation, NiO reacted with TiO_2 to form NiTiO_3 , while some portion of V_2O_5 reacted with TiO_2 to form $\text{V}_2\text{Ti}_3\text{O}_9$ and the rest remained as V_2O_5 as seen in XRD pattern, whereas in the case of CeO_2 , it remained as such with some growth in crystallite size and in the case of Fe_2O_3 , it reacted with TiO_2 to form Fe_2TiO_5 and remained as $\alpha\text{-Fe}_2\text{O}_3$ in co-precipitated ones.

The dispersion values were always better for co-precipitated ones and hence the surface average crystallite size of the respective metals was lower in these samples.

Co-precipitated samples gave high methanation activity compared to ion-exchanged and wet-impregnated ones. The order of

activity is as follows: co-precipitated >> wet-impregnated > ion-exchanged. Methanation activity was found to be highly dependent on nickel concentration present on the surface of the pellets. Significant reduction in activity was observed along with rutilation. Hence, the methanation activity is strongly influenced by support material. There was no change of phase seen after activity studies, which reveals the thermal stability of these samples under the conditions adopted.

As expected, because of better properties, the co-precipitated ones showed higher activity for toluene oxidation. All these catalysts are yet to be reported for this reaction. The percentage conversion decreased drastically upon rutilation. In $\text{CeO}_2/\text{TiO}_2$ samples, even though there existed CeO_2 particles after rutilation, the activity decreased. Hence, the nature of the support material has also a significant role in the activity of these catalysts, in addition to number of active sites, dispersion and surface area. These catalysts were also highly stable under the reaction conditions.

With all these findings, it can be concluded that, TiO_2 as a support should be characterized with high surface area, phase purity and high onset temperature of rutilation, which should be well above the optimum temperature of a designated reaction in which it is employed as a catalyst. Variation in physical properties, depending upon the method of preparation is greater in TiO_2 supported catalysts. Hence, a detailed investigation of properties of the samples prepared through each method is necessary and appropriate. A thorough awareness about the rutilation

temperature of the catalyst is also a must, before exploiting titania supported catalysts industrially.

Suggestions for future work

The rate and turn over frequency of methanation and toluene oxidation activity of these catalysts are also equally important from an industrial point of view. It can be done by setting up a continuous process. However the investigations made here are necessary for developing the catalysts for industrial purpose. Various other industrially important reactions can also be tried over these catalysts after investigating the effect of rutilation, if any, on those reactions.

References

1. Jelks Barksdale in "*Titanium - its occurrence, chemistry and technology.*" The Ronald Press Co., USA, **1966**.
2. Kirk - Othmer "*Encyclopedia of Chemical Technology.*" Wiley-Inter Science Publication, John Wiley & Sons, 3rd Edn, **1983**.
3. "*Technology in Indian titanium dioxide industry.*" DSIR, ministry of Sci.&Tech., New Delhi. **1993**.
4. E.A. Barringer and H.K. Boowen. *J. Am. Ceram. Soc.*,**65**, **1982**, pC199.
5. C.J. Barbe and M. Gretzel. *Mat. Res. Soc. Symp. Proc.***1996**, p43.
6. B.O. Regan and M. Gretzel. *Nature* 353, **1991**, p737.
7. J.H. Wohlgementz; D.B. Warfield and G.A. Johnson. *IEEE*,**1982**, p809.
8. F. Cao; G. Oskam and P.C. Searson. *J. Phys. Chem.B*, 99, **1995**, p17071.
9. A. Gutarra; A. Azens; B. Stjerna and C.G. Gransqvist. *Appl. Phys. Lett.* 64, **1994**, p28.
10. S.Y Huang; L. Kavan; I. Exner and M. Gretzel. *J. Electrochem. Soc.* L142, **1995**, p 142.
11. W.J. Macklin and R. Neat. *J. Solid State Ionics.* 53, **1992**, p694.
12. F. Bonino; L. Busani; M. Manstretta; B. Rovilto and B. Scrosti. *J. Power Sources* 6, **1981**, p261.

13. T. Ohzuku; Z. Takehara and S. Yoshizawa. *ElectrochimActa* , 24, 1979, p219
14. T. Ohzuku; T. Kodama and T. Hirai. *J. Power Sources* 14, 1985, p153.
15. R.V. de Krol; A. Goossens and J. Schoonman. *J. Phys. Chem. B*, 103, 1999, p7151.
16. H. Cheng; J. Ma; Z. Zhao and L. Qi. *Chem. Mater.* 7, 1995, p663.
17. T. Fuyuki and H. Matsunami. *Jpn. J. Appl. Phys.* 25, 1986, p1288.
18. A. Bally; K. Prasad; R. Sanjines; P.E. Schmid; F. Levy; J. Benoit; C. Barthou and P. Benalloul. *Mat. Res. Soc. Symp. Proc.* 424, 1997, p471.
19. R.U. Flood and S. Fitzmaurice. *J. Phys. Chem. B*, 99, 1995, p8954.
20. H. Lindstrom; S. Sodergren; A. Solbrand; H. Rensmo; J. Hjelm; A. Hgfeldt and S.E. Lindquist. *J. Phys. Chem. B*, 101B, 1997, p7710.
21. L. Koran; B.O. Regan; A. Ray and M. Gratzel. *J. Electrochem. Soc.* 346, 1993, p291.
22. P.V. Kamat in “ *Semiconductor Nanoparticles - Physical, Chemical and Catalytic aspects.*” Eds. P.V. Kamat and D. Maisel, Elsevier, Amstergam, 1997.
23. K. Chiba and K. Nakatani. *Thin Solid Films.* 112, 1984, p359.
24. M. Ferroni; V. Guidi and G. Martinelli. *Nano str. Mat* 7, 1996, p709.
25. Y.C. Yeh; T.Y. Tseng and D.A. Chang. *J. Am. Ceram. Soc.*, 73, 1990, p1992.

26. K.L. Sieferting and G.L. Griffin. *J. Electrochem. Soc.*,137, 1990, p814.
27. H. Tang; K. Prasad; R. Sanjines and F. Levy. *Sensors Actuators B*. 26-27, 1995, p71.
28. A.J. Burggraaf; K. Kiezer and B.A. Van Hassel. *Solid State Ionics*. 32 & 33, 1989, p444.
29. Q. Xu and M.A. Anderson. *J. Am. Ceram. Soc.*, 77, 1994, p1939.
30. V.T. Zaspalis; K.Kiezer and A.J. Burggraaf. *Appl.Catal.*74,1991, p249.
31. A. Lambort; J.P. Fabre; C. Guizard and L. Cot. *J. Am. Ceram. Soc.*, 72, 1989, p257.
32. S. Anderson and A.D. Wadsley. *Acta. Crystallograph.*, 15, 1962. p194.
33. Y. Ionue and M. Tsuji. *J. Nucl. Sci. Technol.* 13, 1976, p85.
34. Y. Ionue and M. Tsuji. *Bull. Chem. Soc. Jpn.*, 51, 1978, p794.
35. G.R. Dhoshi and V.N. Sastry. *Indian J. Chem.*, 1977, p904.
36. A.M. Adrianov. *J. Appl. Chem. USSR*, 51, 1978, P1789.
37. R.T. Lidd and Coat jr in “*Hand book of gem identification.*” Gemological Institute of America. Los Angeles. 1966.
38. D. Mac Innes in “*Synthetic gems and allied crystal manufacture.*” Noyes data Corp., Park Ridge, N.J, 1973.
39. G.H. Haerlling. *J. Am. Ceram. Soc.*, 82, 1999, p797.
40. M.Z. -C. Hu; G.A. Miller; E.A. Payzant and C.J. Rown. *J. Mat. Sci.*, 35, 2000, p2927.

41. H. Nishizava and M. Katsube. *J. Solid State Chem.*, 131, **1997**, p43.
42. J.P. Wadington. US patent No: 2, 670, 363. (Feb. 23 **1954**), National Lead Company.
43. M.A. Vannice and R.L. Garten. *J. Catal.*, 56, **1979**, p236.
44. K.C. Pande and R.C. Mehrotra. *Chem. Ind.* **1957**, p114.
45. A.J. Bard. *Science* 207, **1980**, p139.
46. E. Bargarello. *J. Am. Ceram. Soc.*, 104, **1982**, p2996.
47. S. Matsuda and A. Kato. *Appl. Catal.*, 8, **1983**, p149.
48. A. Fujishima and K. Honda. *Nature*, 37, **1972**, p238.
49. T. Tanaka; H. Kumagai; H. Hattori; M. Kudo and S. Hasegawa. *J. Catal.*, 127, **1991**, p221.
50. D.Bockelmann; D. Weichgrebe; R. Goslich and D.W. Bahnemann. *Solar Ener. Mat.& Solar Cells*, 38, **1995**, p441.
51. Y.Lee; Y.M.Gao; K.Dwight and A. Wold. *Mat.Res. Bull.*,27,**1992**, p685.
52. S. Weaver and G. Mills. *J. Phys. Chem. B*, 101, **1997**, p3769.
53. T.R.N. Kutty and M. Avudaithai. *Mat. Res. Bull.*, 23, **1988**, p725.
54. T.R.N. Kutty and S. Ahuja. *Mat. Res. Bull.*, 30, **1995**, p233.
55. G. Dagan and M. Tomkiewicz. *J. Phys. Chem. B*, 97, **1993**, p12651.
56. Y. Takita; H. Yamada; M. Hashida and T, Ishihara. *Chem.Lett.*, **1990**, p715.
57. D.W. Bahnemann. *Israel. J. Chem.*, 33, **1993**, p115.

58. K. Nagakawa; T. Suzuki; T. Kobayashi and M. Haruta. *Chem. Lett.*, **1996**, p1029.
59. A. Nobile jr; V. Van Brunt and M.W. Davis. *J. Catal.* 127, **1991**, p227.
60. S.C. Chuang; J.G. Goodwin jr and I. Wonder. *J. Catal.*, 95,**1985**,p435.
61. K.Y.S. Ng and E. Gulari. *J. Catal.*, 95, **1985**, p33.
62. B.E. Handy; M. Maciejewski and A. Baiker. *J. Catal.*, 134, **1992**, p75.
63. Rutkowski; Marian; Broniek and Roman. *CA.* 114, **1991**, 26992x.
64. J. Santos; J. Philip and J.A. Dumesic. *J. Catal.*, 81, **1983**, p147.
65. J. Santos and J.A. Dumesic in “*Studies in surface science & catalysis.*” Eds. B. Inelik; C. Naccache; G. Coudurier; H. Praliand; P. Gallezot; G.A. Martin & J.C. Vedrine. Elsevier, Amsterdam, 11, **1982**, p43.
66. P. Galli; P. Barbe; G. Guidetti; R. Zannett; A. Marigo; M. Bergozza and A. Fichera. *European Polymer. J.*, 20, **1984**, p967.
67. J.M. Thomas and W.J. Thomas in “*Introduction to the principles of heterogeneous catalysis.*” Academic press, London, **1967**, p279.
68. K. Ziegler; E. Holzkamp; H. Breil and H. Martin. *Angew. Chem.*, 67, **1955**, p541.
69. G. Natta. *J. Polymer Sci.*, 16, **1955**, p143.
70. G. Natta. *Angew. Chem.*, 68, **1956**, p393.
71. G. Natta. and I. Pasquon. *Adv. Catal.*, 11, **1959**, p1.

72. A. Corma; M.A. Camblour; P. Estev; A. Martinez and J. Perez-Pariente. *J. Catal.*, 145, **1994**, p151.
73. A. Corma; P. Estev and A. Martinez. *J. Catal.*, 152, **1995**, p18.
74. M.A. Camblour; M. Constantini; A. Corma; L. Gilbert; P. Estev; A. Martinez and S. Valencia. *J. Chem. Soc. Chem. Commun.* **1996**, p1339.
75. B. Notari. *Catal. Today*, 18, **1993**, p163.
76. S.M. Kuznicki, US pat., No: 4, 938, 939, **1990**, Engelhard Corporation.
77. M.W. Anderson; O. Terasaki; T. Ohsuna; A. Philippou; S.P. Mackay; A. Ferreira; J. Rocha and S. Lidin. *Nature*, 367, **1994**, p347.
78. "Homogeneous and heterogeneous photocatalysis." Eds. E. Pelizzetti and N. Serpone, NATO ASI Series C, **1986**, p174.
79. "Photocatalysis - Fundamental applications." Eds. N. Serpone and E. Pelizzetti. John Wiley & Sons, New York, **1989**.
80. N. Serpone. *Res. Chem. Intermed.*, 20, **1994**, p953.
81. M.R. Hoffmann; S.J. Martin; W.Y. Choi and D.W. Bahnemann. *Chem. Rev.* 95, **1995**, p69.
82. A.L. Linsebigher; G.Q. Lu and J.T. Yates. *Chem. Rev.* 95, **1995**, p735.
83. N. Serpone; D. Lawless; R. Terzian; C. Minero and E. Pelizzetti in "Photochemical conversion and storage of solar energy." Kluwer Academic Publishers, Dordrecht, The Netherlands, **1991**, p451.

84. N.S. Foster; R.D. Nobile and C.A. Koval. *Environ. Engg.*, 27, **1998**, p651.
85. J.W. Jacobs; F.W.H. Kampers; J.M.G. Rikken; C.W.T. Bullelinwma and D.C. Koningsberger. *J. Electrochem. Soc.*, 136, **1989**, p2914.
86. N.S. Foster; A.N. Lancaster; R.D. Nobile and C.A. Kaval. *Ind. Engg. Chem. Res.* 34, **1995**, p3865.
87. F. Forouzan; T.C. Richards and A.J. Bard. *J. Phys. Chem. B*, 100, **1996**, p18123.
88. K.H. Wang; Y.H. Hsiech; M.Y. Chong and C.Y. Chong. *Appl. Catal. B, Environ.*, 21, **1999**, p1.
89. E. Pelizzetti. *Solar Ener. Mat. & Solar Cells.* 38, **1995**, p453.
90. C.S. Turchi and D.F. Ollis. *J. Catal.* 119, **1989**, p483.
91. L.P. Childs and D.F. Ollis. *J. Catal.* 66, **1980**, p383.
92. T. Rajah; A.E. Ostafin; O.I. Micic; D.M. Tiede and M.C. Thurnauer. *J. Phys. Chem. B*, 100, **1996**, p815.
93. K. Tanaka and S.M. Robledo *J. Mol. Catal.*, 144, **1999**, p425.
94. D.W. Bahnemann; D. Bockelmann; R. Goslich; M. Hilgendorff and D. Weichgrebe in "Photo catalytic purification and treatment of water & air." Eds. D.F. Ollis & H.Al Ekabi, Elsevier Sci. Pub., **1993**, p301.
95. N.-G. Park; G. Schlichthorl; J. Vande Langemat; H.M. Cheong; A. Mascarenhas and A.J. Frank. *J. Phys. Chem. B*, 103, **1999**, p3308.
96. M.M. Gomez; J. Lu; J.L. Solis E. Olssan; A. Hagfeldt and C.G. Granqvist. *J. Phys. Chem. B*, 104, **2000**, p8712.

97. R.L. Pozzo; M. Baltanas & A. Cassano. *Catal. Today*, 39, 1997, p219.
98. D. Beydoun and R. Anal. *J. Phys. Chem. B*, 104, 2000, p4397.
99. J.H. Sinfelt in “*Materials science in energy technology.*” Academic Press Inc., 1979, p6.
100. V.E. Henrich and P.A. Cox in “*The surface science of metal oxides.*” Cambridge University Press, 1994.
101. S.J. Tauster; S.C. Fung and R.L. Garten. *J. Am. Chem. Soc.*, 100, 1978, p170.
102. H. Onishi; T. Aruga; C. Egawa and Y. Iwasawa. *Surf. Sci.*, 199, 1988, p54.
103. G. Rooker and W. Gopel. *Surf. Sci.*, 181, 1987, p530.
104. J. Deng; D. Wang; X. Wei; R. Zhai and H. Wang. *Surf. Sci.*, 249, 1991, p213.
105. C.C. Kao; S.C. Tsui and Y.W. Chung. *J. Catal.*, 73, 1982, p136.
106. P.J. Moller and M.C. Wu. *Surf. Sci.*, 224, 1989, p265.
107. J.A. Horsely. *J. Am. Chem. Soc.*, 101, 1979, p2870.
108. H.R. Sadeghi and V.E. Henrich. *J. Catal.*, 109, 1988, p1.
109. C.N.R. Rao; S.R. Yoganarasimhan and P.A. Faeth. *Trans. Faraday Soc.*, 57, 1961, p504.
110. A.F. Wells in “*Structural Inorganic Chemistry.*” 3rd Edn., Oxford University Press, Oxford, UK, 1962, p76.
111. Y. Suwa; M. Inagaki and S. Naka. *J. Mat. Sci.*, 19, 1984, p1397.
112. R.D. Shannon and J.A. Pask. *J. Am. Ceram. Soc.*, 48, 1965, p391.
113. K.J.D. Mackenzie. *Trans. J. Br. Ceram. Soc.*, 74, 1975, p121.

114. J.A. Gambao and D.M. Pasquevich. *J. Am. Ceram. Soc.*, 75, 1992, p2934.
115. D. Shannon. *J. Appl. Phys.*, 35, 1964, p3414.
116. S.R. Yoganarasimhan and C.N.R. Rao. *Trans. Farad. Soc.*, 58, 1962, p1579.
117. K.J.D. Mackenzie. *Trans. J. Br. Ceram. Soc.*, 74, 1975, p29.
118. F.C. Gennari and D.M. Pasquevich. *J. Mat. Sci.*, 33, 1998, p1571.
119. F.C. Gennari and D.M. Pasquevich. *J. Am. Ceram. Soc.*, 82, 1999, p1915.
120. S. Vemury and S.E. Pratsinis. *J. Am. Ceram. Soc.*, 78, 1995, p2984.
121. Y. Lida and S. Ozaki. *J. Am. Ceram. Soc.*, 44, 1961, p120.
122. X.Z. Ding; Z.Z. Qi and Y.Z. He. *Nano str. Mat.*, 4, 1994, p663.
123. K.J.D. Mackenzie. *Trans. J. Br. Ceram. Soc.*, 74, 1975, p77.
124. Z. Yuan and L. Zhang. *Nano str. Mat.*, 10, 1998, p1127.
125. A. Nobile jr and M.W. Davis jr. *J. Catal.*, 116, 1989, p383.
126. K.J.D. Mackenzie and P.J. Melling. *Trans. J. Br. Ceram. Soc.*, 73, 1974, p179.
127. C.N.R. Rao. *Acc. of Chem. Res.*, 17, 1984, p83.

128. M.J. Reddy and D.W. Reddy. *J. Am. Ceram. Soc.*, 70, **1987**, p C-358.
129. F.E. Massoth in "*Advances in catalysis.*" Academic Press, New York. 27, **1978**, p265,
130. G. Muralidhar; F.E. Massoth and J. Shabtai. *J. Catal.*, 85, **1984**, p44.
131. H. Shimada; T. Sato; Y. Yoshimura; J. Hiraishi and A. Nishijima. *J. Catal.*, 110, **1988**, p275.
132. R.B. Quincy; M. Hondlla and D.M. Hercules. *J. Catal.*, 106, **1987**, p85.
133. M. Takeuchi; S. Matsuda; F. Nakajima and H. Okada. *Proc. National meeting of AMC Soc.*, Atlanta, Georgia, **1981**.
134. M. Takeuchi. US patent No: 4, 206, 036. **1980**.
135. S. Matsuda; T. Kano; J. Imahashi and F. Nakajima. *Ind. Engg. Chem. Fundamental*, 21, **1982**, p18.
136. K. Nagakawa; T. Suzuki; T. Kobayashi and M. Haruta. *Chem. Lett.*, **1996**, p1029.

137. K. Mori; A. Miyamoto and Y. Murakami. *J. Catal.*, 95, 1985, p482.
138. G.C. Bond; A.J. Sarkani and G.D. Parfitt. *J. Catal.*, 57, 1979, p476.
139. I.E. Wachs; R.Y. Saleh; S.S. Chan and C.C. Chersich. *Appl. Catal.*, 15, 1985, p339.
140. R.Y. Saleh; I.E. Wachs; S.S. Chan and C.C. Chersich. *J. Catal.*, 98, 1986, p102.
141. G.C. Bond. *J. Catal.*, 116, 1989, p531.
142. R. Haase; U. Illgen; J. Schere and I.W. Schulz. *Appl. Catal.*, 19, 1985, p13.
143. E.I. Andreikov. *React. Kinet. Catal. Lett.*, 22, 1983, p351.
144. Y. Murakami; M. Inomata; A. Miyamoto and K. Mori. *Proc. 7th Inter. Cong. Catal.*, Tokyo, 1980, B 1981, P1344.
145. M. Inomata; A. Miyamoto and Y. Murakami. *J. Chem. Soc. Chem. Commun.*, 1980, p223.
146. A.J. Hengstum; J.G. Van Ommen; H. Bosch and P.J. Gellings. *Appl. Catal.*, 8, 1983, p369.
147. F. Cavari; F. Parrinello and F. Trifirp. *J. Mol. Catal.*, 43, 1987, p117.

148. M. Santi and A. Anderson. *J. Mol. Catal.*, 59, 1990, p233.
149. B.M.Reddy; I.Ganesh and E.P.Reddy. *J. Phys.Chem.B*,101,1997, p1769.
150. A. Vejux and P. Courtine. *J. Solid State Chem.*, 29, 1978, p93.
151. M. Gasior and T. Machej. *J. Catal.*, 83, 1983, p472.
152. G.C. Bond; J.P. Zurita; S. Flamerz; P.J. Gellings; H. Bosch; J. Van Ommen and B.J. Kip. *Appl. Catal.*, 22, 1986, p361.
153. C. Cristini; P. Forzatti and G. Busca. *J. Catal.*, 116, 1989, p586.
154. G.T. Went S.T. Oyama and A.J. Bell. *J. Phys. Chem.B*, 94, 1990, p4240.
155. H. Eckert and I.E. Wachs. *J. Phys. Chem. B*, 93, 1989, p6796.
156. T. Machej; J. Haber; A.M. Turek and I.E. Wachs. *Appl. Catal.*, 70, 1991, p115.
157. G.T. Went; L.-J. Leu and A.T. Bell. *J. Catal.*, 134, 1992, p479.
158. A. Baiker; P. Dollenmeier; M. Gliusk and A. Reller. *Appl. Catal.*, 35, 1989, p351.
159. B.M. Reddy; E.P. Reddy and S.T. Srinivas. *J. Phys. Chem. B*, 96, 1992, P7076.

160. K. Christmann in *"Introduction to surface physical chemistry."* Steinkopff Verlag, Darm Stadt., **1991**,
161. M. Ichikawa. *J. Catal.*, 56, **1979**, p127.
162. L.M. Tau and C.O. Bennett. *J. Catal.*, 89, **1984**, p285.
163. T.K. Kundu; M. Mukherjee and D. Chakravorthy. *J. Mat. Sci.*, 33, **1998**, p1759.
164. L.M. Tau and C.O. Bennett. *J. Catal.*, 89, **1984**, p327.
165. B. Sen and J.L. Falconer. *J. Catal.*, 125, **1990**, p35.
166. M.A. Vannice and R.L. Garten. *J. Catal.*, 63, **1980**, p255.
167. J.S. Smith; P.A. Thrower and M.A.Vannice. *J.Catal.*, 68, **1981**, p270.
168. G.B. Raupp and J.A. Dumesic. *J. Phys. Chem. B*, 88, **1984**, p660.
169. E.L. Kugler and R.L. Garten. US pat., No: 4, 273, 724. June 16, **1981**.
170. G.B. Raupp and J.A. Dumesic. *J. Catal.*, 95, **1985**, p601.
171. J.A. Rabo; A.P. Risch and M.L. Poutsma. *J.Catal.*,53,**1978**, p295.
172. H. Arai; K. Mitsuishi and T. Seiyama. *Chem Lett.*, **1984**, p1291.

173. T. Ishihara; K. Eguchi and H. Arai. *Appl. Catal.*, 30, **1987**, p225.
174. T. Ishihara; K. Eguchi and H. Arai. *Appl. Catal.*, 40, **1988**, p87.
175. N. Horiuchi; T. Ishihara; K. Eguchi & H. Arai. *Chem.Lett.*,**1988**, p499.
176. F. Nakajima. Japan patent No: 52, 6953, **1977**, No: 52, 6954, **1977**, No: 52, 35342, **1977**.
177. K. Matsushida. Japan patent No: 52, 2919, **1977**.
178. F. Nakajima. US patent No: 4,085, 193, **1978**.
179. M. Kancheva; V. Bushev and D. Klissuski. *J. Catal.*, 145, **1994**, p96.
180. M. Inomata; A. Myamoto and Y. Murakami. *J.Catal.*,62, **1980**, p140.
181. A. Myamoto; K. Kobayashi; M. Inomata and Y. Murakami. *J. Phys. Chem. B*, 86, **1982**, p2945.
182. M. Inomata; A. Myamoto and Y. Murakami. *J. Phys. Chem. B*, 85, **1981**, p2372.
183. M. Inomata; K. Mori; A. Myamoto; T. Ui and Y. Murakami. *J. Phys. Chem. B*, 87, **1983**, p754.

184. F. Janssen; F. Vanden Kerkhof; H. Bosh and J. Ross. *J. Phys. Chem. B*, 91, **1987**, p5921.
185. F. Janssen; F. Vanden Kerkhof; H. Bosh and J. Ross. *Ibid* p6633.
186. M. Gasior; J. Haber; T. Machej and T.C. Zeppe. *J. Mol. Catal.*, 43, **1988**, p359.
187. N.-Y. Topsoe. *J. Catal.*, 128, **1991**, p499.
188. Z.C. Kang and Q.X. Bao. *Appl. Catal.*, 26, **1986**, p251.
189. Y. Nagakawa; T. Ouo; H. Miyata and Y. Kubokawa. *J. Chem. Soc. Faraday Trans. 79*, **1983**, p2929.
190. A. Khodakov; B. Olthof; A.T. Bell and E. Ighesia. *J.Catal.*, 181, **1999**, p205.
191. I.E. Wachs and B.M. Weckhuysen. *Appl. Catal. A*, 157, **1997**, p67.
192. E. Payen; M. Guelton and J. Gimbolt. *J. Phys. Chem. B*, 92, **1988**, p1230.
193. G. Centi; D. Pinelli; F. Trifiro; D. Ghoussoub; M. Guelton and L. Gengembre. *J. Catal.*, 130, **1991**, p238.
194. H. Bosch and F. Janssen. *Catal. Today*, 2, **1988**, p369.

195. K. Tanabe and H. Hattori. *Energy Shigen (Resources)*, 2, **1981**, p570.
196. K.I. Aika; H. Hattori and A. Ozaki. *J. Catal.*, 27, **1972**, p424.
197. J.E. Sueiras; N. Homs; P. Ramirez de la Piscina; M. Gracia and J.L.G. Fierro. *J. Catal.*, 98, **1986**, p264.
198. J.Santos; J. Philipos and J.A. Dumesic. *J. Catal.*, 81, **1983**, p147.
199. H. Hattori; M. Itoh and K. Tanabe. *J. Catal.*, 38, **1975**, p172.
200. H. Hattori; M. Itoh and K. Tanabe. *J. Catal.*, 41, **1976**, p46.
201. M. Itoh; H. Hattori and K. Tanabe. *J. Catal.*, 35, **1974**, p225.
202. P. Iengo; G. Apride; M.D. Serio; D. Gazzoli and E. Santacesaria. *Appl. Catal., A*, 178, **1999**, p97.
203. N.E. Quaranta; J. Soria; W.C. Corberan and J.L.G. Fierro. *J. Catal.*, 171, **1997**, p1.
204. J.R. Sohn; Y. Il Pae; H. Jang and M.Y. Park. *J. Catal.*, 127, **1991**, p449.
205. J.R. Sohn and H.J. Kim. *J. catal.*, 101, **1986**, p428.
206. K. Tanaka and J.M. White. *J. Phys. Chem. B*, 86, **1982**, p3977.
207. K. Tanaka and J.M. White. *Ibid*, p4708.

208. K. Tanaka and J.M. White. *J. Catal.*, 79, 1983, p81.
209. E. Akubuiro and X.E. Verykios. *Appl. Catal.*, 14, 1985, p215.
210. G.S. Lane and E.E. Wolf. *J. Catal.*, 105, 1987, p386.
211. Y. Nitta; Y. Ueda and T. Imanaka. *Chem. Lett.*, 1994, p1095.
212. Y. Nitta and K. Kobiro. *Chem. Lett.*, 1995, p165.
213. Y. Nitta; K. Kobiro and Y. Okamoto. *Proc. 70th Ann. Meeting. Chem. Soc. Jpn. I*, 1996, p573.
214. Y. Nitta and K. Kobiro. *Chem. Lett.*, 1996, p897.
215. K. Foger and H. Jaeger. *J. Catal.*, 120, 1989, p465.
216. M. Carbucicchio; G. Centi; P. Forzatti; F. Trifiro and P.L. Villa. *J. Catal.*, 107, 1987, p307.
217. P. Murugavel and H.W. Roesky. *Angew. Chem.*, 36, 1997, p477.
218. D.R.C.Huybrechts; L.D.BrUYcker and P.A.Jacobs. *Nature*, 345, 1990, p240
219. C.C. Wang; Z. Zhang and J.Y. Ying. *Nano str. Mat.*, 9, 1997, p583.
220. W. Choi and M.R. Hoffmann. *Environ. Sci. Technol.*, 25, 1995, p1646.
221. W. Choi and M.R. Hoffmann. *J. Phys. Chem. B*, 100, 1996, p216.

222. H. Kominami; T. Matura; K. Iwai; B. Ohtani; S. Nishimoto and Y. Kera. *Chem. Lett.*, **1995**, p693.
223. H. Kominami; J. Kato; M. Kohno; Y. Kera and B. Ohtani. *Chem. Lett.*, **1996**, p1051.
224. S. Kagaya; Y. Bitoh and K. Hasegawa. *Chem. Lett.*, **1997**, p155.
225. P. Kopf; E. Gilbert and S.H. Eberle. *J. Photochem. Photobiol., A*, **136**, **2000**, p163.
226. I. Sopyan; M. Watanabe; S. Murasawa; K. Hashimoto and A. Fujishima. *Chem. Lett.*, **1996**, p69.
227. M. Muneer; R. Philip and S. Das. *Res. Chem. Intermed.*, **23**, **1997**, p233.
228. K. Ionnis; K. Theophanics; M. Shakellarides; Vasilis; A. Sakkas and A. Albinis. *Environ. Sci. Technol.*, **35**, **2001**, p398.
229. K. Tennakone and I.R.N. Kottegoda. *J. Photochem. Photobiol., A*, **93**, **1996**, p79.
230. G.N. Schranzer; T.D. Guth; J. Salehi; N. S trampach; Liu Nam Hui and M.R. Palmer. *Chem. Phys. Lett.*, **102**, **1983**, p509.
231. C. Anderson and A.J. Bard. *J. Phys. Chem. B*, **101**, **1997**, p2611.

232. M. Anpo; H. Yamashita; Y. Ichihashi; Y. Fuji & M. Honda. *Ibid*, p2632.
233. S.G. Zhang; Y. Fuji; H. Yamashita; K. Koyano; T. Tatsumi and M. Anpo. *Chem. Lett.*, 1997, p659.
234. S.G. Zhang; Y. Ichihashi; H. Yamashita; T. Tatsumi and M. Anpo. *Chem. Lett.*, 1996, p895.
235. Y. Xu and C.H. Langford. *J. Phys. Chem. B*, 101, 1997, p3115.
236. J.E. Tanguay; S.C. Suib and R.W. Coughlin. *J. Catal.*, 117, 1989, p335.
237. C.N.R. Rao. *Mat. Sci. and Engg., B*, 18, 1993, p1.
238. D. Vorkapic and T. Matsoukas. *J. Am. Ceram. Soc.*, 81, 1998, p2815.
239. H. Imai and H. Hirashima. *J. Am. Ceram. Soc.*, 82, 1999, p2301.
240. K. Yanagisawa and J. Ovenston. *J. Phys. Chem. B*, 103, 1999, P7781.
241. Y. Inoue; S. Yin; S. Uchida; Y. Fujishiro; M. Shitsuka; E. Min and T. Sato. *Br. Ceram. Trans.*, 97, 1998, p222.

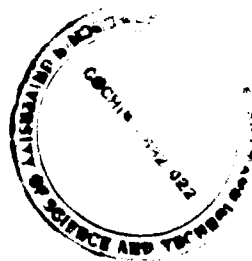
242. O. Masson; V. Rieux; R. Guinebretiere and A. Danger. *Nano str. Mat.*, 7, 1996, p725.
243. W.B Kim; S.H. Choi and J.S. Lee. *J. Phys. Chem. B*, 104, 2000, p8670.
244. T. Arunarkavally; G.V. Kulkarni; G. Sankar and C.N.R. Rao. *Catal. Lett.*, 17, 1993, p29.
245. J.P. Espinos; A.R. Gonzalez - Elipe; A. Caballero; J. Carcia and G. Munuera. *J. Catal.*, 136, 1992, p415.
246. A. Satsuma; S. Takenaka; T. Tanaka; S. Nojima; Y. Kera and H. Miyata. *Chem. Lett.*, 1996, p115.
247. G.T. Went; Li-Jen Leu; R.R. Rosin and A.T. Bell. *J. Catal.*, 134, 1992, p492.
248. G. Busca; G. Centi; L. Marchetti and F. Trifiro. *Langmuir*. 2, 1986, p568.
249. G. Busca. *Ibid*, p577.
250. G. Busca; L. Marchetti; G. Centi and F. Trifiro. *J. Chem. Soc. Faraday Trans.*, 81, 1985, p1003.
251. F. Carten and C.N. Canghlan. *J. Phys. Chem., B*, 64, 1983, p5176.

252. C. Martin and V. Rivas. *React. Kinet. Catal. Lett.*, 33, **1987**, p381.
253. A.J. Van Hengstum; J.G. Van Ommen; H. Bosch and P.J. Gellings. *Appl. Catal.*, 5, **1983**, p207.
254. I. Georgiadou; ch. Papadopoulou; H.K. Matralis; G.A. Voyiatzis; A. Lycourghiotis and ch. Kordulis. *J. Phys. Chem. B*, 102, **1998**, p8459.
255. D.S. Kim; Y. Kurusu; I.E. Wachs; F.D. Hardcastle and K. Segawa. *J. Catal.*, 120, **1989**, p325.
256. H. Coubron; J.M. Herrmann and P. Pichat. *J. Catal.*, 95, **1985**, p539.
257. T. Ishihara; N. Horiuchi; K. Eguchi and H. Arai. *J.Catal.*, 130, **1991**, p202.
258. P.Cortesi; G.Donati and G.Saggese. Br. Pat.EP 0 117755 A2, **1984**, 12.
259. S.J. Kim; S.D. Park and Y.H. Jeong. *J.Am.Ceram.Soc.*,82, **1999**, p927.
260. M. Kundo; K. Shinozaki; R. Ooki and N. Mizutani. *J. Ceram. Soc. Jpn*, 102, **1994**, p742.

261. M. Kundo; H. Funakubo; K. Shinozaki and N. Mizutani. *J. Ceram. Soc. Jpn*, 103, 1995, p552.
262. M. Iwasaki; M. Hara and S. Ito. *J. Mat. Sci. Lett.*, 17, 1998, p1769.
263. M. Yokota and M. Naka. *J. Jpn. Soc. Powder & Powder metal.*, 39, 1992, p235.
264. J. Rubio; J.L. Oteo; M. Villegas and P. Duran. *J. Mat. Sci.*, 32, 1997, p643.
265. S. Gablenz; D. Vottzke; H.P. Abicht and J.N. Zdralek. *J. Mat. Sci. Lett.*, 17, 1998, p537.
266. N. Serpone; D. Lawless and R. Khairut dinov. *J. Phys. Chem. B*, 99, 1995, p16646.
267. C. Kormann; D.W. Bahnemann and H. Hoffmann. *J. Phys. Chem. B*, 92, 1988, p5196.
268. S.J. Oyama; G.T. Went; K.B. Lewis; A.T. Bell and G.A. Somarajai. *J. Phys. Chem. B*, 93, 1989, p6786.
269. M. Boudart; A. Delbouille; J.A. Dumesic; S. Khammouma and H. Topsoe. *J. Catal.*, 37, 1975, p486.

270. F.D. Snell and C.L. Hilton in "*Encyclopedia of industrial chemical analysis.*" 7,1968, p65. Inter Sci. Publ., John Wiley & Sons, New York.
271. J.A. Longford. *J. Appl. Cryst.*, 11, 1978, p102.
272. Wauthoz; M.Ruwet; T.Machej and P.Grange. *Appl. Catal.*,69,1991, p149.
273. I.M. Kolthoff; P.J. Elving and E.B. Sandell in "*Treatise on analytical chemistry.*" Inter Sci. Publishers, New York, Part II, 5, 1961, p49.
274. I.M. Kolthoff; P.J. Elving and E.B. Sandell. *Ibid*, 2, 1962, p404.
275. C.L. Wilson and D.W. Wilson in "*Comprehensive analytical chemistry.*" Elsevier Publishing Co., I^c, 1962, p499.
276. N.H. Furman in "*Standard methods of chemical analysis.*" D. Van Nostrand Co. Inc., Princeton, New Jersey, 6th Edn., 1, 1966, p1215.
277. N.H. Furman. *Ibid*, p539.
278. *Degussa Technical Bulletin- Pigment Report*, 56, 1990, p13.
279. K.B. Kester and J.L. Falconer. *J. Catal.*, 89, 1984, p380.
280. F. Qu and P.C. Morris. *J. Phys. Chem. B*, 104, 2000, p 5232.

281. G.D. Parfitt and K.S.W. Sing in "*Characterization of powder surfaces.*" Academic Press, 1976, p2.
282. D. Farin and D. Anvir. *J. Catal.*, 120, 1989, p55.
283. W. Goodman. *Acc. Chem. Res.*, 17, 1984, p194.
284. Ruckenstein and S.H. Lee. *J. Catal.*, 104, 1987, p259.
285. Z. Ozdogan; P.D. Gochis and J.L. Falconer. *J. Catal.*, 83, 1983, p257.
286. C.H. Bartholomew; P.B. Pannell and J.L. Bulter. *J.Catal.*,65,1980, p335.
287. M.A. Vannice. *J. Catal.*, 66, 1980, p242.
288. L. Xu; S. Bao; R.J. O'Brien; A. Raje and B.H. Davis. *Chem Tech*, Jan 1998, p47.
289. Larkins; P. Frank and Z. Khan Azhraf. *Appl. Catal.*, 47, 1989, p209.
290. M.A. Vannice; S.Y. Wang and S.H. Moon. *J. Catal.*, 71, 1981, p15.



291. Adamice; S.E. Wanke; B. Tesche and U. Klenger in "*Metal-support and metal additive effect in catalysis.*" Elsevier Sci. Publishing Co., Amsterdam. **1983**, p77,
292. H.F. Mark; D.F. Othmer; C.G. Overberger and G.T. Seaborg in "*Encyclopedia of chemical technology.*" Inter Sci. Publ. John Wiley and Sons. New York. 3, 3rd Edn., **1978**, p781.
293. A. Trovarelli; C. de Leitenburg and G. Dolcetti. *Chem Tech*, June **1997**, p32.